# Structure and Dynamics
## of the
# VAULT COMPLEX

# Structure and Dynamics of
# the Vault Complex

De structuur en dynamiek van het vault complex

**Proefschrift**

ter verkrijging van de graad van doctor
aan de Erasmus Universiteit Rotterdam
op gezag van de Rector Magnificus
Prof.dr. S.W.J. Lamberts
en volgens besluit van het College voor Promoties.

De openbare verdediging zal plaatsvinden op
woensdag 14 januari 2004 om 15.45 uur

door

**Arend van Zon**
geboren te Gouda

**Promotiecommissie:**

Promotor:            Prof.dr. P. Sonneveld

Overige leden:       Prof.dr. I.P. Touw
                     Prof.dr. R. Kanaar
                     Prof.dr. R.J. Scheper

Copromotor:          Dr. E.A.C. Wiemer

# Contents

# CHAPTER 1

## Introduction: The vault complex

*Chapter 1*

**Abstract**

Vaults are large ribonucleoprotein particles found in eukaryotic cells. They are composed of multiple copies of a $M_r$ 100,000 major vault protein (MVP) and two minor vault proteins of $M_r$ 193,000 (VPARP) and $M_r$ 240,000 (TEP1) as well as small untranslated RNAs of 86-141 bases. The vault components are arranged into a highly characteristic hollow barrel-like structure of 35 x 65 nm in size. Vaults are predominantly localized in the cytoplasm where they associate with cytoskeletal elements. A small fraction of vaults are found to be associated with the nucleus. As of yet the precise cellular function of the vault complex is unknown. However, their distinct morphology and intracellular distribution suggest a role in intracellular transport processes. Here we review the current knowledge on the vault complex, its structure, components and possible functions.

*Chapter 1*

**Discovery of the vault complex**

Vault particles were first observed in 1986 as contaminants in preparations of clathrin coated vesicles from rat liver (1). The ovoid vault particles displayed highly regular dimensions and possessed a complex barrel-shaped morphology. The structures were named vaults, a term that describes the morphology of the particles that contain multiple arches reminiscent of the vaulted ceilings in cathedrals. The vault particles are identified as 13 MDa ribonucleoprotein complexes with dimensions of approximately 35 x 65 nm. In fact, vaults are the largest ribonucleoprotein particles described to date (2, 3) and are approximately threefold larger than eukaryotic ribosomes and tenfold larger than signal recognition particles (SRP) or small nuclear ribonucleoproteins (snRNPs) (4). An intriguing question is how these large particles remained undetected for so long. The reason is a technical one as pointed out by Rome *et al.* (5). The commonly used stains for electron microscopy, the heavy metal salts osmium tetroxide and uranyl acetate, have a high affinity for charged components of membranes and nucleic acids, but particles like vaults with a high protein content and a relatively low amount of RNA are stained poorly. This results in nearly invisible vault particles when cells are examined by transmission electron microscopy using these positive stains. Vaults could only be visualized after purification and a negative staining procedure (Fig. 1.1A). Structures with similar dimensions and morphology have been detected in numerous eukaryotic species as diverse as mammals, avians, amphibians, fish, echinoderms, mollusks, the slime mold *Dictyostelium discoideum* and protozoa (2, 5). Nevertheless, vaults are probably not an essential and integral part of the eukaryotic cell in general, as they were not detected in *Saccharomyces cerevisia*e (6), *Caenorhabditis elegans*, *Drosophila melanogaster* and the plant *Arabidopsis thaliana*. At least, no clear vault protein orthologs could be detected in the genomes of these organisms.

**Vault components**

Analysis of vaults from mammals revealed that the complex contains at least four distinct components (1); three high molecular weight proteins and several small untranslated RNA molecules. A $M_r$ 100,000 protein, designated major vault protein (MVP), dominates the structure and constitutes over 70% of the molecular mass of the complex. Two additional proteins of $M_r$ 193,000 and $M_r$ 240,000 comprise the minor vault proteins. The $M_r$ 193,000 subunit was found to contain poly(ADP-ribose) polymerase (PARP) activity and was therefore named vault PARP (VPARP or p193) (7). The $M_r$ 240,000 subunit appeared to be identical to the telomerase-associated protein 1 (TEP1 or p240) (8). This vault subunit is shared with at least one other ribonucleoprotein complex, the telomerase complex. The vault RNA (vRNA) accounts for about 5% of the mass of vaults (1). A stoichiometric model has been proposed where each vault particle is composed of 96 MVP molecules, eight molecules of VPARP, two molecules of TEP1 and at least six molecules of vault RNA (9). It was noted that the high molar frequency of MVP relative to the minor vault proteins is
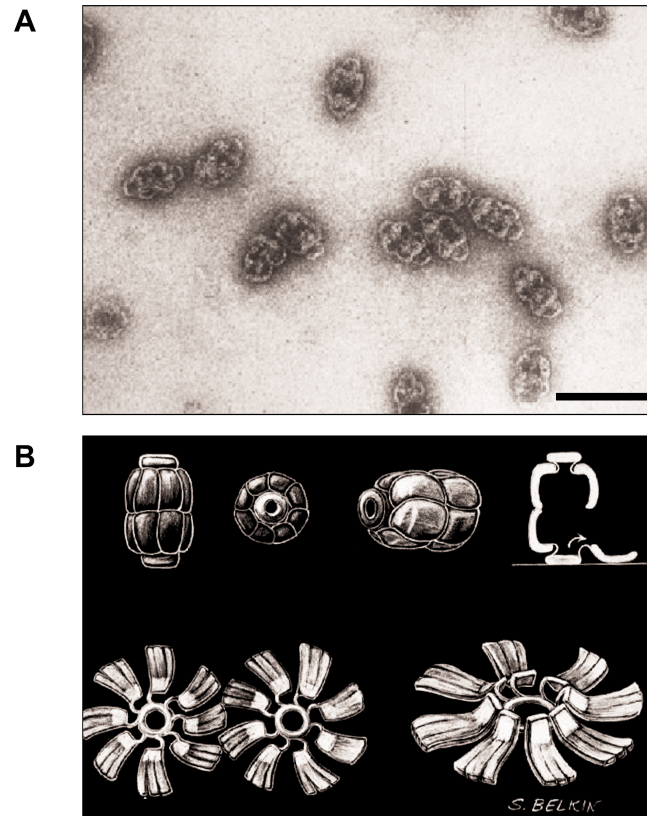
Figure 1.1. **Electron micrograph of vault particles and early vault model.** A, Electron micrograph of purified rat liver vault particles negatively stained with uranyl acetate. Bar corresponds to 100 nm. B, Early schematic model of the vault complex showing its barrel-like structure, which can fold open into two eight-petaled flower-like structures. The proposed stochiometry predicts each petal to be composed of six MVP molecules. The caps of the vault particle, in this model depicted as the ring holding the MVP petals together, were suggested to consist of the minor vault proteins and vRNA. Figures reproduced from the Journal of Cell Biology (1986) 103: 699-709 and Journal of Cell Biology (1991) 112: 225-235 by copyright permission of the Rockefeller University Press.

unlike the composition of other ribonucleoproteins, but is reminiscent to coated vesicle composition or the molecular redundancy observed in cytoskeletal structures, like microtubules and stress fibers, or in certain viruses. An interesting hypothesis - although as of yet unsubstantiated - is that vaults may have originated from a viral endosymbiont (10).

*The major vault protein*
Following the cloning of the *MVP* cDNA from *Dictyostelium discoideum* and rat (11, 12), MVP orthologs were identified in numerous species (13-15). The primary sequence of the various MVPs reveals a high degree of conservation, with an overall identity of ~90% between mammalian MVPs and a considerable identity (~60%) of mammalian MVPs with MVPs from most lower eukaryotes. Comparison of the murine and human *MVP* genes indicated that also the genomic organization, including promoter elements, is highly conserved (15). The human gene for *MVP*, located on chromosome 16p13.1-p11.2 (16), is differentially expressed resulting in high MVP levels in lung, liver and intestines and relatively low levels in skeletal muscle and brain. Two alternative human splice variants have been described. An alternative splice acceptor site at the 3' end of the first intron results in a longer MVP transcript with an additional open reading frame upstream the regular initiation codon. The extra open reading frame may repress MVP translation and regulate MVP expression (17, 18). However, such an alternative splice event does not seem to occur in mice (15).

Several distinct structural domains were identified within the human major vault protein (Fig. 1.2). First, a long $\alpha$-helical domain near its C-terminus (amino acid 652-800) forms a coiled coil structure (19, 20). In a yeast-based two-hybrid system, the coiled coil domain was found to be responsible for the interaction between MVP molecules and therefore essential for vault formation (20). Deletion or partial deletion of the coiled coil completely abolished the interaction (Chapter 4). A coiled coil domain is present in all MVPs known, stressing the importance of this domain. Second, the N-terminal half of MVP contains at least five degenerated 45-50 amino acid repeats. Within this repeat structure two, and possibly three, calcium-binding EF-hands could be distinguished (amino acid 118-283). EF-hands are composed of two $\alpha$-helices separated by a loop structure that consists of about 12 amino acids, which are involved in the binding of calcium (21). *In vitro* the major vault protein was able to bind calcium, in particular its N-terminal half (20, Chapter 4). Preliminary experiments indicated that calcium was necessary for the folding and assembly of MVP molecules into complete vault particles. Very recently, the tumor suppressor PTEN was found to interact with MVP and intact vaults (22). Analysis of the interaction of MVP with PTEN in a two-hybrid setting mapped the interaction domain to amino acids 113-171 of MVP, which encompassed two EF hands. Interestingly, *in vitro* binding experiments revealed that the association between MVP and PTEN required calcium.

*Vault poly(ADP-ribose) polymerase*
The $M_r$ 193,000 minor vault protein VPARP was originally identified through its interaction with MVP in a yeast-based two-hybrid system (7) and comprises an integral part of the vault complex. However, its subcellular distribution only partly overlaps with that of MVP, as shown in biochemical fractionation and immunofluorescence experiments (7, 23). A non-vault associated fraction of VPARP
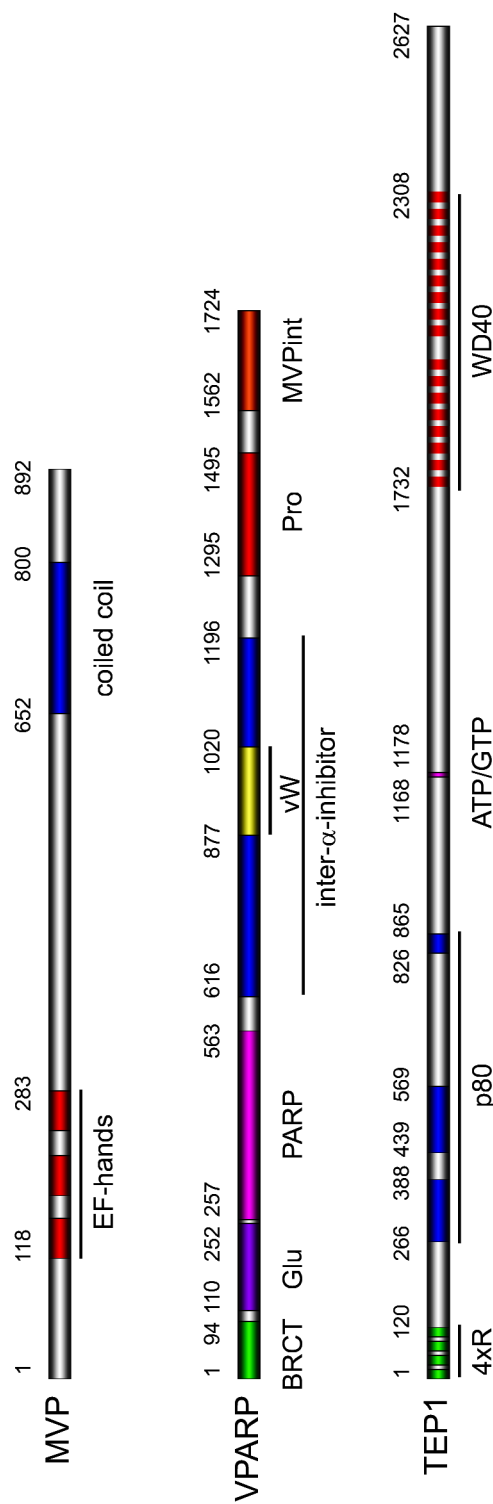
Figure 1.2. **Architecture of the human vault proteins.** Schematic representation of the three vault proteins: the major vault protein (MVP); the vault poly(ADP-ribose) polymerase (VPARP) and the telomerase-associated protein (TEP1). Indicated in different colors are protein domains with a putative functional and/or structural significance. MVP contains a degenerated repeat structure consisting of five stretches of approximately 50 amino acids. In at least three repeats putative calcium binding EF-hands could be distinguished. A conserved coiled coil domain is present in the C-terminal half of all MVPs described to date. In VPARP a BRCT, PARP, Von Willebrand (vW), inter-α-inhibitor domain and a region that interacts with MVP are indicated. In addition, a glutamate acid (Glu) and a proline (Pro) rich domain could be identified. TEP1 contains a small domain consisting of four 30 amino acid repeats (4xR) at its N-terminus. In its C-terminal half a WD40 repeat structure is present. Furthermore, there is a region homologous to the *Tetrahymena* p80 telomerase protein (p80) and an ATP/GTP binding motif. The numbers correspond to the amino acid residues marking the start and end of the various domains.

15

is present in the cytoplasm and nucleus. In mitotic cells VPARP was found associated with the mitotic spindle (7). It is not yet clear if the non-vault associated VPARP fulfils a completely separate function unrelated to vaults or whether there is a functional linkage.

The gene for VPARP is located on human chromosome 13q11 (24) and is heterogeneously expressed in human tissues with the highest level of VPARP transcripts detectable in kidney. The human VPARP, also referred to as PH5P (25) and ADPRTL1 (24), contains a region of about 300 amino acids (amino acid 257-563) that exhibits a 28% sequence identity with the catalytic domain of poly(ADP-ribose) polymerase (PARP1). It was demonstrated that VPARP catalyzes the ADP-ribosylation of itself and to a lesser extent of MVP (7). Although the significance of VPARP activity for vault function is not yet known, it is interesting to note that assembled vault particles retain this enzymatic activity. Poly ADP-ribosylation of proteins is a reversible post-translational modification that plays a significant role in the maintenance of genomic DNA stability (for review see Smith *et al.* (26)). So far, seven additional proteins with PARP activity have been described (27). The prototype of this family is PARP1, which is a nuclear protein that binds to single or double strand DNA breaks. Upon binding, PARP1 activates its catalytic domain that transfers ADP-ribose groups from $NAD^+$ to itself and to proteins involved in maintenance of chromatin structure and DNA metabolism. The resulting delay in DNA replication permits the cell to recruit DNA repair enzymes to the site of the DNA break (28, 29). Also other members of the PARP family are involved in DNA repair (PARP2), whereas others act as telomere length regulators, like tankyrase 1 and 2. The identification and characterization of additional VPARP substrates may shed a light on VPARP and/or vault function.

Several protein domains can be distinguished in the human VPARP that relate to its PARP activity and interaction with other vault components (Fig. 1.2). A region located at the N-terminal side of the catalytic PARP domain is rich in glutamic acid residues (amino acid 110-252), and may serve as an auto-modification site, analogous to sequences in PARP1. The presence of a BRCA1 C-terminus (BRCT) domain (amino acid 1-94) at the N-terminus of VPARP is another similarity between VPARP and PARP1. The BRCT domain (30, 31) in PARP1 is separated from the catalytic domain by ~145 amino acids, similar to the distance that separates these two domains in VPARP (7, 32). Notably, the BRCT domain was first discovered in the BRCA1 genes and was found to define a superfamily of cell cycle checkpoint-DNA damage response proteins. The BRCT domain is considered to be important for protein-protein interactions (33). Nevertheless, it does not seem to play a role in the assembly of vault particles, since in a yeast two-hybrid system no interactions were found between the BRCT domain and the other vault proteins (20, Chapter 4). Instead, a domain at its C-terminus (amino acid 1562-1724) was found to mediate the association of VPARP with the N-terminal half of MVP (7, 20, Chapter 4). The proline-rich region (amino

acid 1295-1495) at the N-terminal side of the MVP-interaction domain may serve as a flexible joint between the interacting domain and the enzymatically active part of VPARP. VPARP also contains a domain (amino acid 616-1196) that is common in a plasma glycoprotein family, the inter-α-inhibitor family (25). Most inter-α-inhibitor family members are made up of so-called heavy chains with one bikunin chain that harbors two protease inhibitory domains of the Kunitz type (34). They all harbor a domain of about 160 residues in length, which is similar to a Von Willebrand type A domain (32, 35). Von Willebrand type A domains (amino acid 877-1020 of VPARP) are widespread in adhesive proteins and receptors (35). This suggests a heterophillic binding capacity of VPARP for a polypeptide target.

*Telomerase-associated protein 1*
The $M_r$ 240,000 minor vault protein was shown to be identical to the mammalian telomerase-associated protein 1 (TEP1). Although, it was demonstrated that TEP1 specifically interacts with the telomerase RNA (36, 37), the role of TEP1 within the telomerase complex is not yet clear. Telomerase activity is not dependent on TEP1, as it can be reconstituted *in vitro* with just the catalytic protein subunit TERT and the telomerase RNA (38-40). Furthermore, the disruption of the murine gene encoding *TEP1* did not result in a changed telomere length and telomerase activity (41). The human *TEP1* gene was mapped by immunofluorescence *in situ* hybridization (FISH) to chromosome 14q11.2 (42). Using a yeast based three-hybrid system it was shown that amino acid 1-871 of the murine TEP1 specifically associate with human vRNAs (8), analogous to its binding of telomerase RNA. No telomerase RNA could be detected within the vault complex and vaults do not contain telomerase activity (8). Possibly, the binding of either vRNA or telomerase RNA determines whether TEP1 associates with vaults or with the telomerase complex.

In the C-terminal part of TEP1 an extensive WD40 repeat structure is found (amino acid 1732-2308) encompassing 16 WD40 repeats. Such repeats are known for their ability to form β-propeller structures (43, 44), which are versatile protein-protein interaction domains. Molecular modeling of the WD40 repeats of TEP1 into a β-propeller resulted in a model that fitted the eight-fold symmetry of the vault complex (9). It was hypothesized that the TEP1 WD40 repeats imposed the observed symmetry on the vault complex. This theory was discarded when eight-fold symmetric vault particles were isolated from *TEP1* knockout tissues. The N-terminus of TEP1 contains four repeats of 30 amino acids whose function is still unknown. Furthermore, an ATP/GTP binding motif (WALKER A domain) was identified at amino acids 1168-1178, implying that TEP1 function requires energy. A detailed two-hybrid analysis was unable to map amino acid stretches in TEP1 that mediate the binding to the other vault proteins (Chapter 4). Even co-expression of vRNA (hvg1), whose association with TEP1 may modulate its structure and interacting capabilities, failed to identify an association. Possibly several interacting vault proteins, complete vault structures and/or other proteins are necessary for TEP1 to bind vaults.

*Vault RNA*

The vault RNA constitutes less than 5% of the mass of the complex and is believed to be a functional rather than a structural component, as degradation of the vRNA did not affect the vault morphology (1, 9, 10, 45). The vault RNA has a species-specific length ranging from 86 to 141 bases and the number of vRNAs expressed in various organisms differs. Rats and mice only express a single vRNA of 141 bases, whereas bullfrogs (*Rana catesbeiana*) express two vRNA species of 89 and 94 bases. Interestingly, humans harbor three related vRNAs (hvg1, hvg2 and hvg3) of 98, 88 and 88 bases, respectively. The hvg genes are arranged in a triple repeat structure on chromosome 5, a situation that probably arose through gene duplication. The exact reason for the existence of multiple vRNAs in some species is unknown. One may speculate however that the functional range of the relatively long rodent vRNA is covered by multiple smaller vRNAs in other species. In all vRNAs the typical internal polymerase III promoter elements are highly conserved. Furthermore, all vRNAs are predicted to fold into similar stem-loop structures (45). An intriguing observation, with respect to the function of the vRNAs, is the association of the vRNAs with the vault complex in several human cancer cell lines. It was shown that all three human vRNAs are bound to the vault complex, but not in a ratio that reflected their expression levels (Chapter 5). Apparently, the individual human vRNAs have different affinities for TEP1. The bulk of vRNA associated with vaults was hvg1 and only small amounts of hvg2 and hvg3 could be detected. Interestingly, in at least three multidrug resistant cell lines consistently more hvg3 was found associated with the vaults compared to their drug sensitive counterparts (46, Chapter 5). This suggests that the ratio in which vRNA species are associated to vaults may be of functional significance.

**Vault structure**

The structure of the vault complex was examined by various electron microscopical techniques (3, 9, 10). Quantitative scanning transmission electron microscopy showed that vault particles contain two centers of mass (10). Open and closed forms of the vault complex were observed using freeze etch techniques. The open forms resembling flower-like structures, in which eight rectangular petals are joined to a central ring. These flower-like structures were usually seen in pairs, suggesting that an intact vault particle consist of two folded flowers (Fig. 1.1B). It is unclear whether vaults can unfold and refold in this fashion *in vivo*. A more detailed structural vault model was generated using a cryo-electron microscopy image reconstruction technique (reviewed by Stewart *et al.* (47)). Basically, isolated vault particles were quickly frozen in liquid ethane and subsequently viewed by transmission electron microscopy. Images of individual vaults in various orientations were captured and by combining multiple images a high-resolution three-dimensional model could be generated (Fig. 1.3). Striking features of the 31 Å resolution vault-model are the smooth surface of the complex, the barrel-shaped mid-section and the two protruding caps (3, 9). The barrel has an invaginated waist of 380 Å in diameter and the two caps have a maximum

diameter of 240 Å. The thickness of the walls of the hollow complex is about 20-52 Å and the cavity (~5 x $10^7$ Å$^3$) is spacious enough to enclose particles as large as ribosomes. In fact, often the cryo-electron micrographs showed extra density within the central barrel-shaped cavity of the vaults implying the presence of a cargo inside the vault (3). Note that in order to internalize or release large macromolecular cargoes vaults would have to open up.

The particle reconstruction technique was also used to map the location of individual vault components within the complex. When RNase-treated and untreated vaults were compared, it was shown that the vRNAs are located in the tip of the cap structures (9, 10). Analysis of vault particles isolated from *TEP1* knockout livers initially showed normal vault particles (48) displaying the characteristic eight-fold symmetry. However, a close examination showed a reduced electron density at the extreme ends of both cap structures, similar as observed in RNase-treated vaults. This is in agreement with a role for TEP1 in vRNA binding. The precise position of VPARP within the vault complex is currently under investigation, but it is thought to be located in the caps as well.

The initial idea that the barrel-shaped midsection consisted of MVP molecules and that the caps were completely composed of the minor vault proteins and vRNAs was abandoned when rat MVP was expressed in insect cells (Sf9), which do not contain endogenous vault particles or vault proteins (49). Surprisingly, the expression of MVP alone resulted in the formation of particles that had the biochemical characteristics (e.g. behavior in a sucrose gradient) of normal vaults. They display the distinct vault-like morphology, including the protruding caps. The caps were only a bit misshapen and distorted.

Although the vault model implies a static structure, little or no information is available on the rigidity and dynamics of the vault particles and its components *in vivo*. For example, do vaults exchange subunits or are they present in a disassembled state in the cells ready to be assembled when needed? There are some observations reported in the literature suggesting that vaults *in vivo* are less rigid than the vaults isolated by differential and velocity sucrose gradient centrifugation. First, vaults isolated from *Dictyostelium* amoebae seem to display more variability in shape and integrity (6). Second, in purified vault preparations from rat liver the vRNA component is usually well protected against degradation by RNases, whereas in a crude microsmal extract containing vaults, vRNA is easily degraded (6).

**Intracellular localization of vaults**

The number of vaults per cell has been estimated to be as many as 10,000 to 100,000 copies (50). The majority of these reside in the cytoplasm where they interact with cytoskeletal elements. Co-localization of vaults with the ends of actin stress fibers was reported in stationary rat fibroblasts (51) and in the tips of differentiated rat

**A**



**B**
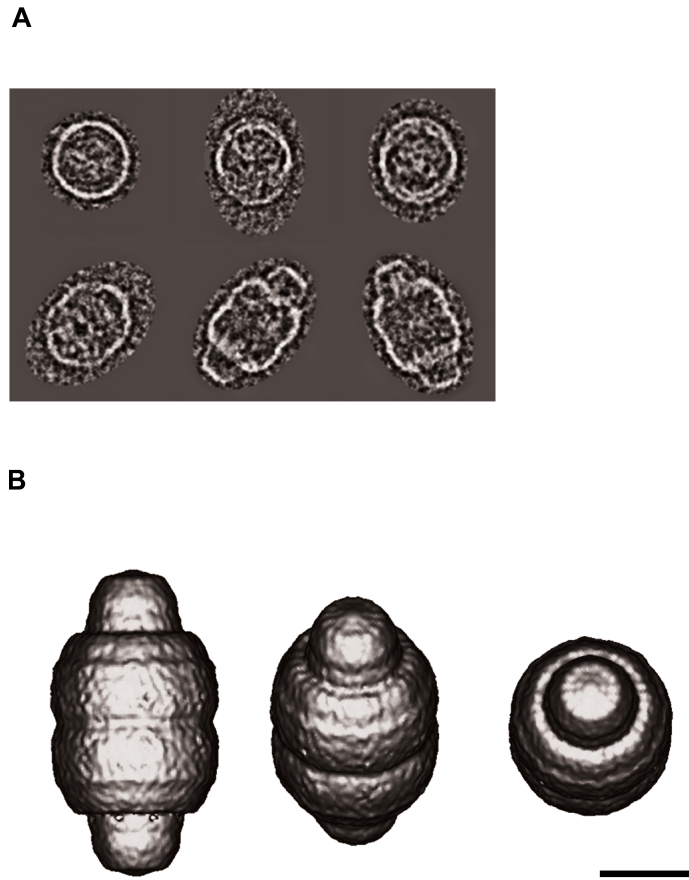


Figure 1.3. **Reconstruction of the vault complex at a 31 Å resolution.** A, Cryo-electron microscopy images showing individual vault particles in different orientations. B, Single-particle reconstruction techniques were used to generate a three-dimensional model of the vault complex. The combination of more than 1300 images resulted in the depicted vault model at a 31 Å resolution. Bar corresponds to 100 Å. Figures reproduced from Kong *et al.* (1999) Structure 7: 371-379 with permission from Elsevier Science.

phaeochromocytoma (PC12) cells (52). Likewise, vaults were found in close association with microtubules in PC12, chinese hamster ovary (CHO) and non-small cell lung carcinoma cells (52-54, Chapter 3). Moreover, in sea urchin eggs vaults were *in vitro* co-purified with microtubules and ribosomes through several cycles of polymerization and depolymerization (53). Next to the cytoskeleton association, several groups reported an association of vaults with the nucleus in particular the nucleoli, the nuclear membrane and/or the nuclear pore complex (53, 55, 56). However, in general less than 5% of the total vault fraction is found associated with the nucleus in mammalian cells.

**The function of vaults**

Despite the characterization of individual vault components and the development of a detailed structural model in recent years, the cellular function of vaults has still not been elucidated. Based on the subcellular localization and the typical hollow barrel-like structure of the complex, a role in intracellular transport has been proposed by several investigators. The partial co-localization of vaults with cytoskeletal elements may indicate that vaults are transported along the cytoskeleton or that vaults are involved in cytoskeletal maintenance. Supporting evidence for vault mediated cytoskeletal transport comes from studies in the electric ray *Torpedo* in which vaults were shown to be transported within axons between soma and nerve terminals (57, 58). Immunoelectron microscopical analysis revealed a close association of vaults and synaptic vesicles in the nerve terminals of the electric organ. It was hypothesized that material that has to be secreted associates with vaults and is transported via microtubules to the synaptic vesicles (19). Cytoskeletal mediated transport would enable vaults to directionally shuttle cargo from and to specific cellular locations. However, to convincingly demonstrate the existence of such a transport system additional studies are necessary addressing vault dynamics, for instance by investigating the effects of actin and microtubule-affecting drugs, the energy dependence of transport and the involvement of molecular motors.

The idea of vaults taking part in a nucleo-cytoplasmic transport route was based on observations in rat fibroblasts in which part of the vaults were found to be associated with the nuclear membrane often in close proximity to the nuclear pore complex (55). The initial suggestion that vaults were in fact the elusive central plugs is probably not correct. The central plug is now generally being regarded as material in transit through the nuclear pore rather than as a separate physical entity (see for example Stoffler *et al.* (59)). The observations made by Chugani *et al.* (55) may represent vaults docking at the cytoplasmic site of the nuclear pore complex in order to take up or give off cargo. A possible cargo might be ribosomes, since MVP was co-purified with ribosomes in developing sea urchin embryos. Furthermore, Abbondanza *et al.* (56) found that MVP co-immunoprecipitated with the human estrogen receptor and that treatment of cells with estradiol increases the level of MVP associated with estrogen receptor in nuclear extracts. The putative vault cargoes do not necessarily have to be inside vault complex, but may also be stuck to the outside of the complex.

*Vaults and multidrug resistance*

The molecular identification of the lung resistance-related protein (LRP) as the human MVP linked the vault complex to multidrug resistance (MDR) (60). LRP was originally found to be overexpressed in a non-small cell lung cancer cell line selected for doxorubicin resistance that did not overexpress P-glycoprotein (61). In subsequent studies it was found that MVP/vaults were overexpressed in many human tumor cell lines characterized by a MDR phenotype (23, 50, 62-64). Moreover, MVP expression

closely reflected known chemoresistant characteristics in a broad panel of unselected tumor cell lines and untreated clinical cancers of different histogenetic origins (61, 63, 64). A number of clinical studies identified MVP as an independent prognostic factor for poor response to chemotherapy in various malignancies (see for review Scheffer *et al.* (65)). In favor of a role for vaults in cellular detoxification is the fact that MVP is highly expressed in tissues that are chronically exposed to elevated levels of xenobiotoics (e.g. bronchus epithelium), metabolic active tissue (e.g. adrenal cortex) and macrophages (63).

Based on its putative transport function as well as the drug handling and cellular distribution of fluorescent anthracyclines in vault expressing cell lines, it was postulated that vaults act by transporting drugs away from their subcellular targets. Evidence supporting a role for vaults in the extrusion of anthracyclines from the nuclei of resistant cells came from the group of Akiyama (66-68). Treatment of the colon carcinoma cell line (SW620) with sodium butyrate induced vault expression and resulted in cells resistant to various cytostatic drugs. Expression of MVP-specific ribozymes led to the reversion of this drug resistance phenotype (67, 68). Furthermore, isolated nuclei incubated with doxorubicin in the presence of anti-(MVP) antibodies retained more drug compared to the nuclei that were not treated with the antibodies. These experiments suggest that MVP/vaults are directly involved in drug transport and as such contribute to the MDR phenotype. By contrast, expression of MVP stably transfected in the ovarian carcinoma cell line A2780 led to increased numbers of vault particles, but failed to confer drug resistance to etoposide, doxorubicin and vincristine (60, 62). Siva *et al.* conclude that vaults may be necessary, but are not sufficient for drug resistance.

**Knockout models**

Several researchers attempted to determine the significance of vaults for cellular homeostasis and development by generating knockout models. In *Dictyostelium*, unlike the situation found in other organisms, three different but related *MVP* genes are present that code for MVPA, MVPB and MVPC of $M_r$ 94,000, 92,000 and 92,000, respectively (11, 13). Disruption of two (*MVPA* and *MVPB*) of the three *MVP* genes impedes growth under nutritional stress, suggesting a role for vaults in fundamental processes such as proliferation and cell survival. In mammals, the situation is different as single genes code for the vault proteins. To date, two knockout models have been generated in which either *MVP* or *TEP1* has been disrupted (41, 48, 69). In both instances the mice were viable and healthy, breed normally and did not display obvious abnormalities. No distinguishable vault particles could be detected in *MVP* knockout tissues. In addition, the levels of the remaining vault components are dramatically reduced by the absence of MVP (Chapter 6). By contrast, vault particles were still present in *TEP1* knockout tissues but it was demonstrated that these were not only devoid of TEP1 but also of vRNA. It was found that TEP1 is required for a stable

association of the vault RNA with the vault complex (48). Recently, the generation of a *VPARP* knockout model was announced at a meeting (27). Although the characterization of this model has not yet been reported, the mice are viable.

The *MVP* knockout mouse has been exploited to test some of the proposed vault functions in particular the involvement of vaults in multidrug resistance and in the development and/or function of dendritic cells. The sensitivity of MVP deficient cells to a panel of cytostatic agents was determined. It was found that both embryonic stem cells as well as bone marrow cells did not show an increased sensitivity to these drugs when compared to wild-type cells (69). The activities of the multidrug resistance related transporters P-glycoprotein, MRP1 and BCRP1 were not altered in vault deficient cells ruling out the possibility that these proteins compensate for the loss of vaults. The *in vivo* toxicity of doxorubicin in *MVP* knockout mice was also examined. Both knockout and control mice responded similarly to the drug treatment. It was concluded that - at least in mice - vaults are not directly involved in drug resistance. Recently, it was reported that MVP is upregulated during the development of human dendritic cells (70). Moreover, the presence of MVP specific antibodies, presumably interfering with the function of MVP or vaults, resulted in reduced expression levels of dendritic cell markers and co-stimulatory molecules and a decreased capacity to induce T-cell proliferative and IFN-γ releasing responses. However, in the *MVP* knockout mice the development and function of dendritic cells, derived from mononuclear bone marrow cells, appeared normal (71). In addition, *in vivo* immunization assays showed that neither the T-cell mediated immune response nor the T-cell dependent humoral response were affected by the disruption of *MVP*, indicating intact antigen presenting and migration capacities of the dendritic cells.

**Aims and outline of the thesis**

This study aims at gaining a better understanding of the biogenesis, dynamics and interaction with other cellular components of mammalian vaults; particularly in view of a role of this ribonucleoprotein particle in intracellular transport.

In the first part (Chapters 2 and 3) attention is focused on the dynamics and intracellular localization of the vault complex. Chapter 2 deals with the dynamics of the vault complex and its ability to assemble into highly regular tube-like structures under certain conditions and Chapter 3 describes the interaction of vaults with microtubules. The second part (Chapters 4-6) addresses various structural aspects of vaults. Chapter 4 is concerned with the identification of various domains in the three vault proteins with emphasis on protein-protein interactions. Chapter 5 describes the expression and association of the vault RNA in relation to a suggested function of vaults in multidrug resistance. Chapter 6 reports that the absence of the major vault protein in cells and tissues of *MVP* knockout mice severely affects the stability of the remaining vault components VPARP, TEP1 and vault RNA. In Chapter 7 the

involvement of vaults in the efflux and sequestration of anthracyclines and as such their contribution to resistance to these drugs is studied. Finally, Chapter 8 gives a general discussion of the work presented in this thesis.

## References

1.      Kedersha, N. L. and Rome, L. H. Isolation and characterization of a novel ribonucleoprotein particle: large structures contain a single species of small RNA. J Cell Biol, 103: 699-709, 1986.

2.      Kedersha, N. L., Miquel, M. C., Bittner, D., and Rome, L. H. Vaults. II. Ribonucleoprotein structures are highly conserved among higher and lower eukaryotes. J Cell Biol, 110: 895-901, 1990.

3.      Kong, L. B., Siva, A. C., Rome, L. H., and Stewart, P. L. Structure of the vault, a ubiquitous celular component. Structure Fold Des, 7: 371-379, 1999.

4.      Batey, R. T., Rambo, R. P., Lucast, L., Rha, B., and Doudna, J. A. Crystal structure of the ribonucleoprotein core of the signal recognition particle. Science, 287: 1232-1239, 2000.

5.      Rome, L., Kedersha, N., and Chugani, D. Unlocking vaults: organelles in search of a function. Trends in Cell Biol, 1: 47-50, 1991.

6.      Kickhoefer, V. A., Vasu, S. K., and Rome, L. H. Vaults are the answer, what is the question? Trends in Cell Biol, 6: 174-178, 1996.

7.      Kickhoefer, V. A., Siva, A. C., Kedersha, N. L., Inman, E. M., Ruland, C., Streuli, M., and Rome, L. H. The 193-kD vault protein, VPARP, is a novel poly(ADP-ribose) polymerase. J Cell Biol, 146: 917-928, 1999.

8.      Kickhoefer, V. A., Stephen, A. G., Harrington, L., Robinson, M. O., and Rome, L. H. Vaults and telomerase share a common subunit, TEP1. J Biol Chem, 274: 32712-32717, 1999.

9.      Kong, L. B., Siva, A. C., Kickhoefer, V. A., Rome, L. H., and Stewart, P. L. RNA location and modeling of a WD40 repeat domain within the vault. Rna, 6: 890-900, 2000.

10.     Kedersha, N. L., Heuser, J. E., Chugani, D. C., and Rome, L. H. Vaults. III. Vault ribonucleoprotein particles open into flower-like structures with octagonal symmetry. J Cell Biol, 112: 225-235, 1991.

11.     Vasu, S. K., Kedersha, N. L., and Rome, L. H. cDNA cloning and disruption of the major vault protein alpha gene (mvpA) in Dictyostelium discoideum. J Biol Chem, 268: 15356-15360, 1993.

12.     Kickhoefer, V. A. and Rome, L. H. The sequence of a cDNA encoding the major vault protein from Rattus norvegicus. Gene, 151: 257-260, 1994.

13.     Vasu, S. K. and Rome, L. H. Dictyostelium vaults: disruption of the major proteins reveals growth and morphological defects and uncovers a new associated protein. J Biol Chem, 270: 16588-16594, 1995.

14.     Herrmann, C., Zimmermann, H., and Volknandt, W. Analysis of a cDNA encoding the major vault protein from the electric ray Discopyge ommata. Gene, 188: 85-90, 1997.

15.     Mossink, M., van Zon, A., Fränzel-Luiten, E., Schoester, M., Scheffer, G., Scheper, R., Sonneveld, P., and Wiemer, E. The genomic sequence of the murine major vault protein and its promoter. Gene, 294: 225, 2002.

16. Slovak, M. L., Ho, J. P., Cole, S. P., Deeley, R. G., Greenberger, L., de Vries, E. G., Broxterman, H. J., Scheffer, G. L., and Scheper, R. J. The LRP gene encoding a major vault protein associated with drug resistance maps proximal to MRP on chromosome 16: evidence that chromosome breakage plays a key role in MRP or LRP gene amplification. Cancer Res, 55: 4214-4219, 1995.

17. Lange, C., Walther, W., Schwabe, H., and Stein, U. Cloning and initial analysis of the human multidrug resistance-related MVP/LRP gene promoter. Biochem Biophys Res Commun, 278: 125-133, 2000.

18. Holzmann, K., Ambrosch, I., Elbling, L., Micksche, M., and Berger, W. A small upstream open reading frame causes inhibition of human major vault protein expression from a ubiquitous mRNA splice variant. FEBS Lett, 494: 99-104, 2001.

19. Herrmann, C., Kellner, R., and Volknandt, W. Major vault protein of electric ray is a phosphoprotein. Neurochem Res, 23: 39-46, 1998.

20. van Zon, A., Mossink, M. H., Schoester, M., Scheffer, G. L., Scheper, R. J., Sonneveld, P., and Wiemer, E. A. Structural domains of vault proteins: a role for the coiled coil domain in vault assembly. Biochem Biophys Res Commun, 291: 535-541, 2002.

21. Moncrief, N. D., Kretsinger, R. H., and Goodman, M. Evolution of EF-hand calcium-modulated proteins. I. Relationships based on amino acid sequences. J Mol Evol, 30: 522-562, 1990.

22. Yu, Z., Fotouhi-Aroakani, N., Wu, L., Maoui, M., Wang, S., Banville, D., and Shen, S. H. PTEN Associates with the vault particles in Hela cells. J Biol Chem, 277:40247-40252, 2002.

23. Schroeijers, A. B., Siva, A. C., Scheffer, G. L., de Jong, M. C., Bolick, S. C., Dukers, D. F., Slootstra, J. W., Meloen, R. H., Wiemer, E., Kickhoefer, V. A., Rome, L. H., and Scheper, R. J. The $M_r$ 193,000 vault protein is up-regulated in multidrug-resistant cancer cell lines. Cancer Res, 60: 1104-1110, 2000.

24. Still, I. H., Vince, P., and Cowell, J. K. Identification of a novel gene (ADPRTL1) encoding a potential Poly(ADP- ribosyl)transferase protein. Genomics, 62: 533-536, 1999.

25. Jean, L., Risler, J. L., Nagase, T., Coulouarn, C., Nomura, N., and Salier, J. P. The nuclear protein PH5P of the inter-alpha-inhibitor superfamily: a missing link between poly(ADP-ribose)polymerase and the inter-alpha-inhibitor family and a novel actor of DNA repair? FEBS Lett, 446: 6-8, 1999.

26. Smith, S. The world according to PARP. Trends Biochem Sci, 26: 174-179, 2001.

27. Shall, S. Poly (ADP-ribosylation)--a common control process? Bioessays, 24: 197-201, 2002.

28. de Murcia, G. and Menissier de Murcia, J. Poly(ADP-ribose) polymerase: a molecular nick-sensor. Trends Biochem Sci, 19: 172-176, 1994.

29. D'Amours, D., Desnoyers, S., D'Silva, I., and Poirier, G. G. Poly(ADP-ribosyl)ation reactions in the regulation of nuclear functions. Biochem J, 342:

249-268, 1999.

30. Callebaut, I. and Mornon, J. P. From BRCA1 to RAP1: a widespread BRCT module closely associated with DNA repair. FEBS Lett, 400: 25-30, 1997.

31. Koonin, E. V., Altschul, S. F., and Bork, P. BRCA1 protein products ... Functional motifs... [letter]. Nat Genet, 13: 266-268, 1996.

32. Bork, P., Hofmann, K., Bucher, P., Neuwald, A. F., Altschul, S. F., and Koonin, E. V. A superfamily of conserved domains in DNA damage-responsive cell cycle checkpoint proteins. Faseb J, 11: 68-76, 1997.

33. Zhang, X., Morera, S., Bates, P. A., Whitehead, P. C., Coffer, A. I., Hainbucher, K., Nash, R. A., Sternberg, M. J., Lindahl, T., and Freemont, P. S. Structure of an XRCC1 BRCT domain: a new protein-protein interaction module. Embo J, 17: 6404-6411, 1998.

34. Salier, J. P., Rouet, P., Raguenez, G., and Daveau, M. The inter-alpha-inhibitor family: from structure to regulation. Biochem J, 315: 1-9, 1996.

35. Bork, P. and Rohde, K. More von Willebrand factor type A domains? Sequence similarities with malaria thrombospondin-related anonymous protein, dihydropyridine- sensitive calcium channel and inter-alpha-trypsin inhibitor. Biochem J, 279: 908-910, 1991.

36. Harrington, L., McPhail, T., Mar, V., Zhou, W., Oulton, R., Bass, M. B., Arruda, I., and Robinson, M. O. A mammalian telomerase-associated protein [see comments]. Science, 275: 973-977, 1997.

37. Nakayama, J., Saito, M., Nakamura, H., Matsuura, A., and Ishikawa, F. TLP1: a gene encoding a protein component of mammalian telomerase is a novel member of WD repeats family. Cell, 88: 875-884, 1997.

38. Beattie, T. L., Zhou, W., Robinson, M. O., and Harrington, L. Polymerization defects within human telomerase are distinct from telomerase RNA and TEP1 binding. Mol Biol Cell, 11: 3329-3340, 2000.

39. Weinrich, S. L., Pruzan, R., Ma, L., Ouellette, M., Tesmer, V. M., Holt, S. E., Bodnar, A. G., Lichtsteiner, S., Kim, N. W., Trager, J. B., Taylor, R. D., Carlos, R., Andrews, W. H., Wright, W. E., Shay, J. W., Harley, C. B., and Morin, G. B. Reconstitution of human telomerase with the template RNA component hTR and the catalytic protein subunit hTRT. Nat Genet, 17: 498-502, 1997.

40. Koyanagi, Y., Kobayashi, D., Yajima, T., Asanuma, K., Kimura, T., Sato, T., Kida, T., Yagihashi, A., Kameshima, H., and Watanabe, N. Telomerase activity is down regulated via decreases in hTERT mRNA but not TEP1 mRNA or hTERC during the differentiation of leukemic cells. Anticancer Res, 20: 773-778, 2000.

41. Liu, Y., Snow, B. E., Hande, M. P., Baerlocher, G., Kickhoefer, V. A., Yeung, D., Wakeham, A., Itie, A., Siderovski, D. P., Lansdorp, P. M., Robinson, M. O., and Harrington, L. Telomerase-associated protein TEP1 is not essential for telomerase activity or telomere length maintenance *in vivo*. Mol Cell Biol, 20: 8178-8184, 2000.

42. Saito, T., Matsuda, Y., Suzuki, T., Hayashi, A., Yuan, X., Saito, M., Nakayama,

J., Hori, T., and Ishikawa, F. Comparative gene mapping of the human and mouse TEP1 genes, which encode one protein component of telomerases. Genomics, 46: 46-50, 1997.

43.     Neer, E. J., Schmidt, C. J., Nambudripad, R., and Smith, T. F. The ancient regulatory-protein family of WD-repeat proteins [published erratum appears in Nature 1994 Oct 27;371(6500):812]. Nature, 371: 297-300, 1994.

44.     Smith, T. F., Gaitatzes, C., Saxena, K., and Neer, E. J. The WD repeat: a common architecture for diverse functions. Trends Biochem Sci, 24: 181-185, 1999.

45.     Kickhoefer, V. A., Searles, R. P., Kedersha, N. L., Garber, M. E., Johnson, D. L., and Rome, L. H. Vault ribonucleoprotein particles from rat and bullfrog contain a related small RNA that is transcribed by RNA polymerase III. J Biol Chem, 268: 7868-7873, 1993.

46.     van Zon, A., Mossink, M. H., Schoester, M., Scheffer, G. L., Scheper, R. J., Sonneveld, P., and Wiemer, E. A. Multiple human vault RNAs. Expression and association with the vault complex. J Biol Chem, 276: 37715-37721, 2001.

47.     Stewart, P. L., Chiu, C. Y., Haley, D. A., Kong, L. B., and Schlessman, J. L. Review: resolution issues in single-particle reconstruction. J Struct Biol, 128: 58-64, 1999.

48.     Kickhoefer, V. A., Liu, Y., Kong, L. B., Snow, B. E., Stewart, P. L., Harrington, L., and Rome, L. H. The Telomerase/Vault-associated Protein TEP1 Is Required for Vault RNA Stability and Its Association with the Vault Particle. J Cell Biol, 152: 157-164, 2001.

49.     Stephen, A. G., Raval-Fernandes, S., Huynh, T., Torres, M., Kickhoefer, V. A., and Rome, L. H. Assembly of vault-like particles in insect cells expressing only the major vault protein. J Biol Chem, 276: 23217-23220, 2001.

50.     Kickhoefer, V. A., Rajavel, K. S., Scheffer, G. L., Dalton, W. S., Scheper, R. J., and Rome, L. H. Vaults are up-regulated in multidrug-resistant cancer cell lines. J Biol Chem, 273: 8971-8974, 1998.

51.     Kedersha, N. L. and Rome, L. H. Vaults: large cytoplasmic RNP's that associate with cytoskeletal elements. Mol Biol Rep, 14: 121-122, 1990.

52.     Herrmann, C., Golkaramnay, E., Inman, E., Rome, L., and Volknandt, W. Recombinant major vault protein is targeted to neuritic tips of PC12 cells. J Cell Biol, 144: 1163-1172, 1999.

53.     Hamill, D. R. and Suprenant, K. A. Characterization of the sea urchin major vault protein: a possible role for vault ribonucleoprotein particles in nucleocytoplasmic transport. Dev Biol, 190: 117-128, 1997.

54.     Berger, W., Elbling, L., and Micksche, M. Expression of the major vault protein LRP in human non-small-cell lung cancer cells: activation by short-term exposure to antineoplastic drugs. Int J Cancer, 88: 293-300, 2000.

55.     Chugani, D. C., Rome, L. H., and Kedersha, N. L. Evidence that vault ribonucleoprotein particles localize to the nuclear pore complex. J Cell Sci, 106: 23-29, 1993.

56. Abbondanza, C., Rossi, V., Roscigno, A., Gallo, L., Belsito, A., Piluso, G., Medici, N., Nigro, V., Molinari, A. M., Moncharmont, B., and Puca, G. A. Interaction of vault particles with estrogen receptor in the MCF-7 breast cancer cell. J Cell Biol, 141: 1301-1310, 1998.

57. Li, J. Y., Volknandt, W., Dahlstrom, A., Herrmann, C., Blasi, J., Das, B., and Zimmermann, H. Axonal transport of ribonucleoprotein particles (vaults). Neuroscience, 91: 1055-1065, 1999.

58. Herrmann, C., Volknandt, W., Wittich, B., Kellner, R., and Zimmermann, H. The major vault protein (MVP100) is contained in cholinergic nerve terminals of electric ray electric organ. J Biol Chem, 271: 13908-13915, 1996.

59. Stoffler, D, Fahrenkrog, B., and Aebi, U. The nuclear pore complex: from molecular architecture to functional dynamics. Curr Opin Cell Biol, 11: 391-401, 1999.

60. Scheffer, G. L., Wijngaard, P. L., Flens, M. J., Izquierdo, M. A., Slovak, M. L., Pinedo, H. M., Meijer, C. J., Clevers, H. C., and Scheper, R. J. The drug resistance-related protein LRP is the human major vault protein. Nat Med, 1: 578-582, 1995.

61. Scheper, R. J., Broxterman, H. J., Scheffer, G. L., Kaaijk, P., Dalton, W. S., van Heijningen, T. H., van Kalken, C. K., Slovak, M. L., de Vries, E. G., van der Valk, P., and *et al.* Overexpression of a M(r) 110,000 vesicular protein in non-P- glycoprotein-mediated multidrug resistance. Cancer Res, 53: 1475-1479, 1993.

62. Siva, A. C., Raval-Fernandes, S., Stephen, A. G., LaFemina, M. J., Scheper, R. J., Kickhoefer, V. A., and Rome, L. H. Up-regulation of vaults may be necessary but not sufficient for multidrug resistance. Int J Cancer, 92: 195-202, 2001.

63. Izquierdo, M. A., Scheffer, G. L., Flens, M. J., Giaccone, G., Broxterman, H. J., Meijer, C. J., van der Valk, P., and Scheper, R. J. Broad distribution of the multidrug resistance-related vault lung resistance protein in normal human tissues and tumors. Am J Pathol, 148: 877-887, 1996.

64. Izquierdo, M. A., Shoemaker, R. H., Flens, M. J., Scheffer, G. L., Wu, L., Prather, T. R., and Scheper, R. J. Overlapping phenotypes of multidrug resistance among panels of human cancer-cell lines. Int J Cancer, 65: 230-237, 1996.

65. Scheffer, G. L., Schroeijers, A. B., Izquierdo, M. A., Wiemer, E. A., and Scheper, R. J. Lung resistance-related protein/major vault protein and vaults in multidrug-resistant cancer. Curr Opin Oncol, 12: 550-556, 2000.

66. Ohno, N., Tani, A., Uozumi, K., Hanada, S., Furukawa, T., Akiba, S., Sumizawa, T., Utsunomiya, A., Arima, T., and Akiyama, S. Expression of functional lung resistance--related protein predicts poor outcome in adult T-cell leukemia. Blood, 98: 1160-1165, 2001.

67. Kitazono, M., Okumura, H., Ikeda, R., Sumizawa, T., Furukawa, T., Nagayama, S., Seto, K., Aikou, T., and Akiyama, S. Reversal of LRP-associated drug resistance in colon carcinoma SW-620 cells. Int J Cancer, 91: 126-131, 2001.

68. Kitazono, M., Sumizawa, T., Takebayashi, Y., Chen, Z. S., Furukawa, T., Nagayama, S., Tani, A., Takao, S., Aikou, T., and Akiyama, S. Multidrug resistance and the lung resistance-related protein in human colon carcinoma SW-620 cells [see comments]. J Natl Cancer Inst, 91: 1647-1653, 1999.

69. Mossink, M. H., Van Zon, A., Fränzel-Luiten, E., Schoester, M., Kickhoefer, V. A., Scheffer, G. L., Scheper, R. J., Sonneveld, P., and Wiemer, E. A. Disruption of the Murine Major Vault Protein (MVP/LRP) Gene Does Not Induce Hypersensitivity to Cytostatics. Cancer Res, 62: 7298-7304, 2002.

70. Schroeijers, A. B., Reurs, A. W., Scheffer, G. L., Stam, A. G., de Jong, M. C., Rustemeyer, T., Wiemer, E. A., de Gruijl, T. D., and Scheper, R. J. Up-regulation of drug resistance-related vaults during dendritic cell development. J Immunol, 168: 1572-1578, 2002.

71. Mossink, M. H., De Groot, J., Van Zon, A., Fränzel-Luiten, E., Schoester, M., Scheffer, R. J., Sonneveld, G. L., Scheper, P., and Wiemer, E. A. Unimpaired dendritic cell functions in *MVP/LRP* knockout mice. Immunology, 110: 58-65, 2003.

CHAPTER 2

The formation of vault-tubes:
A dynamic interaction between vaults
and VPARP

*Chapter 2*

**Abstract**

Vaults are barrel-shaped cytoplasmic ribonucleoprotein particles that are composed of a major vault protein (MVP), two minor vault proteins (TEP1, VPARP) and small untranslated RNA molecules. Not all expressed TEP1 and VPARP in cells is bound to vaults. TEP1 is known to associate with the telomerase complex whereas VPARP is also present in the nuclear matrix and in cytoplasmic clusters (VPARP-rods). We examined the subcellular localization and the dynamics of the vault complex in a non-small cell lung cancer cell line expressing MVP tagged with green fluorescent protein. Using quantitative FRAP it was demonstrated that vaults move temperature independently by diffusion. It was noted however that incubation at room temperature (21°C) resulted in the formation of distinct tube-like structures in the cytoplasm. Raising the temperature could reverse this process. When the vault-tubes were formed, there were fewer or no VPARP-rods present in the cytoplasm, suggesting an incorporation of the VPARP into the vault-tubes. MVP molecules have to interact with each other via their coiled coil domain in order to form vault-tubes. Furthermore, the stability of microtubules influenced the efficiency of vault-tube formation at 21°C. The dynamics and structure of the tubes were examined using confocal microscopy. Our data indicate a direct and dynamic relationship between vaults and VPARP, providing further clues to unravel the function of vaults.

**Introduction**

Vaults are the largest ribonucleoprotein particles described to date. They were named for their typical lobular morphology, which is reminiscent of the vaulted ceilings in cathedrals (1). Mammalian vaults are composed of multiple copies of three different proteins (p240, p193 and p100) and several small untranslated RNA molecules of 88-141 bases. The vault components assemble into a 13 MDa hollow barrel-like structure of about 35 x 65 nm (2, 3) that is predominantly localized in the cytoplasm. Nevertheless, a small part (~5%) of MVP is consistently associated with the nucleus (4, 5). Although the cellular function of vaults is still unknown, their subcellular localization and distinct morphology point to a role for vaults in intracellular, particularly nucleo-cytoplasmic, transport (4-11). It was noted that vaults are frequently upregulated in multidrug resistant cell lines and tumors of different histogenetic origin. Furthermore, they are highly expressed in tissues exposed to xenobiotics. It has been suggested that vaults function in cellular detoxification processes by transporting harmful agents from their cellular targets (for review see Scheffer *et al.* (12)).

The p100 subunit or major vault protein (MVP) constitutes over 70% of the molecular mass of vaults and is the main determinant of the vault structure (13). Interaction between MVP molecules is mediated by the coiled coil domain present in the C-terminal half of the protein (14, Chapter 4). The p240 protein is identical to the telomerase-associated protein 1 (TEP1) and appears to be shared between at least two ribonucleoprotein complexes i.e. vaults and the telomerase complex (15, 16). TEP1 is capable of binding vault RNA and is required for the overall stability and stable association of the vault RNA with the vault complex (17). The vault RNA itself is thought to be a functional vault component rather than a structural one (3, 18, 19). The p193 protein or VPARP exhibits a poly(ADP-ribose) polymerase activity and can poly(ADP-ribosylate) MVP and, to a lesser extent, itself (20). Whether there are other substrates for VPARP is presently unknown. VPARP is a member of a growing family of enzymes, which include PARP1 and tankyrase (21, 22). Although having a similarity of 29 - 60% between their PARP domains, the PARP proteins in general do not resemble each other outside the PARP domain, suggesting they have separate cellular functions. Unique features of VPARP are a BRCA1 C-terminus (BRCT) domain (aa 1-94) and an inter-$\alpha$-inhibitor domain (aa 616-1195); both may be involved in protein-protein interactions. The C-terminus of VPARP (aa 1562-1724) has been shown to associate with the N-terminal part of MVP (14, 20, Chapter 4). Immunofluorescence and biochemical fractionation studies clearly indicate that not all VPARP is bound to vaults; VPARP is also present in the nuclear matrix and in distinct cytoplasmic clusters (20, 23 and this manuscript). It is not clear whether VPARP fulfils separate functions - unrelated to vault function - in its non-vault associated form.

Although the vault components and structure have been characterized in detail, little is known about the intracellular distribution and mobility of vaults *in vivo* and their relation to non-vault associated minor vault proteins. To visualize the vault complex, we fused green fluorescent protein to the major vault protein. Bleaching experiments demonstrated that vaults in the cytoplasm move temperature independently by diffusion. However, incubation of cells at 21°C resulted in the formation of highly regular and dynamic vault-tubes. We present evidence for a role of the cytoplasmic non-vault associated VPARP-rods in vault-tube formation.
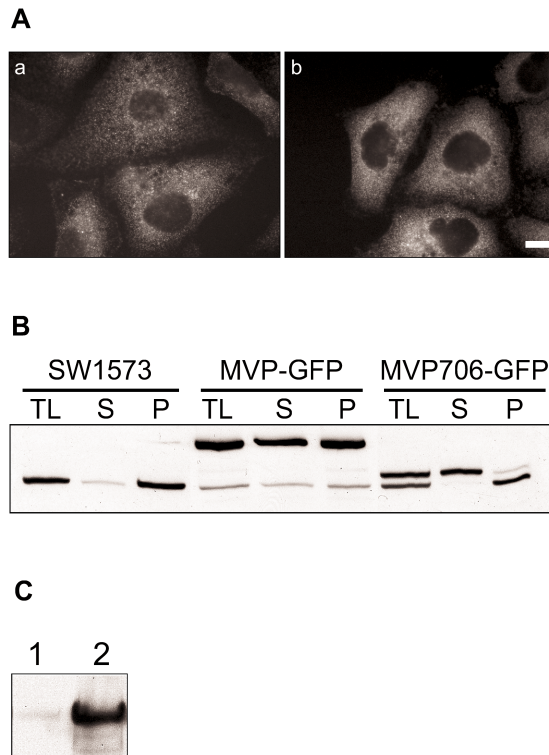
**A**



**B**



**C**



Figure 2.1. **Incorporation of GFP-tagged MVP molecules in vaults.** A, The SW1573 transfectant expressing MVP-GFP (*a*) was examined by fluorescence microscopy. The cell line SW1573 (*b*) was processed for indirect immunofluorescence and stained with anti-(MVP) (LRP-56). Bar corresponds to 10 μm. B, Vault particles were pelleted from a total cell lysate (TL) of SW1573, SW1573/MVP-GFP transfectants and SW1573 transfectants expressing a GFP-tagged truncated MVP (SW1573/MVP706-GFP) by a 100,000 x *g* centrifugation step. Immunoblotting using rabbit polyclonal anti-(MVP) was performed to determine the presence of MVP and the GFP-fusion proteins in the resulting pellet (P) and supernatant (S) fractions. Note that SW1573/MVP-GFP and SW1573/MVP706-GFP show two bands, representing endogenous (lower band) and GFP-tagged MVP or truncated MVP (upper band). C, Immunoblot analysis showing the presence of the minor vault protein VPARP in immunoprecipitates obtained from MVP-GFP transfectants using anti-(GFP) (lane 2). Lane 1 contains control immunoprecipitates in which a polyclonal rabbit pre-immune serum was used.

**Materials and methods**

*Cell lines and culture conditions*
The following human cell lines were used: the cervix epitheloid carcinoma cell line HeLa, the non-small cell lung carcinoma cell line SW1573 and its doxorubicin selected multidrug resistant (MDR) variant SW1573/2R120 (24). The cell line SW1573 was transfected with a construct encoding a C-terminal GFP tagged MVP or truncated MVP (aa 1-706); the resulting cell lines were named SW1573/MVP-GFP and SW1573/MVP706-GFP. All cell lines were maintained in DMEM (Life technologies, Paisley, Scotland), supplemented with 10% (vol/vol) fetal calf serum, 1 mM pyruvate, 100 U/ml penicillin and 100 µg/ml streptomycin (Life Technologies, Paisley, Scotland) at 37°C under an atmosphere containing 5% $CO_2$. The drug resistant cell line, SW1573/2R120, was cultured in the presence of 120 nM doxorubicin. The transfected cell lines were cultured in medium containing 200 µg/ml of G-418 (Life Technologies, Paisley, Scotland).

*GFP tagged MVP, MVP deletion constructs and transfection*
An expression construct was generated by cloning the full-length human MVP cDNA in frame to the 5' end of the enhanced green fluorescent protein coding sequence. Full-length MVP cDNA cloned in pBS-KSII was used as a PCR template with the following primers: forward primer 5'-CCCAAGCTTGTCACCATGGCAACTGA-AGAG and reverse primer 5'-CGGGATCCCGCAGTACAGGCACCACGTGG introducing a *Hind*III and *Bam*HI restriction site to facilitate cloning in pEGFP-N1 (Clonetech laboratories Inc., Palo Alto, USA). The PCR conditions were as follows: 95°C for 2 minutes, then 35 cycles of 95°C for 30 seconds, 58°C for 1 minute and 72°C for 3 minutes followed by 72°C for 10 minutes using *Pfu* DNA polymerase (Stratagene, La Jolla, CA). The amplified DNA fragments were size fractionated by agarose gel electrophoresis, isolated and extracted from agarose gel and ligated into pCR-Blunt (Invitrogen, Carlsbad, CA). The MVP fragments were released from the vector by digestion with the appropriate restriction enzymes and subsequently cloned into the GFP expression vector. A cDNA fragment of human MVP encoding amino acid 1-706 was amplified by standard PCR using 5'-CCCAAGCTTGTCACCATG-GCAACTGAAGAG as a forward primer and 5'-CCGGATCCTCCAAAAGTT-CCTTGCGAGC as reverse primer. To prevent PCR artifacts we used *Pfu* polymerase combined with a low number of PCR cycli. Amplified fragments containing appropriate restriction sites were cloned in pZeroblunt (Invitrogen, Carlsbad, CA). Subsequently, the *Hind*III-*Bam*HI MVP fragments were cloned in the *Hind*III and *Bam*HI digested and dephosphorylated vector pEGFP-N1 (Clontech, Palo Alto, CA). The resulting expression plasmid MVP706-GFP expresses GFP fused to a MVP truncated at its C-terminal end. Transfection of the SW1573 cell line was performed by calcium-phosphate precipitation as described previously (25). Approximately 48 hours after transfection, transfectants were selected by addition of 800 µg/ml of G-
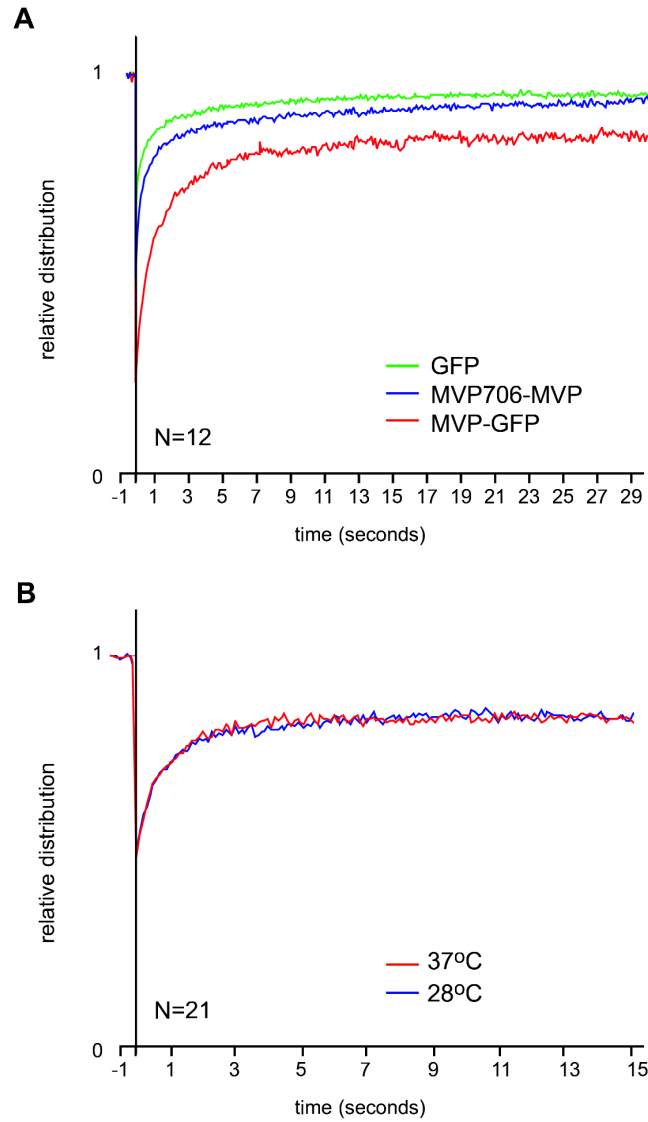
Figure 2.2. **Dynamics of the vault complex measured by FRAP.** A, The graph shows the mobility of fluorescent MVP-GFP (red line) compared to free GFP (green line) and a GFP-tagged truncated MVP that is not incorporated into vaults (MVP706-GFP, blue line), each measured in 12 cells. Fluorescence intensity prior to the bleach pulse was set at 1. Note that the recovery of fluorescence is never 100% due to removal of fluorescence by the bleach pulse that differs between proteins depending on their residence time in the strip during bleaching. B, The redistribution of fluorescent MVP-GFP within a bleached strip was monitored at 37°C (red line) and at 28°C (blue line) with intervals of 100 milliseconds. The graph depicts the data of an experiment in which 21 cells were measured.

418. The G-418 resistant and GFP expressing cells were isolated using a fluorescence activated cell sorter (FACS) and cultured in the presence of 200 μg/ml G-418.

*Antibodies*
The mouse monoclonal anti-(VPARP) (mAb p193-4), mouse monoclonal anti-(MVP) (LRP-56) and the rabbit polyclonal anti-(MVP) were generated as described previously (23). The mouse monoclonal anti-(β-tubulin) and a species-specific isotype antibody were purchased from the Sigma-Aldrich Corporation (St. Louis, MO) and the rabbit polyclonal anti-(GFP) was purchased at Clonetech Laboratories Inc. (Palo Alto, CA). Species-specific anti-(Ig) antibodies conjugated to tetramethyl rhodamine isothiocyanate (TRITC), fluorescein isothiocyanate (FITC) or horseradish peroxidase (HRP) were obtained from Jackson ImmunoResearch Laboratories Inc. (West Grove, PA).

*Immunoprecipitation, cell fractionation, SDS-PAGE and Western blot analysis*
Antibodies were coupled to Protein A-Sepharose beads (Amersham Pharmacia Biotech, Uppsala, Sweden) according to the recommendations of the manufacturer. Immunoprecipitations from protein lysates prepared in lysis buffer (50 mM Tris-Cl pH 7.4, 1.5 mM $MgCl_2$, 75 mM NaCl, 0.5% (vol/vol) Nonidet P-40), supplemented with a proteinase inhibitor cocktail (Complete™, Roche, Mannheim, FRG), were carried out for two hours at 4°C. Subsequently, the beads were washed with lysis buffer and twice with PBS after which the beads were suspended in protein sample buffer. Immunoprecipitated proteins were analyzed by SDS-PAGE and Western blotting. A cellular fraction, enriched for vaults, was prepared as follows: cells were harvested and resuspended in lysis buffer supplemented with a proteinase inhibitor cocktail. All subsequent steps were performed at 4°C. The cell lysate was incubated on ice for 5 minutes and cleared from nuclei by centrifugation for 20 minutes at 20,000 x *g*. The supernatant was centrifuged at 100,000 x *g* for 90 minutes, resulting in a pellet fraction enriched for vaults. Equal portions of the resulting supernatant and pellet fraction were subjected to SDS-PAGE after which the size-fractionated proteins were transferred to nitrocellulose. Remaining protein binding sites on Western blots were blocked by TBST (50 mM Tris-Cl pH 7.5, 100 mM NaCl, 0.05% (vol/vol) Tween 20) containing 5% (wt/vol) non-fat dry milk (Bio-Rad Laboratories, Hercules, CA). Consecutively, primary and secondary antibody incubations were carried out in the same buffer. Immune-complexes were detected using the BM Chemiluminescence Blotting Substrate (POD) kit (Roche, Mannheim, FRG) and visualized on Hyperfilm™ ECL™ (Amersham Pharmacia Biotech, Uppsala, Sweden).

*Fluorescence microscopy*
Cells were grown on poly-L-lysine coated coverslips after which they were fixed with 3% (vol/vol) formaldehyde in PBS for 20 minutes. Subsequently, the cells were permeabilized by 1% (vol/vol) Triton-X100 in PBS for 5 minutes. The remaining protein binding sites were blocked with 1% (wt/vol) BSA in PBS for 30 minutes.

Primary and secondary antibody incubations were performed in the same buffer for 60 minutes at room temperature (21°C) using 25 µg/ml p193.4 mAb, 10 µg/ml LRP-56 and FITC or TRITC conjugated goat anti-(mouse Ig) in a dilution as recommended by the manufacturer. Between each antibody incubation step the coverslips were washed six times in PBS. Coverslips were mounted on microscope slides in anti-fade (4% (wt/vol) n-propyl gallate in glycerol) or VectaShield mounting medium (Vector Laboratories, Inc., Burlingame, CA). The fluorescent staining pattern was studied using a Leica DMRXA microscope and pictures were created using Leica QFish version V 2.3e.

*Confocal microscopy and Fluorescence Recovery After Photobleaching (FRAP)*
A Zeiss (Jena, FRG) confocal laser-scanning microscope (CLSM) equipped with a thermostatted stage was used for confocal microscopy and FRAP experiments. Excitation illumination was by an argon ion laser at 488 nm. Images were taken at a lateral resolution of 102 nm using a 40X 1.3 n.a. objective. To determine cytoplasmic mobility of vaults, a 2 µm wide strip spanning the width of the cytoplasm was bleached by a short bleach pulse (200 milliseconds) at relatively high laser intensity. Subsequently, fluorescence intensity was monitored within the bleached strip at 100 milliseconds intervals. The relative fluorescence intensity data was then fitted to diffusion curves obtained by Monte Carlo computer simulation of diffusion, immobile fraction and binding time in an ellipsoid representing the cytoplasm with a sphere inside where the molecules cannot go (representing the nucleus) (26). To determine the dynamics of protein associated with vault-tubes, the laser beam was focused in the center of a vault-tube and the region in the beam was bleached for 4 seconds (at relatively low laser power). Fluorescence redistribution was followed in time.

**Results**

*GFP-tagged MVP proteins are incorporated into intact vaults*
In order to investigate the subcellular distribution and dynamics of the vault complex, GFP was fused to the C-terminus (MVP-GFP) of MVP. The subcellular distribution of the GFP fusion protein expressed in the non-small cell lung carcinoma cell line SW1573 was examined by fluorescence microscopy. A particulate MVP-GFP fluorescence was distributed through the cytoplasm with a denser staining in the perinuclear region (Fig. 2.1A, *a*). The fluorescent pattern was similar to the localization of MVP in untransfected cells as detected by immunofluorescence using a mouse monoclonal anti-(MVP) (Fig. 2.1A, *b*). Incubation using an isotype control antibody confirmed the specificity of the fluorescent signal (data not shown). To verify whether the expressed GFP fusion protein is actually incorporated into intact vault particles, we used differential centrifugation. Vault particles have enough mass to be pelleted from a crude cell lysate in a 100,000 x *g* centrifugation step. The GFP fusion protein was partly recovered in the 100,000 x *g* pellet fraction, together with endogenous MVP (Fig. 2.1B). The ratio of GFP-tagged MVP versus endogenous MVP in the pellet (P)
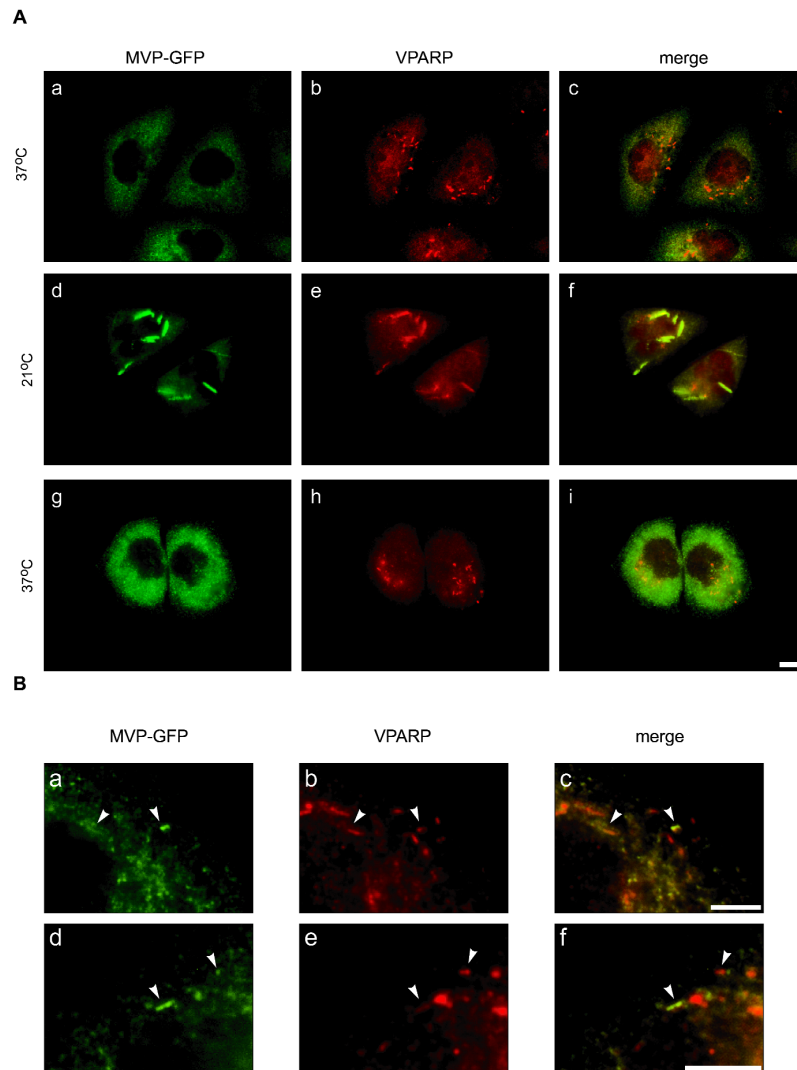
**A**



**B**



Figure 2.3. **Formation of vault-tubes.** A, SW1573/MVP-GFP cells were incubated at 37°C (*a–c*), at 21°C for 60 minutes (*d-f*) and at 37°C for 30 minutes after the treatment at 21°C (*g–i*). Shown is the MVP-GFP fluorescent signal (*a,d,g*), the indirect immunofluorescence staining for VPARP (*b,e,h*) and the merged images (*c,f,I*). Incubation at 21°C resulted in the formation of large cytoplasmic, tube-like structures (vault-tubes, *d*). Under the same conditions VPARP staining reveals a dramatic decrease in the number of non-vault associated VPARP-rods. The VPARP signal almost completely colocalizes with the tube structures (*e* and *f*). Both the MVP and VPARP distribution returns to normal when the cells cultured at 21°C were placed at 37°C for 30 minutes (*g–i*). Bar corresponds to 10 μm. B, Partial colocalization of GFP-tagged MVP (*a* and *d*) and the VPARP-rods (*b* and *e*) in the merged picture (*c* and *f*) after incubation of SW1573/MVP-GFP cells at 21°C for 10 minutes. The arrowheads point to sites where MVP-GFP clusters have formed, which are in close proximity of VPARP-rods. Bars indicate 5 μm.

fraction reflects their expression levels as determined in the total lysate (TL), indicating that both proteins are equivalent in competing for incorporation into vault particles. Nevertheless, about 35-40% of both the endogenous and GFP-tagged MVP is found in the supernatant fraction. Similarly, upon fractionation of SW1573 cells part of the MVP (10-15%) was recovered in the supernatant (S). The recovery of MVP and MVP-GFP in the supernatant fraction may reflect the *in vivo* situation in which a portion of the MVP is not incorporated into complexes large enough to be pelleted at 100,000 x *g*. Alternatively, it might be a fractionation artifact. To ascertain that the MVP-GFP is incorporated in genuine vaults, we performed an immunoprecipitation with a rabbit polyclonal anti-(GFP) antiserum. The subsequent analysis of the immunoprecipitates by immunoblotting demonstrated that the minor vault protein VPARP is associated with the vaults containing MVP-GFP (Fig. 2.1C).

*Dynamics of the vault complex measured by FRAP*
We examined vault dynamics in living SW1573 cells expressing MVP-GFP using fluorescence recovery after photobleaching (FRAP). In a FRAP assay specifically suited for determination of effective diffusion coefficients ($D_{eff}$), we compared the mobility of MVP-GFP (vaults) with that of free GFP. As a control we used a SW1573 transfectant expressing a GFP-tagged deletion mutant of MVP (MVP706-GFP) that is not incorporated into vault particles as demonstrated by biochemical fractionation (Fig. 2.1B).

In the cytoplasm a narrow strip (2 μm) was bleached by a short laser pulse (200 milliseconds) at high laser intensity, after which recovery of the fluorescent signal in the strip was determined at intervals of 100 milliseconds. We observed a full recovery of both GFP and MVP-GFP fluorescence, indicating that all MVP-GFP, whether incorporated into vaults or not, is mobile (Fig. 2.2A). The diffusion coefficients were calculated from these measurements by least square fitting to curves from computer simulations in which diffusion, bound fraction and residence time were varied (see Materials and Methods and Hoogstraten *et al.* (26)). GFP molecules fitted best to a model where all molecules were mobile and had a $D_{eff}$ of 14 ± 2.4 μm$^2$/s. The MVP-GFP data also fitted best to a model where no bound fraction was present and with a $D_{eff}$ of 2 ± 0.4 μm$^2$/s the MVP-GFP molecules were much slower than free GFP. Using the effective diffusion coefficient of GFP determined in our experimental set-up, we estimated that a complex of 10-13 MDa will have a diffusion coefficient of approximately 2 μm$^2$/s. Therefore, we conclude that *in vivo* the majority of MVP-GFP molecules is incorporated into vault particles. It was noted that the effective diffusion coefficient of the mutant MVP molecules (MVP706-GFP of about 107 kDa) as determined by least square fitting to the computer simulation curves was ~13 μm$^2$/s. This value is close to that of free GFP, confirming the fact that the MVP706-GFP molecules are not incorporated into larger complexes. To check whether vault movement was dependent on temperature, FRAP measurements were performed at 37°C and 28°C. It has been reported that a relatively small decrease in temperature

(from 310 K to 301 K) has little effect on diffusion in living cells (26-28). We observed no significant difference in vault mobility in three independent experiments (Fig. 2.2B). These results indicate that the majority of vaults are freely mobile and move by diffusion.

*Redistribution of MVP-GFP into tube-like structures*
Although the diffusion of vaults was not affected at 28°C, we noticed a typical and highly consistent redistribution of the MVP-GFP fluorescence when the transfected cells were incubated at 21°C (room temperature). The characteristic particulate fluorescent pattern observed in cells expressing MVP-GFP cultured at 37°C is shown (Fig 2.3A, *a* and Fig. 2.1A, *a*). Incubation of these cells at 21°C for 30-60 minutes resulted in the appearance of elongated fluorescent structures, resembling tubes (Fig. 2.3A, *d*). These vault-tubes appeared in 50 to 80% of the cells and disappeared within 30 minutes when the temperature was raised to 37°C (Fig. 2.3A, *g*). Degrading vault-tubes seemed to break open along their longitudinal axis forming curled sheets, which eventually dissolve to give rise to the regular vault fluorescent pattern (data not shown). When SW1573/MVP-GFP cells were stained for the minor vault protein VPARP (Fig. 2.3A, *b*), the fluorescent pattern only partly overlapped with the MVP-GFP fluorescence (Fig. 2.3A, *c*). In addition to the fine particulate staining that colocalizes with MVP-GFP, VPARP is also present in the nucleus and in distinct elongated structures. These VPARP-rods are predominantly, but not exclusively, present in the perinuclear region (Fig. 2.3A, *b*).

When vault-tubes were allowed to form at 21°C, most of the cytoplasmic VPARP-rods could no longer be detected separately from the MVP-GFP fluorescence (Fig. 2.3A, *e* and *f*). This indicates that the VPARP molecules of the rods are either incorporated in the vault-tubes or that the tubes are formed at the site of the VPARP-rods. By incubating cells at 21°C for a short time (10 minutes) we were able to detect interactions between the VPARP-rods and clusters of MVP-GFP molecules (Fig. 2.3B). Vault-tubes were not yet formed, but an accumulation of GFP-tagged MVP at the VPARP-rods is observed (Fig. 2.3B). This implies a recruitment of MVP-GFP (or vaults) to the VPARP-rods, what eventually may lead to vault-tubes. Restoring the temperature to 37°C not only led to the disintegration of the vault-tubes, but also to the reappearance of the non-vault associated VPARP-rods (Fig. 2.3A, *h* and *i*).

*The subcellular localization of VPARP*
We verified the presence of VPARP-rods in different - non-transfected - cell lines. A similar subcellular distribution of VPARP - a diffuse localization in both the nucleus and cytoplasm and the presence of cytoplasmic VPARP-rods - was observed in the non-transfected SW1573 and HeLa cells (Fig. 2.4A, *a* and *b*) as well as in the drug resistant SW1573/2R120 and African green monkey kidney (COS) cells (data not shown). The specificity of the VPARP staining was confirmed by the absence of fluorescent signal when an isotype control was used (Fig. 2.4A, *c*). The length of the
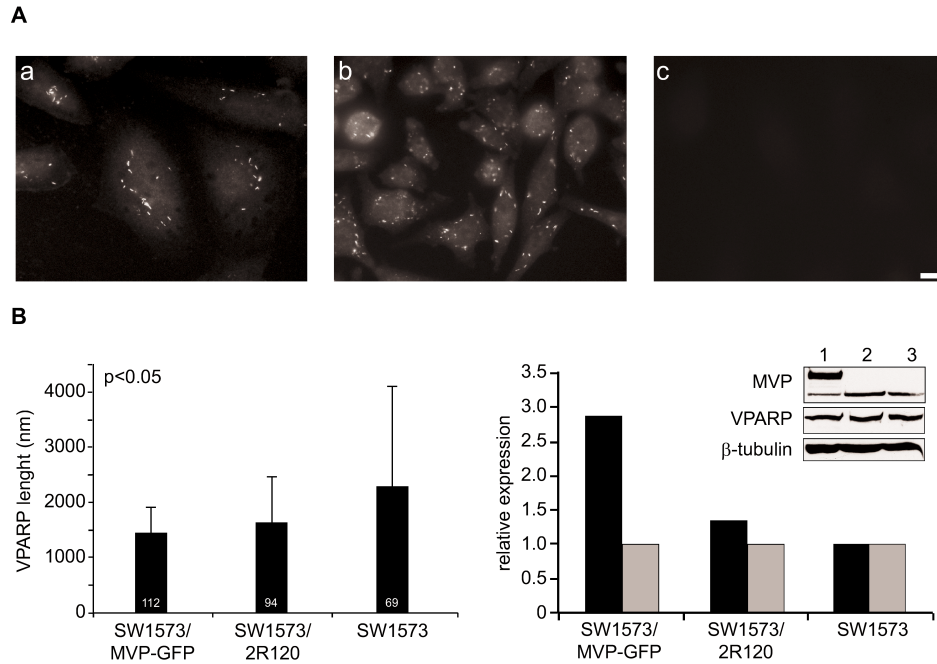
**A**



**B**



Figure 2.4. **Cytoplasmic VPARP-rods and their relation to MVP expression levels.** A, Anti-(VPARP) staining of untransfected SW1573 (*a*) and HeLa (*b*) cells showed the normal VPARP distribution, including the VPARP-rods. Background staining was absent as revealed by the staining of SW1573 cells with an isotype antibody (*c*). Bar corresponds to 10 μm. B, The left-hand graph depicts the average length of the VPARP-rods in untransfected SW1573 cells, in its vault-overexpressing drug resistant derivative SW1573/2R120 and in the SW1573/MVP-GFP transfectant. The numbers in the bars indicate the number of VPARP-rods measured. The data were analyzed by the Student's *t*-test. The P-value was in all cases below 0.05, indicating statistically significant differences. The right-hand graph shows the quantification of the MVP (black bars) and VPARP (gray bars) levels as determined by immunoblotting (see inlay; lane 1: SW1573/MVP-GFP, lane 2: SW1573/2R120 and lane 3: SW1573 with equal amounts of total protein loaded). The levels of VPARP and MVP in the SW1573 cells are arbitrarily set at 1 and corrected for loading using the β-tubulin signal as a reference. Note that the two protein bands visible in the MVP panel in lane 1 represent the endogenous MVP and the MVP-GFP fusion product.

VPARP-rods differed in a cell line dependent manner. Especially the differences in length between the parental SW1573 and the MVP-GFP transfected SW1573 pointed to a correlation between MVP expression levels and the length of the VPARP-rods. We therefore measured VPARP-rod length in SW1573 cells, its drug resistant, vault overexpressing, derivative SW1573/2R120 and the SW1573/MVP-GFP transfectant. The average length varied from 1.5 μm in SW1573/MVP-GFP to 2.3 μm in SW1573 cells (Fig. 2.4B, left-hand graph). Although the orientation of the

VPARP-rods may vary, the differences in length are significant (p<0.05), confirming our visual observations. The length of the VPARP-rods may have differed because of the differences in expression level of VPARP. Nevertheless, Western blot analysis indicated that the total levels of expressed VPARP were similar in these cell lines (Fig. 2.4B, right-hand graph). As expected, MVP was upregulated in the drug resistant cells (usually around 1.5 fold compared with the parental SW1573 cell line) and in the MVP-GFP transfectant cells (almost threefold). The size of the cytoplasmic VPARP-rods appeared to inversely correlate with the MVP expression levels.

*The coiled coil domain of MVP is necessary for vault-tube formation*
To exclude the possibility that the occurrence of vault-tubes at 21°C is due to overexpression of MVP-GFP or the addition of the GFP-tag, the formation of vault-tubes was investigated in SW1573/2R120 and parental, non-transfected, SW1573 cells (Fig. 2.5A). Vault-tubes, detected by indirect immunofluorescence, were observed in both cell lines, indicating that they are not caused by the overexpression of GFP tagged MVP. To test whether MVP-MVP interactions are necessary for vault-tube formation we used the stable SW1573 transfectant expressing a GFP-tagged deletion mutant of
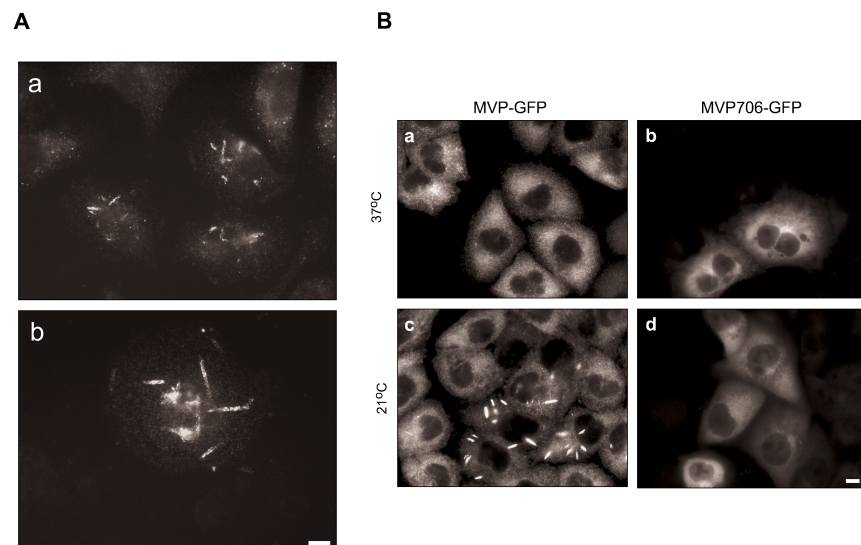


Figure 2.5. **Coiled coil domain of MVP essential for incorporation into vault-tubes.** A, Vault-tube formation, by a 60 minute incubation at 21°C, could be observed in non-transfected SW1573 (*a*) and SW1573/2R120 (*b*) cells immuno-detected with anti-(MVP) (LRP-56 mAb). Bar corresponds to 10 μm. B, Stably transfected SW1573 cells expressing either full-length MVP (*a* and *c*) or the amino acids 1-706 of MVP (*b* and *d*) fused to GFP were incubated at 21°C for 60 minutes. The GFP-tagged proteins in which a part of the coiled coil domain of MVP is deleted (MVP706-GFP) are not incorporated into vault-tubes. Bar corresponds to 10 μm.

MVP. The MVP is truncated at its C-terminal end, resulting in a partial deletion of the coiled coil domain (MVP706-GFP). The coiled coil domain at the C-terminal half of MVP is essential for the interaction of MVP molecules and consequently for the assembly of vault particles (14, Chapter 4). The deletion mutant is unable to interact with other MVP molecules and is not incorporated into vault particles (see Fig. 2.1B, Fig. 2.2A and Van Zon *et al.* (14)). Expression of the truncated fusion protein resulted in a less particulate, more diffuse, fluorescent staining pattern as compared to the full-length MVP-GFP (Fig. 2.5B, *a, b*). Incubation at 21°C led to the formation of GFP-labeled vault-tubes in control cells, but not in the coiled coil mutant (Fig. 2.5B, *c, d*). This indicates that MVP molecules have to interact with each other via their coiled coil domain in order to form vault-tubes. It is therefore probable that vault-tubes contain intact vaults.

*Dimensions and dynamics of the vault-tubes*
Confocal microscopy revealed that vault-tubes, which are formed at 21°C, are cylinders with highly regular dimensions (Fig. 2.6A). In living SW1573/MVP-GFP cells, the vault-tubes had an average length of 7 ± 2 μm (range 4.5 - 12 μm; n=16) and a width of 1.5 ± 0.3 μm (n=18). To study whether vault-tubes are stable or dynamic structures (where MVP molecules bind and release frequently), we performed fluorescence recovery after photobleaching (FRAP) experiments on these structures (Fig. 2.6B). Surprisingly, approximately 100 seconds after the laser pulse the fluorescence in the bleached area had completely recovered, indicating that the vault-tubes are dynamic structures, in which individual MVP molecules have residence times of on average 100 seconds. Attempts to quantify the fluorescent redistribution were hampered by the fact that the vault-tubes are relatively narrow and tend to move, leading to inaccurate measurements. In the current experimental set-up we cannot distinguish whether the observed exchange of fluorescence is the result of individual MVP-GFP molecules moving to and from vault-tubes or whether it represents the exchange of whole vault particles.

*Integrity of microtubules affects vault-tube formation*
Vaults have been suggested to function in cytoplasmic transport, possibly via the microtubules (8, 9). The question arises to what extent the microtubules are involved in the vault-tube formation. There are no visible differences in the β-tubulin staining in cells cultured at 37°C and 21°C, indicating no dramatic effects on the microtubules when the temperature drops to 21°C. To investigate whether microtubule destabilization or stabilization results in vault-tube formation, we treated SW1573/MVP-GFP cells with either 30 μM nocodazole or 20 μM Taxol for 60 minutes (Fig. 2.7). The depolymerization of microtubules by nocodazole did not result in vault-tube formation at 37°C nor did the taxol incubation, which stabilizes microtubules. However, when the treated cells were incubated at 21°C for 60 minutes clear differences in the amount of cells with vault-tubes were observed. Vault-tubes were observed in approximately 80% (n=608) of the nocodazole treated cells. By

contrast, 60% (n=684) of the control cells contained vault-tubes whereas only 3% (n=645) of the taxol treated cells showed vault-tube formation. Apparently the stability of the microtubules plays a significant role in tube formation at 21°C. However, destabilization or stabilization alone is not sufficient to initiate vault-tube assembly at 37°C.

**Discussion**

Vaults are large ribonucleoprotein particles that may play a role in intracellular transport; however their precise cellular function is unknown. Here, we investigated the dynamics and subcellular distribution of vaults using GFP-tagged MVP molecules expressed in non-small cell lung carcinoma cells. All experiments shown were performed with SW1573 cell expressing a C-terminal tagged MVP, however, identical results were found using a N-terminal tagged MVP fusion protein. Clearly, the outcome of the experiments was not affected by the position of the GFP-tag. At room temperature (21°C), we observed extensive rearrangements in vault distribution and dynamics leading to the formation of vault-tubes. Individual MVP molecules had to interact with each other in order to form the vault-tubes and the non-vault bound VPARP pool is used during the vault-tube formation. We therefore believe that complete vault particles are incorporated into the vault-tubes, a process that is completely reversible.

Most of our studies were performed with SW1573 cells expressing MVP tagged with GFP. Therefore, we verified that these tagged proteins are incorporated into genuine vaults. The subcellular localization and appearance of the MVP-GFP fluorescence is similar to the MVP pattern observed in immuno-stained untransfected cells. Like regular vaults, the GFP-tagged vaults can be precipitated by centrifugation at 100,000 x *g*. These biochemical fractionation data show an equal ratio of MVP and MVP-GFP in the pellet fraction compared to the total lysate. This indicates that both proteins are equivalent in competing for incorporation or assembly. In both the parental and the MVP-GFP overexpressing cell line we found a fraction of MVP/MVP-GFP in the supernatant after centrifugation. This might be an artifact of the biochemical fractionation or it may represent an *in vivo* situation in which not all MVP molecules are incorporated into vault particles. Evidence that MVP-GFP molecules are incorporated into vault particles came from the *in vivo* FRAP measurements. Although it is likely that the cytoplasmic organization (e.g. cytoskeleton, endoplasmic reticulum) affects vaults kinetics, our data indicated that the majority of MVP-GFP moved as free 10-13 MDa complexes. However, owing to the limited resolution of the microscopic methods used, we cannot completely rule out the possibility that a small fraction behaves differently. The effective diffusion coefficient of the expressed MVP-GFP was similar to the one predicted for vault complexes (see Results section), indicating that *in vivo* the majority of MVP-GFP is incorporated into vault particles. The intracellular localization of VPARP only partly overlapped with that of MVP.
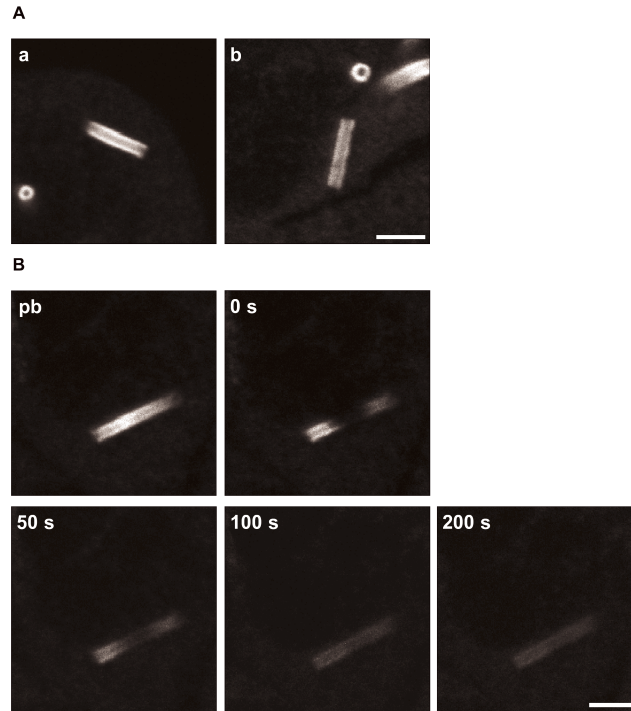
Figure 2.6. **Dimensions and dynamics of the vault-tubes.** A, Images obtained by confocal laser scan microscopy on living SW1573/MVP-GFP cells cultured at 21°C clearly show that vault-tubes are hollow cylinders. Depicted are transverse and longitudinal optical sections of the vault-tubes. Bar corresponds to 5 μm. B, Dynamics of the vault-tubes were studied with fluorescence recovery after photobleaching (FRAP). Shown are images from a representative FRAP experiment of a vault-tube before the bleach pulse (pb), directly after bleaching (0 s) and 50, 100 and 200 seconds after the bleach pulse. The rapid recovery of fluorescent staining in the bleached area indicated that vault-tubes are dynamic structures. Bar corresponds to 5 μm.

Unlike vaults, VPARP is present in the nucleus and in elongated structures in the cytoplasm (VPARP-rods). In line with TEP1, which is a shared protein with the telomerase complex (16), the non-vault associated VPARP may have separate functions independent of the vault complex. Nevertheless, our results indicate a dynamic link between the non-vault associated VPARP fraction and vault particles. First, the VPARP-rod length seems to inversely correlate with the MVP expression levels. Relatively high MVP expression levels associate with short VPARP-rods. When more MVP is present in a cell, more vault particles are formed (13, 29) and probably more VPARP is incorporated in these vaults. Consequently, less non-vault bound VPARP is present in the cell, leading to shorter VPARP-rods. Second, when vault-tubes are allowed to form at 21°C, the VPARP-rods can no longer be detected separately from the tubes. Probably, the VPARP is temporarily incorporated in the

vault-tubes. Both the localization of vaults and the VPARP-rods are reversed when the cells are again incubated at 37°C. Finally, we could detect clustering of MVP-GFP on the VPARP-rods when cells were incubated at 21°C for a short time. This indicated the existence of a true physical interaction between MVP-GFP molecules (or vaults) and the VPARP-rods.
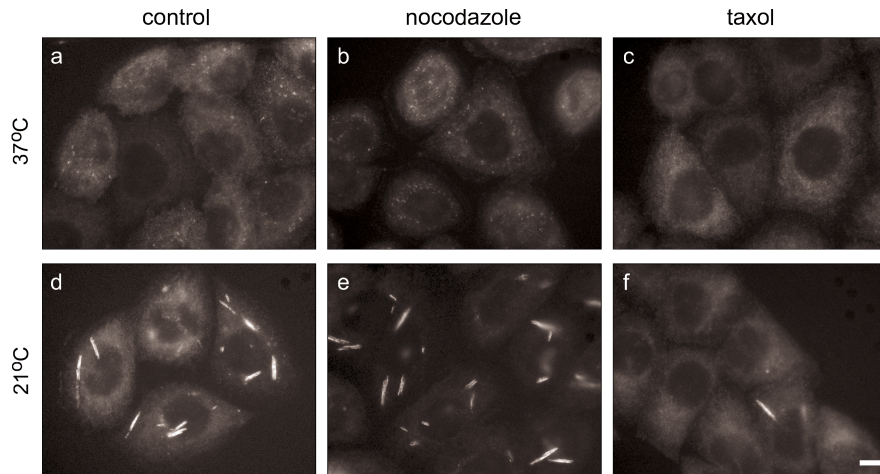


Figure 2.7. **Vault-tube formation and the stability of microtubules.** SW1573/MVP-GFP cells were cultures at 37°C for 60 minutes in the absence (*a* and *d*) or presence of 30 μM nocodazole (*b* and *e*) or 20 μM taxol (*c* and *f*). Subsequently, the cells were placed at 21°C for 60 minutes and monitored for vault-tube formation by fluorescence microscopy. Bar corresponds to 10 μm.

An intriguing question concerns the nature of the cytoplasmic VPARP-rods. In a yeast based two-hybrid system, we showed previously that VPARP is not able to interact with itself (14). Therefore, VPARP-rods probably need other proteins or structures to sustain themselves. The VPARP-rods are relatively small (2 μm x 0.5 μm) compared to the large vault-tubes (7 μm x 1.5 μm). Assuming that the vault-tube is completely covered with vaults in a standing position, one could calculate that there will be around 7,500 vault particles per micrometer of vault-tube. Probably, the symmetrical vault itself determines the morphology of the vault-tubes. It was observed *in vitro* that vaults are able to aggregate side-to-side in large pseudo-crystalline arrays (18). We showed clustering of vault particles *in vivo*, indicating that this might be a natural ability of the vault particles.

Because vault particles have been associated with intracellular transport, a function in which the microtubules may participate, we studied the involvement of the microtubules in the vault-tube formation. One scenario might be that the microtubules are damaged by the incubation at room temperature and that this may cause the vault-tubes to form, but depolymerization of the microtubules at 37°C did not result in vault-tubes. However, when the cells were incubated at room temperature

depolymerized microtubules had a stimulating effect on vault-tube formation and stabilization of the microtubules an inhibiting effect. The microtubule stability plays a role in the vault-tube formation, however other impulses are necessary to initiate vault-tube assembly. Lowering of the temperature also affects the efficiency of enzymatic reactions and may influence protein conformation. Preliminary results showed that small vault-tubes appear when cells cultured at 37°C are treated with PARP-inhibitors, like 3-aminobenzamide or DPQ (3,4-dihydro-5-[4-(1-piperidinyl) butoxy]-1(2*H*)-isoquinoline), which suggest that the inhibition of the enzymatic activity of VPARP may play a role in tube formation. Although these results are interesting, also the VPARP activity appears a small element in the complex event of the vault-tube formation.

*Chapter 2*

## References

1. Kedersha, N. L. and Rome, L. H. Isolation and characterization of a novel ribonucleoprotein particle: large structures contain a single species of small RNA. J Cell Biol, 103: 699-709, 1986.

2. Kong, L. B., Siva, A. C., Rome, L. H., and Stewart, P. L. Structure of the vault, a ubiquitous celular component. Structure Fold Des, 7: 371-379, 1999.

3. Kong, L. B., Siva, A. C., Kickhoefer, V. A., Rome, L. H., and Stewart, P. L. RNA location and modeling of a WD40 repeat domain within the vault. Rna, 6: 890-900, 2000.

4. Abbondanza, C., Rossi, V., Roscigno, A., Gallo, L., Belsito, A., Piluso, G., Medici, N., Nigro, V., Molinari, A. M., Moncharmont, B., and Puca, G. A. Interaction of vault particles with estrogen receptor in the MCF-7 breast cancer cell. J Cell Biol, 141: 1301-1310, 1998.

5. Chugani, D. C., Rome, L. H., and Kedersha, N. L. Evidence that vault ribonucleoprotein particles localize to the nuclear pore complex. J Cell Sci, 106: 23-29, 1993.

6. Li, J. Y., Volknandt, W., Dahlstrom, A., Herrmann, C., Blasi, J., Das, B., and Zimmermann, H. Axonal transport of ribonucleoprotein particles (vaults). Neuroscience, 91: 1055-1065, 1999.

7. Herrmann, C., Volknandt, W., Wittich, B., Kellner, R., and Zimmermann, H. The major vault protein (MVP100) is contained in cholinergic nerve terminals of electric ray electric organ. J Biol Chem, 271: 13908-13915, 1996.

8. Herrmann, C., Golkaramnay, E., Inman, E., Rome, L., and Volknandt, W. Recombinant major vault protein is targeted to neuritic tips of PC12 cells. J Cell Biol, 144: 1163-1172, 1999.

9. Hamill, D. R. and Suprenant, K. A. Characterization of the sea urchin major vault protein: a possible role for vault ribonucleoprotein particles in nucleocytoplasmic transport. Dev Biol, 190: 117-128, 1997.

10. Kitazono, M., Sumizawa, T., Takebayashi, Y., Chen, Z. S., Furukawa, T., Nagayama, S., Tani, A., Takao, S., Aikou, T., and Akiyama, S. Multidrug resistance and the lung resistance-related protein in human colon carcinoma SW-620 cells [see comments]. J Natl Cancer Inst, 91: 1647-1653, 1999.

11. Kitazono, M., Okumura, H., Ikeda, R., Sumizawa, T., Furukawa, T., Nagayama, S., Seto, K., Aikou, T., and Akiyama, S. Reversal of LRP-associated drug resistance in colon carcinoma SW-620 cells. Int J Cancer, 91: 126-131, 2001.

12. Scheffer, G. L., Schroeijers, A. B., Izquierdo, M. A., Wiemer, E. A., and Scheper, R. J. Lung resistance-related protein/major vault protein and vaults in multidrug-resistant cancer [In Process Citation]. Curr Opin Oncol, 12: 550-556, 2000.

13. Stephen, A. G., Raval-Fernandes, S., Huynh, T., Torres, M., Kickhoefer, V. A., and Rome, L. H. Assembly of vault-like particles in insect cells expressing only the major vault protein. J Biol Chem, 276: 23217-23220, 2001.

14. van Zon, A., Mossink, M. H., Schoester, M., Scheffer, G. L., Scheper, R. J., Sonneveld, P., and Wiemer, E. A. Structural domains of vault proteins: a role for the coiled coil domain in vault assembly. Biochem Biophys Res Commun, 291: 535-541, 2002.

15. Harrington, L., McPhail, T., Mar, V., Zhou, W., Oulton, R., Bass, M. B., Arruda, I., and Robinson, M. O. A mammalian telomerase-associated protein [see comments]. Science, 275: 973-977, 1997.

16. Kickhoefer, V. A., Stephen, A. G., Harrington, L., Robinson, M. O., and Rome, L. H. Vaults and telomerase share a common subunit, TEP1. J Biol Chem, 274: 32712-32717, 1999.

17. Kickhoefer, V. A., Liu, Y., Kong, L. B., Snow, B. E., Stewart, P. L., Harrington, L., and Rome, L. H. The Telomerase/Vault-associated Protein TEP1 Is Required for Vault RNA Stability and Its Association with the Vault Particle. J Cell Biol, 152: 157-164, 2001.

18. Kedersha, N. L., Heuser, J. E., Chugani, D. C., and Rome, L. H. Vaults. III. Vault ribonucleoprotein particles open into flower-like structures with octagonal symmetry. J Cell Biol, 112: 225-235, 1991.

19. van Zon, A., Mossink, M. H., Schoester, M., Scheffer, G. L., Scheper, R. J., Sonneveld, P., and Wiemer, E. A. Multiple human vault RNAs. Expression and association with the vault complex. J Biol Chem, 276: 37715-37721, 2001.

20. Kickhoefer, V. A., Siva, A. C., Kedersha, N. L., Inman, E. M., Ruland, C., Streuli, M., and Rome, L. H. The 193-kD vault protein, VPARP, is a novel poly(ADP-ribose) polymerase. J Cell Biol, 146: 917-928, 1999.

21. Smith, S. The world according to PARP. Trends Biochem Sci, 26: 174-179, 2001.

22. D'Amours, D., Desnoyers, S., D'Silva, I., and Poirier, G. G. Poly(ADP-ribosyl)ation reactions in the regulation of nuclear functions. Biochem J, 342: 249-268, 1999.

23. Schroeijers, A. B., Siva, A. C., Scheffer, G. L., de Jong, M. C., Bolick, S. C., Dukers, D. F., Slootstra, J. W., Meloen, R. H., Wiemer, E., Kickhoefer, V. A., Rome, L. H., and Scheper, R. J. The $M_r$ 193,000 vault protein is up-regulated in multidrug-resistant cancer cell lines. Cancer Res, 60: 1104-1110, 2000.

24. Kuiper, C. M., Broxterman, H. J., Baas, F., Schuurhuis, G. J., Haisma, H. J., Scheffer, G. L., Lankelma, J., and Pinedo, H. M. Drug transport variants without P-glycoprotein overexpression from a human squamous lung cancer cell line after selection with doxorubicin. J. Cell Pharmacol., 1: 35-41, 1990.

25. Parker, B. A. and Stark, G. R. Regulation of simian virus 40 transcription: sensitive analysis of the RNA species present early in infections by virus or viral DNA. J Virol., 31: 360-369, 1979.

26. Hoogstraten, D., Nigg, A. L., Heath, H., Mullenders, L. H., van Driel, R., Hoeijmakers, J. H., Vermeulen, W., and Houtsmuller, A. B. Rapid Switching of TFIIH between RNA Polymerase I and II Transcription and DNA Repair In Vivo. Mol Cell, 10: 1163-1174, 2002.

27. Politz, J. C., Tuft, R. A., Pederson, T., and Singer, R. H. Movement of nuclear poly(A) RNA throughout the interchromatin space in living cells. Curr Biol, 9: 285-291, 1999.

28. Phair, R. D. and Misteli, T. High mobility of proteins in the mammalian cell nucleus. Nature, 404: 604-609, 2000.

29. Siva, A. C., Raval-Fernandes, S., Stephen, A. G., LaFemina, M. J., Scheper, R. J., Kickhoefer, V. A., and Rome, L. H. Up-regulation of vaults may be necessary but not sufficient for multidrug resistance. Int J Cancer, 92: 195-202, 2001.

CHAPTER 3

Interaction between vault particles
and microtubules

*submitted*

*Chapter 3*

**Abstract**

Vaults are large barrel-shaped ribonucleoproteins that may function in intracellular transport processes in the cytoplasm. They consist of multiple copies of three different proteins; the $M_r$ 100,000 major vault protein (MVP), the $M_r$ 193,000 vault poly(ADP-ribose) polymerase (VPARP) and the $M_r$ 240,000 telomerase-associated protein (TEP1) as well as small untranslated RNA molecules of 88 - 141 bases (vault RNA). The interaction between vaults and cytoskeletal elements and the effect of microtubules on vault dynamics were studied in non-small cell lung cancer cells in which vaults are fluorescently labelled with the green fluorescent protein (GFP). Fluorescence microscopy experiments showed that vaults are dispersed throughout the cytoplasm; a small fraction is closely associated with microtubules, but not with actin filaments. Immunoprecipitation experiments confirmed and extended these results showing a co-precipitation of vaults and β-tubulin. Using quantitative fluorescence recovery after photobleaching (FRAP) we demonstrated that vault mobility in part depends on microtubules; vaults moving slower when microtubules are depolymerised by nocodazole whereas under these conditions the mobility of GFP was not affected. Our data support a role for vaults as intracellular transport modules by providing evidence for a microtubule-based vault motility.

**Introduction**

Vaults are large, evolutionarily conserved, ribonucleoprotein particles that are composed of multiple copies of three different proteins; the $M_r$ 100,000 major vault protein (MVP), the $M_r$ 193,000 vault ADP(poly-ribose) polymerase (VPARP) and the $M_r$ 240,000 telomerase-associated protein (TEP1) as well as vault RNAs of 88-141 bases (see for recent reviews: 1, 2). The vault components are arranged into a typical hollow, barrel-like structure with an invaginated waist and two protruding caps (3, 4). The morphology of the complex is reminiscent of the vaulted ceilings in cathedrals, hence the name vaults. MVP is the main determinant of the vault structure and accounts for over 70% of its molecular mass (5, 6). The minor vault protein TEP1, and probably VPARP, are localized in the caps together with the vault RNAs (3, 4). A stoichiometric model predicts that each vault particle consists of 96 molecules of MVP, eight molecules of VPARP, two molecules of TEP1 and at least six molecules of vault RNA.

The precise role of the minor vault proteins TEP1 and VPARP within the complex and their contribution to overall vault function are not yet known. TEP1, a vault subunit that is shared with the telomerase complex, is capable of binding telomerase RNA but also vault RNAs and is responsible for the association of vault RNAs with the vault complex (7, 8). The analysis of *TEP1* knockout mice revealed that TEP1 is not essential for telomerase activity or telomere length regulation (9). Vault particles devoid of TEP1, which could be isolated from TEP1 deficient mice, lacked vault RNA. In addition, the stability of vault RNA was markedly decreased in *TEP1* knockout tissues (7). VPARP is the only vault component that displays enzymatic activity and is capable of ADP-ribosylating itself and MVP (10). Nevertheless, the functional importance of the ADP-ribosylation activity is unknown and currently under investigation. The vault RNA constitutes less than 5% of the mass of the complex and is believed to be a functional rather than a structural component, as degradation of vault RNA did not affect vault morphology (3, 5).

The intracellular distribution of vaults has been studied in various cell types and organisms (11). In mammalian cells vaults are predominantly localized in the cytoplasm. However, a small fraction (~5%) of the vaults is consistently found associated with the nucleus (12, 13) in particular the nuclear membrane and nuclear pore complex (13 and Van Zon *et al.*, unpublished results). Immunofluorescence and immunohistochemical experiments pointed to an association of vaults with cytoskeletal elements either actin filaments or microtubules (11, 13-15). In addition, vaults in sea urchin eggs seem to be closely associated with microtubules as they co-purified though several cycles of microtubule polymerisation and depolymerisation (16).

The distinct morphology and subcellular localization of the vault complex led to the hypothesis that vaults function in intracellular transport, particularly nucleo-cytoplasmic transport. Although electron dense material has been observed inside isolated vaults (3), a specific cargo of vaults has not yet been characterized. Several putative cargoes have been proposed, like nuclear hormone receptors (12), mRNA and/or ribosomes (16), and xenobiotics/drugs (1, 2). Recently, two proteins have been identified that interact with intact vaults; the tumor suppressor PTEN (17) and La auto-antigen (18). The ability to co-immunoprecipitate vaults with antibodies against the estrogen receptor (12) or PTEN suggests that these proteins bind to the outside of the complex. This is different from the electron microscopy data and therefore it remains unclear whether the putative cargo is inside vaults or attached to the outside.

Here we investigated the significance of the association of vaults with cytoskeletal elements for vault dynamics in non-small cell lung cancer cells. Immunofluorescence experiments showed a co-localization of GFP-tagged vault particles and microtubules. The existence of such an interaction was corroborated by the co-precipitation of β-tubulin with vault particles. Finally, fluorescence recovery after photobleaching (FRAP) experiments indicated that disassembly of microtubules influences vault mobility.

## Materials and methods

*Cell lines and culture conditions*
The following human cancer cell lines were used: the non-small cell lung carcinoma cell line SW1573 (19) and a stable SW1573 transfectant (SW1573/MVP-GFP) expressing an MVP-GFP fusion protein (20). The cell lines were maintained in DMEM (Life Technologies, Paisley, UK), supplemented with 10% (vol/vol) fetal calf serum, 1 mM pyruvate, 100 U/ml penicillin and 100 μg/ml streptomycin (Life Technologies, Paisley, UK) at 37°C under an atmosphere containing 5% $CO_2$. The cell line SW1573/MVP-GFP was routinely cultured in the presence of 200 μg/ml G-418 (Geneticin, Life Technologies, Paisley, UK).

*Antibodies and microfilament staining*
The mouse monoclonal anti-(MVP) (mAb LRP56) and rabbit polyclonal anti-(MVP) were generated as described previously (21). The mouse monoclonal anti-(β-tubulin) and isotype control (IgG2b) were purchased from the Sigma-Aldrich Corporation (St. Louis, MO, USA). All species-specific anti-(Ig) antibodies conjugated to horseradish peroxidase (HRP) or tetramethyl rhodamine isothiocyanate (TRITC) were obtained from Jackson ImmunoResearch Laboratories Inc. (West Grove, PA, USA). Actin filaments were stained using Texas Red®-X-phalloidin (Molecular Probes, Eugene, OR, USA).
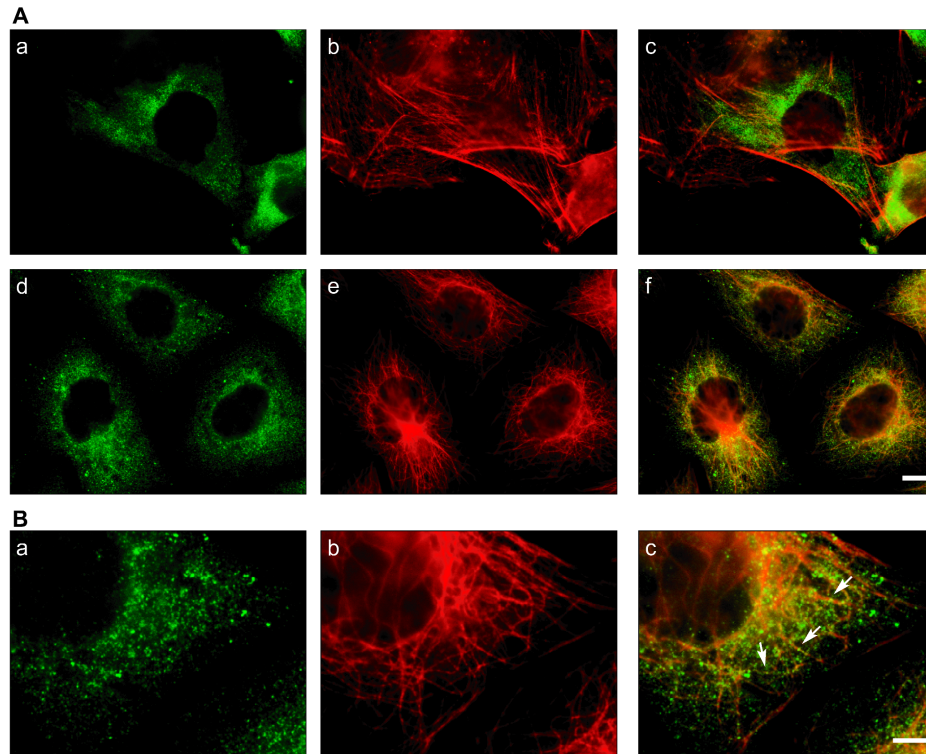
Figure 3.1. **Colocalization of MVP with microtubules.** A, SW1573/MVP-GFP transfectants were fixed, permeabilized and stained for actin filaments (*b*) or microtubules (*e*) in red using phalloidin and anti-(β-tubulin), respectively. The expression of MVP-GFP is shown in green (*a* and *d*). Merging of images reveals a partial colocalization (in yellow) of microtubules and the GFP-tagged vault complexes (*f*) whereas no colocalization of vaults with actin filaments could be observed (*c*). Bar corresponds to 10 μm. B, Higher magnification of vaults indicated by MVP-GFP (*a*), microtubules (*b*) and their partial colocalization when images are merged (*c*, arrows). Bar corresponds to 5 μm.

*Fluorescence microscopy*

SW1573/MVP-GFP cells were grown on poly-L-lysine coated coverslips, fixed with 3% (vol/vol) formaldehyde in PBS for 20 minutes and permeabilized by a 5 minute incubation in 1% (vol/vol) Triton-X100 in PBS after which the cover-slips were washed with PBS. Non-specific protein binding sites were blocked by incubating the cover-slips for 30 minutes in PBS containing 1% (wt/vol) BSA. Subsequently, the cells were incubated for one hour at room temperature with the appropriate anti-(β-tubulin) or Texas Red®-X-phalloidin dilutions made up in the same buffer. After washing the coverslips six times with PBS, bound anti-(β-tubulin) was visualized using anti-(mouse Ig) conjugated to TRITC. After extensive washing, the coverslips were mounted on microscope slides in anti-fade (4% (wt/vol) n-propyl gallate in glycerol).

The fluorescent staining pattern was examined using a Leica DMRXA microscope and images were created using Leica QFish version V 2.3e.

*Immunoprecipitations, SDS-PAGE and Western blotting*
Anti-(MVP) (LRP56) and an isotype control IgG2b were coupled to Dynabeads®-protein A (Dynal Biotech GmbH, Hamburg, FRG) according to the recommendations by the manufacturer. Cell lysates were prepared from SW1573 and SW1573/MVP-GFP as follows: cells were washed twice with phosphate buffered saline (PBS) and harvested by scraping. The cell pellets were subsequently resuspended in lysis buffer (50 mM Tris-Cl pH 7.5, 1.5 mM MgCl$_2$, 75 mM NaCl, 2 mM EDTA, 2 mM EGTA, 1 mM GTP, 0.5% (vol/vol) Nonidet P-40) supplemented with a cocktail of protease inhibitors (Complete™ Roche Molecular Biochemicals). During the preparation of the cell lysates, solutions were kept at room temperature (21°C) in order to prevent disintegration of the microtubuli. Before using the lysates in immunoprecipitations insoluble components were removed by centrifuging the samples at 13,000 x *g* for 2 minutes. Each lysate was split in half and used in immunoprecipitations with either anti-(MVP) or its isotype control. Immunoprecipitations were carried out for 2.5 hours at room temperature. Subsequently, the beads were washed five times with lysis buffer containing protease inhibitors. The use of Dynabeads®-protein A that were washed using a magnetic particle concentrator (Dynal, Oslo, Norway) precluded the pelleting of the beads by centrifugation and eliminated the chance of non-specific precipitation of microtubules. After the last wash the beads were resuspended in 100 μl protein loading buffer (50 mM Tris-Cl pH 6.8, 2% (wt/vol) SDS, 10% (vol/vol) β-mercaptoethanol, 10% (vol/vol) glycerol and 0.1% (wt/vol) Bromeophenol blue). Immunoprecipitates were subjected to SDS-PAGE after which size-fractionated proteins were electroblotted to nitrocellulose. The protein blots were blocked in TBST (50 mM Tris-Cl pH 7.5, 100 mM NaCl and 0.05 % (vol/vol) Tween 20) containing 5% (wt/vol) non-fat dry milk. MVP and β-tubulin were detected using a rabbit polyclonal anti-(MVP) and a monoclonal anti-(β-tubulin), respectively. Species specific anti-(Ig) antibodies conjugated to horseradish peroxidase were used as second antibody. Immune-complexes were detected using the BM Chemiluminescence Blotting Substrate (POD) kit (Roche, Mannheim, FRG) and visualized on Hyperfilm™ ECL™ (Amersham Pharmacia Biotech, Uppsala, Sweden).

*Fluorescence recovery after photobleaching (FRAP) assays*
A Zeiss (Jena, FRG) confocal laser-scanning microscope (CLSM) equipped with a heatable scan stage was used for confocal microscopy and FRAP experiments. Excitation illumination was from an argon ion laser (488 nm) using a 40X 1.3 n.a. objective. High-resolution images were at a lateral resolution of 102 nm. To determine cytoplasmic mobility of vaults in SW1573/MVP-GFP cells, a laser beam was focused in the cytoplasm for 4 seconds (at relatively low laser power) allowing a large part of the mobile molecules to diffuse through the laser cone area and get bleached. Note that

if no immobile molecules are present, eventually all molecules will get bleached. However, if a fraction of the molecules is immobile these will only get bleached inside the laser focus resulting in an uneven distribution of bleached molecules with less fluorescence in the laser spot. In addition, if immobilisation is transient a subsequent slow redistribution of fluorescence will occur, as immobile molecules release and diffuse through the cytoplasm. The time it takes for this secondary fluorescence redistribution to be complete is a measure for average binding time of individual molecules (based on Houtsmuller *et al.* (22)). Similar experiments were performed in the presence of the microtubule depolymerizing agent nocodazole (30 μM for 30 minutes).
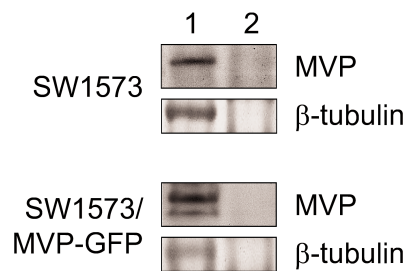


Figure 3.2. **Co-immunoprecipitation of vaults and β-tubulin.** Cell lysates were prepared from SW1573 and SW1573/MVP-GFP cells. Vaults were isolated by immunoprecipitation using anti-(MVP) (mAb LRP56; lane 1) bound to Dynabeads-protein A as described in the materials and methods section. The conditions were carefully chosen to prevent complete degradation and non-specific precipitation of the microtubules. Control immunoprecipitations were carried out using an isotype IgG2b control antibody (lane 2). Immunoprecipitates were subjected to SDS-PAGE and electroblotted to nitrocellulose. MVP and β-tubulin were detected by incubating the blot with anti-(β-tubulin) and after stripping with anti-(MVP).

**Results**

*Partial co-localization of GFP-tagged vaults and microtubules*

Vaults are predominantly found in the cytoplasm where they are believed to function in intracellular transport processes. Directional transport of cargo by vaults could take place via association of vaults with cytoskeletal elements (11, 15, 16). We previously showed that expression of a MVP-GFP fusion protein in non-small cell lung cancer cells (SW1573) results in GFP-tagged vault particles through the incorporation of MVP-GFP in vaults (20, Chapter 2). The SW1573 transfectant stably expressing MVP-GFP (SW1573/MVP-GFP) was fixed, permeabilized and processed for immunofluoresence. Microtubules were identified using anti-(β-tubulin) antibodies and actine microfilaments were stained using phalloidin. Vaults, identified by GFP, were dispersed throughout the cytoplasm as indicated by the fine particulate fluorescent pattern, similar to the staining pattern observed with anti-(MVP) in

immunofluorescence in SW1573 cells (20). We did not detect a colocalization of GFP-tagged vaults with the Texas-Red phalloidin-stained actin filaments (Fig. 3.1A, *a–c*). However, a partial overlap in fluorescent patterns was observed in the cells stained for microtubules as is illustrated by the appearance of a yellow fluorescent pattern when the images were merged (Fig. 3.1A, *d–f*). A higher magnification revealed that part of the vaults is in close proximity to microtubules (Fig. 3.1B, *a–c*).

*Co-immunoprecipitation of β-tubulin with vaults*

To verify the observed association between vaults and microtubules, we performed immunoprecipitation experiments. Cell lysates were prepared from SW1573 and SW1573/MVP-GFP cells. The buffer and conditions used, were designed to keep vaults and microtubules intact. Because it is known that microtubules depolymerize at low temperatures (4°C), the cell lysates were prepared at 21°C. Likewise, the immunoprecipitations with the mouse monoclonal anti-(MVP) LRP56 or a control IgG2b were carried out at room temperature for 2.5 hours. To prevent non-specific precipitation of microtubules during wash steps we used protein A-dynabeads that were collected using a magnet. The immunoprecipitates were analyzed by SDS-PAGE and immunoblotting. Figure 3.2 shows that MVP and the MVP-GFP fusion protein of $M_r$ 125,000 in the SW1573/MVP-GFP cell lysate were selectively isolated. No MVP or MVP-GFP could be detected in the control immunoprecipitations. Staining of the same blot for β-tubulin revealed co-immunoprecipitations of this protein, corroborating the observed interaction between microtubules and vaults.

*Dynamics of the vault complex measured by FRAP*

To further investigate whether microtubules dynamically associate with MVP, we subjected SW1573/MVP-GFP cells to FRAP analysis. For 4 seconds a laser beam bleaches a spot in the cytoplasm. The mobility of the vaults was determined by measuring fluorescence intensity in time, in rings around the bleached spot (Fig. 3.3A). The speed of fluorescence redistribution is a measure for the mobility of the labeled molecules. The experiments suggest that vaults are present in two dynamic pools; a fast component that is revealed in the initial part of the curve (solid line) and a secondary slower fraction. Interestingly, upon a 30-minute nocodazole treatment (dashed line), the biphasic nature of the curves is abolished and the majority of the vaults adopt the slower mobility. The effect of the nocodazole treatment prior the FRAP measurement is visualized after processing the treated cells for indirect immunofluorescence and staining with anti-(β-tubulin) (Fig. 3.3B). To study the effect of nocodazole on general cytoplasmic movement, the mobility of free GFP was assessed by FRAP on transiently transfected SW1573 cells; no differences in mobility were observed when the cells were pre-treated with nocodazole (data not shown).

**Discussion**

Vaults have been linked to various basic cellular processes like nucleo-cytoplasmic transport, telomere length regulation, differentiation, detoxification, xenobiotic transport and ribonucleoprotein assembly (1, 2). However, insight into the molecular mechanism by which vaults affect these processes is often lacking. Although the precise cellular function of vaults remains elusive, a recurring theme is a role for vaults in intracellular transport. Supporting a transport function is the fact that vaults are hollow barrel-like structures appropriate for transporting cargoes of considerable size (3, 4). If vaults truly function as transport modules of some kind one expects them to move in an orderly fashion through the cell possibly guided by cytoskeletal elements. We exploited the ability of MVP-GFP to be incorporated into vaults particles (20), providing a vital stain for vaults that enables us to study the intracellular distribution and dynamics of vaults in relation to the cytoskeleton.

In SW1573 transfectants expressing MVP-GFP part of the fluorescent vault particles could be observed in close proximity to microtubules, confirming earlier immunofluorescence studies using other mammalian cell lines like chinese hamster ovary and PC12 (phaeochromocytoma cells of rat adrenal medulla origin) cells (15). More direct evidence for an association of microtubules with vaults came from immunoprecipitation experiments showing that $\beta$-tubulin co-precipitates with intact vault particles. Using fluorescent recovery after photobleaching (FRAP) we examined the significance of this interaction for *in vivo* vault movement. Vault dynamics was determined by FRAP in SW1573/MVP-GFP cells cultured in the presence or absence of nocodazole. Destabilization of microtubules consistently resulted in a delayed recovery of the fluorescent signal after a laser pulse. Apparently, the absence of intact microtubules slows the movement of GFP-tagged vaults but it does not affect the dynamics of GFP. Previous FRAP experiments, involving the SW1573/MVP-GFP transfectant, in which a small strip of 2 µm in the cytoplasm was bleached and the fluorescence recovery measured (strip-FRAP), indicated that the majority of vaults move by diffusion (20, Chapter 2). A similar setting was used to determine the involvement of the cytoskeleton in vault dynamics and small differences in dynamics after nocodazole treatment were detected (data not shown). Nevertheless, no significant differences could be measured due to the small size of the bleached area. Therefore, in the present FRAP experiments a much larger area is bleached (spot-FRAP) enabling us to detect vault movement over longer distances in the cell. The fact that the overall movement of vaults is slowed down when microtubules are disintegrated indicates that vault movement is in part dependent on microtubules. It is tempting to speculate that vaults directionally move along microtubule tracks reminiscent of organelle movement within cells (23-25). Unfortunately, no individual vault particles could be followed due to the simple fact that the cytoplasm is packed with vault particles.
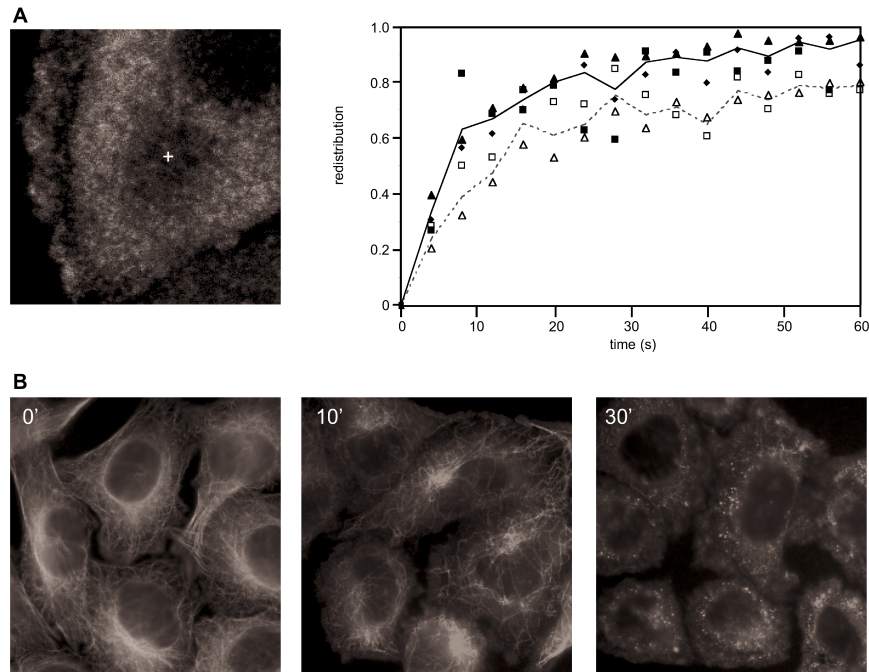
Figure 3.3. **Dynamics of the vault complex measured by FRAP.** A, Example of a spot bleached in the cytoplasm of SW1573/MVP-GFP cells. The white cross indicates the center of the spot that was bleached by a laser beam in the cytoplasm after bleaching (4 seconds). The graph shows the redistribution of fluorescent molecules in time in the absence (■, ◆ and ▲) and presence (□ and △) of 30 μM nocodazole. Each of the symbols represents the average value from an independent experiment in which 15 cells were analyzed. The solid line indicates the mean of the three independent experiments carried out in the absence of nocodazole (n=45). The dashed line indicates the mean of the two independent experiments in the presence of nocodazole (n=30). Similar experiments were performed with SW1573 expressing GFP, in which no effect of the nocodazole treatment was seen (data not shown). B, SW1573/MVP-GFP cells were treated with 30 μM of nocodazole prior the FRAP measurements, which results in a depolymerization of microtubules. Microtubules are immuno-stained with anti-(β-tubulin) after 0, 10 and 30 minutes of incubation with nocodazole. After a 30-minute incubation the cells were used for the FRAP experiments shown in figure 3.3A. Bar corresponds to 10 μm.

Recently, we found that vaults are able to rearrange themselves into large cytoplasmic tube-like structures (vault-tubes) when cells were incubated at room temperature. Vault-tube formation is a reversible process as a temperature raise to 37°C led to the disappearance of the tubes and restored the normal cellular vault distribution (20). We also studied the influence of microtubule stability on the formation of the vault-tubes and found that a destabilization of the microtubules significantly increased the amount of cells that contained the vault-tubes. Stabilization on the other hand decreased the amount of vault-tubes. Similar to the results described above these findings indicate

the existence of an intricate relationship between vaults and the cytoskeleton; with microtubules affecting vault distribution, dynamics and perhaps vault activity.

The question arises as to how vaults are linked to microtubules. Interestingly, we found a region in MVP that may function as a microtubule-binding domain (MTB), on the basis of similarity to MTBs described in various proteins including CLIPs (26, 27). The 70 amino acid MTB domains are rich in glycine and valine residues and contain the core sequence PXGKND. At position 289 of MVP there is a PDGKNQ motif surrounded by glycine- and valine-rich sequences. Another possibility for vaults to interact with microtubules is via the minor vault protein VPARP. This protein was shown to be associated to the mitotic spindle, independent of the other vault components (10).

We have shown that intact vaults interact with microtubules and demonstrated for the first time that vault movement is partly dependent on intact microtubules. However, many questions remain concerning the microtubule based vault dynamics. Most importantly, do vaults really move directionally along microtubules, which proteins are involved and is the transport active or passive? The presented data may support and initiate future research to answer these important questions.

## References

1.  Van Zon, A., Mossink, M. H., Scheper, R. J., Sonneveld, P., and Wiemer, E. A. C. The Vault Complex. Cell Mol Life Sci, 60(9): 1828-1837, 2003.
2.  Suprenant, K. A. Vault ribonucleoprotein particles: sarcophagi, gondolas, or safety deposit boxes? Biochemistry, 41: 14447-14454, 2002.
3.  Kong, L. B., Siva, A. C., Kickhoefer, V. A., Rome, L. H., and Stewart, P. L. RNA location and modeling of a WD40 repeat domain within the vault. RNA, 6: 890-900, 2000.
4.  Kong, L. B., Siva, A. C., Rome, L. H., and Stewart, P. L. Structure of the vault, a ubiquitous celular component. Structure Fold Des, 7: 371-379, 1999.
5.  Kedersha, N. L. and Rome, L. H. Isolation and characterization of a novel ribonucleoprotein particle: large structures contain a single species of small RNA. J Cell Biol, 103: 699-709, 1986.
6.  Stephen, A. G., Raval-Fernandes, S., Huynh, T., Torres, M., Kickhoefer, V. A., and Rome, L. H. Assembly of vault-like particles in insect cells expressing only the major vault protein. J Biol Chem, 276: 23217-23220, 2001.
7.  Kickhoefer, V. A., Liu, Y., Kong, L. B., Snow, B. E., Stewart, P. L., Harrington, L., and Rome, L. H. The Telomerase/Vault-associated Protein TEP1 Is Required for Vault RNA Stability and Its Association with the Vault Particle. J Cell Biol, 152: 157-164, 2001.
8.  Kickhoefer, V. A., Stephen, A. G., Harrington, L., Robinson, M. O., and Rome, L. H. Vaults and telomerase share a common subunit, TEP1. J Biol Chem, 274: 32712-32717, 1999.
9.  Liu, Y., Snow, B. E., Hande, M. P., Baerlocher, G., Kickhoefer, V. A., Yeung, D., Wakeham, A., Itie, A., Siderovski, D. P., Lansdorp, P. M., Robinson, M. O., and Harrington, L. Telomerase-associated protein TEP1 is not essential for telomerase activity or telomere length maintenance *in vivo*. Mol Cell Biol, 20: 8178-8184, 2000.
10. Kickhoefer, V. A., Siva, A. C., Kedersha, N. L., Inman, E. M., Ruland, C., Streuli, M., and Rome, L. H. The 193-kD vault protein, VPARP, is a novel poly(ADP-ribose) polymerase. J Cell Biol, 146: 917-928, 1999.
11. Kedersha, N. L. and Rome, L. H. Vaults: large cytoplasmic RNP's that associate with cytoskeletal elements. Mol Biol Rep, 14: 121-122, 1990.
12. Abbondanza, C., Rossi, V., Roscigno, A., Gallo, L., Belsito, A., Piluso, G., Medici, N., Nigro, V., Molinari, A. M., Moncharmont, B., and Puca, G. A. Interaction of vault particles with estrogen receptor in the MCF-7 breast cancer cell. J Cell Biol, 141: 1301-1310, 1998.
13. Chugani, D. C., Rome, L. H., and Kedersha, N. L. Evidence that vault ribonucleoprotein particles localize to the nuclear pore complex. J Cell Sci, 106: 23-29, 1993.
14. Berger, W., Elbling, L., and Micksche, M. Expression of the major vault protein LRP in human non-small-cell lung cancer cells: activation by short-term

exposure to antineoplastic drugs. Int J Cancer, 88: 293-300, 2000.

15.     Herrmann, C., Golkaramnay, E., Inman, E., Rome, L., and Volknandt, W. Recombinant major vault protein is targeted to neuritic tips of PC12 cells. J Cell Biol, 144: 1163-1172, 1999.

16.     Hamill, D. R. and Suprenant, K. A. Characterization of the sea urchin major vault protein: a possible role for vault ribonucleoprotein particles in nucleocytoplasmic transport. Dev Biol, 190: 117-128, 1997.

17.     Yu, Z., Fotouhi-Aroakani, N., Wu, L., Maoui, M., Wang, S., Banville, D., and Shen, S. H. PTEN Associates with the vault particles in Hela cells. J Biol Chem, 277:40247-40252, 2002.

18.     Kickhoefer, V. A., Poderycki, M. J., Chan, E. K., and Rome, L. H. The La RNA binding protein interacts with the vault RNA and is a vault- associated protein. J Biol Chem, 277:41282-41286, 2002.

19.     Kuiper, C. M., Broxterman, H. J., Baas, F., Schuurhuis, G. J., Haisma, H. J., Scheffer, G. L., Lankelma, J., and Pinedo, H. M. Drug transport variants without P-glycoprotein overexpression from a human squamous lung cancer cell line after selection with doxorubicin. J. Cell Pharmacol., 1: 35-41, 1990.

20.     Van Zon, A., Mossink, M. H., Schoester, M., Houtsmuller, A. B., Scheffer, G. L., Scheper, R. J., Sonneveld, P., and Wiemer, E. A. The formation of vault-tubes: a dynamic interaction between vaults and vault PARP. J Cell Sci, 116: 4391-4400, 2003.

21.     Schroeijers, A. B., Siva, A. C., Scheffer, G. L., de Jong, M. C., Bolick, S. C., Dukers, D. F., Slootstra, J. W., Meloen, R. H., Wiemer, E., Kickhoefer, V. A., Rome, L. H., and Scheper, R. J. The $M_r$ 193,000 vault protein is up-regulated in multidrug-resistant cancer cell lines. Cancer Res, 60: 1104-1110, 2000.

22.     Houtsmuller, A. B., Rademakers, S., Nigg, A. L., Hoogstraten, D., Hoeijmakers, J. H., and Vermeulen, W. Action of DNA repair endonuclease ERCC1/XPF in living cells. Science, 284: 958-961, 1999.

23.     Rogers, S. L. and Gelfand, V. I. Membrane trafficking, organelle transport, and the cytoskeleton. Curr Opin Cell Biol, 12: 57-62, 2000.

24.     Goodson, H. V., Valetti, C., and Kreis, T. E. Motors and membrane traffic. Curr Opin Cell Biol, 9: 18-28, 1997.

25.     Allan, V. J. and Schroer, T. A. Membrane motors. Curr Opin Cell Biol, 11: 476-482, 1999.

26.     Riehemann, K. and Sorg, C. Sequence homologies between four cytoskeleton-associated proteins. Trends Biochem Sci, 18: 82-83, 1993.

27.     Hoogenraad, C. C., Akhmanova, A., Grosveld, F., De Zeeuw, C. I., and Galjart, N. Functional analysis of CLIP-115 and its binding to microtubules. J Cell Sci, 113: 2285-2297, 2000.

# Structural domains of vault proteins:
# A role for the coiled coil domain
# in vault assembly

*Chapter 4*

**Abstract**

Vaults consist of multiple copies of three proteins (MVP, VPARP and TEP1) and several untranslated RNAs. The function of vaults is unknown but the typical and evolutionary conserved structure indicates a role in intracellular transport. Although all vault components have been identified and characterized, not much is known about vault protein assembly. In this study we identified and analyzed structural domains involved in vault assembly with emphasis on protein-protein interactions. Using a yeast two-hybrid system we demonstrate within MVP an intramolecular binding site and show that MVP molecules interact with each other via their coiled coil domain. We show that purified MVP is able to bind calcium, most likely at calcium-binding EF-hands. No interactions could be detected between TEP1 and other vault proteins. However, the N-terminal half of MVP binds to a specific domain in the C-terminus of VPARP. Furthermore, VPARP contains amino acid stretches mediating intramolecular binding.

**Introduction**

Vaults, large ribonucleoprotein particles, are predominantly found in the cytoplasm. However, part of the vaults may be associated with the nucleus or the nuclear membrane (1-3). The typical morphology of the complex is responsible for its name, since the hollow structure consists of multiple arches reminiscent of the vaulted ceilings in cathedrals (4). Although the cellular function of the vault complex is still unknown, vault morphology and subcellular localization suggest a general role in intracellular transport. Studies in various organisms present data that support the concept of vaults as transport modules of some kind, although its cargo has not been characterized (1-3, 5-7). In recent years the vault complex has been linked to multidrug resistance in tumor cells (see for reviews: 8, 9). There is experimental evidence suggesting that at least part of the basis for vault-mediated drug resistance might lie in its ability to prevent nuclear accumulation of anthracyclins (10, 11).

The 13 MDa mammalian vault structure is highly regular and consists of approximately 96 molecules of the 100 kDa major vault protein (MVP), two molecules of the 240 kDa minor vault protein TEP1, eight molecules of the 193 kDa minor vault protein VPARP and at least six copies of a small untranslated RNA of 88-141 bases (12). The MVP molecules form the core of the complex, which is a barrel-like structure with an invaginated waist and two protruding caps. The complex can unfold into two symmetrical flower-like structures with eight petals each supposedly consisting of six MVP molecules (13). TEP1 and probably VPARP are located in the two protruding caps (12, 14, 15). Vault RNA is associated with the TEP1 protein (12, 16, 17). In fact, using *TEP1$^{-/-}$* mouse embryonic fibroblasts it was shown that TEP1 is required for stable association of the vault RNA with the vault particle (17). Kong *et al.* (14) proposed that the WD40 repeats found in the C-terminal part of TEP1 determine the structure of the eight-fold symmetric vault particle. However, after examining vaults isolated from *TEP1$^{-/-}$* mice this proposal was abandoned as it was found that vault symmetry was preserved (17). Note that TEP1 is a shared protein with the telomerase complex, but it does not seem to be necessary for telomerase activity (16, 18). VPARP contains a distinct domain with similarity to the catalytic domain of poly (ADP-ribose) polymerase (PARP). It was demonstrated that VPARP catalyses ADP-ribosylation of itself and MVP, hence its name (19). Several additional domains were identified, like a BRCT domain and a Von Willebrand factor type A domain within the inter-$\alpha$-inhibitor domain (19, 20). Interesting from a structural point of view is the region at the C-terminal end of VPARP (aa 1562-1724) that has been shown to interact with MVP (19). Despite the characterization of all vault components and the macromolecular assembly they form, very little is known about the biogenesis of the complex and the factors that mediate this process. To understand the formation of this highly ordered structure we identified and functionally characterized distinct structural domains present in the three vault proteins.
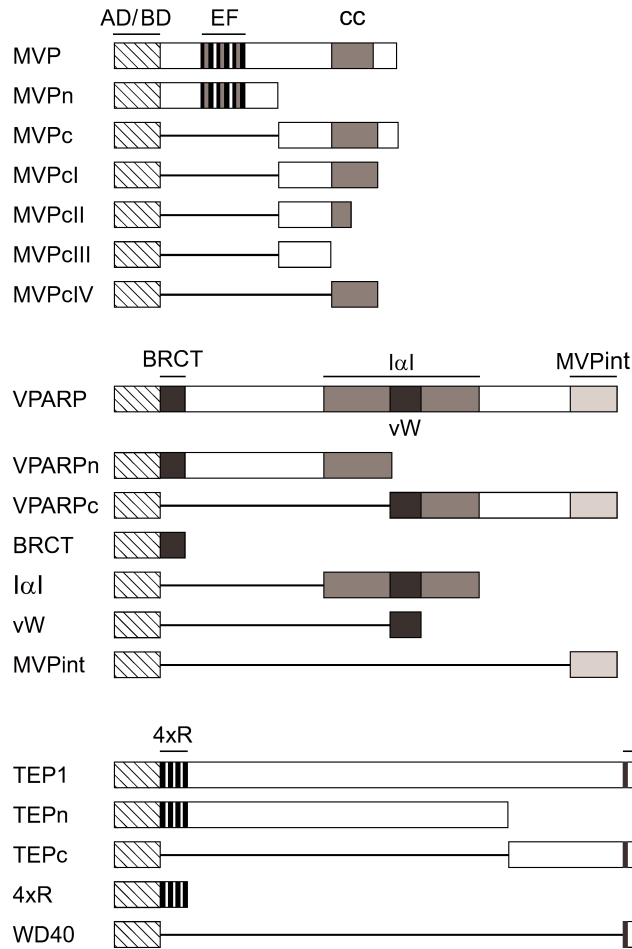
Figure 4.1. **Yeast two-hybrid constructs.** Plasmids encoding fusion proteins of a DNA-binding domain (BD) or a transactivation domain (AD) with complete vault proteins, or parts of them, were constructed. MVP fusion proteins included full-length MVP, the N-terminal part of MVP (MVPn; amino acid (aa) 1-447), the C-terminal part of MVP (MVPc; aa 448-893), aa 448-800 containing the complete coiled coil (MVPcI), aa 448-733 containing half of the coiled coil (MVPcII), aa 448-651 with no coiled coil (MVPcIII) and the coiled coil domain itself (MVPcIV; aa 652-800). VPARP fusion proteins included full-length VPARP, N-terminal part of VPARP (VPARPn; aa 1-862), C-terminal part of VPARP (VPARPc; aa 863-1724), BRCT domain (aa 1-94), inter-α-inhibitor domain (IαI; aa 616-1195), Von Willebrand domain (vW; aa 878-987) and the MVP interaction domain (MVPint; aa 1562-1724). TEP1 fusion proteins included full-length TEP1, N-terminal part of TEP1 (TEPn; aa 1-1313), C-terminal part of TEP1 (TEPc; aa 1314-2627), four times repeat structure (4xR; aa 1-120) and the WD40 repeats (aa 1723-2410). Domains are indicated as follows: EF, EF-hand repeat structure; cc, coiled coil; BRCT, BRCT domain; IαI, Inter-α-inhibitor domain; vW, Von Willebrand domain; MVPint, MVP interaction domain; 4xR, four times repeat structure and WD40, WD40 repeats.

**Materials and methods**

*Bacteria and yeast strains*
*Escherichia coli* DH5α was the transformation recipient for all plasmids. For the two-hybrid screening the yeast *Saccharomyces cerevisiae* L40 (*MAT*a *trp1 leu2 his3 LYS2::lexA-HIS3 URA3::lexA-lacZ*) was used. This strain was grown at 30°C in YPAD (1% yeast extract, 2% Bacto peptone, 0.01% adenine, 2% glucose) or MY (0.12% yeast nitrogen base (without amino acids and ammonium sulfate), 0.5% ammonium sulfate, 1% succinic acid, 0.6% sodium hydroxide, 2% glucose) supplemented as required (0.01% ade, arg, cys, leu, lys, thr, trp, ura and 0.005% asp, his, ile, met, phe, pro, ser, tyr, val). For solid plates 2% agar was added.

*Yeast two-hybrid constructs*
The yeast two-hybrid constructs were generated by cloning PCR amplified fragments of human MVP, VPARP and TEP1 into derivatives of pVP16 (pKNSD50-52; containing the transactivation domain, AD) and pBTM116 (pKNSD53-55; containing the Lex A DNA binding domain, BD) (21). The MVP cDNA fragments were derived from full-length cDNA cloned in pBSKSII (Stratagene, La Jolla, CA). Fragments of VPARP were amplified by PCR using a cDNA clone, ha02779 (KIAA0177) (22). This construct lacks the first 276 bp of the VPARP ORF and bases 1024 and 1025 are deleted. To repair the VPARP ORF we cloned the first 1400 base

Table 4.1. **Yeast two-hybrid analysis of the major vault protein**

| AD↓BD→ | MVP | MVPn | MVPc | MVPcI | MVPcII | MVPcIII | MVPcIV |
|---|---|---|---|---|---|---|---|
| MVP | + | – | + | + | – | – | + |
| MVPn | – | – | + | + | + | + | – |
| MVPc | + | + | + | + | . | . | + |
| MVPcI | + | + | + | + | . | . | + |
| MVPcII | – | + | . | . | – | – | – |
| MVPcIII | – | + | . | . | – | – | . |
| MVPcIV | + | – | + | + | – | . | + |

This table presents the observed interactions between various MVP domains in a yeast two-hybrid screen. The '+' indicates an interaction and '-' indicates combinations that did not interact. Two MVP molecules interact with each other via their coiled coil domains. Deletion or partial deletion of this domain abolishes the interaction, as is clear from the first row and the first column. However, in the second row and second column another interaction can be observed, namely between the N-terminal and C-terminal part of MVP. This intramolecular binding site is not dependent on the coiled coil domain. The dots '·' indicate contradictory results that cannot be judged (see Materials and methods).

pairs by RT-PCR. As a PCR template we used cDNA prepared from total RNA isolated from human mononuclear cells derived from peripheral blood. We introduced a *Kpn*I restriction site at the 5' end (forward primer: 5'-GAggtaccATGGTGATG-GGAATCTTTG) and made use of an *Aat*II restriction site at the 3' end (reverse primer: 5'-TCCgacgtcTGTTCTTTGCACACC) of the fragment. The PCR product was isolated from gel, digested with *Kpn*I and *Aat*II and used to replace the *Kpn*I - *Aat*II fragment in ha02779. TEP1 fragments were amplified by PCR using pCR3-Myc-HuTEP1-FL, which contains a *myc*-tagged full-length TEP1 cDNA insert. All primers were designed with 18-22 nucleotide anchors complementary to the sequence of interest, in addition to the appropriate restriction enzyme sites for cloning purposes. In essence, PCR conditions were as follows: 94°C for 5 minutes, then 30 cycles of 94°C for 1 minute, 50-55°C for 2 minutes and 72°C for 2-5 minutes followed by 72°C for 8 minutes. The exact annealing temperatures depended on the $T_m$ values of the individual primer pairs. Routinely, *Pfu* DNA polymerase (Stratagene, La Jolla, CA) or alternatively the Expand High Fidelity PCR System (Roche Diagnostics, Mannheim, Germany) was used to prevent PCR artefacts. PCR products were isolated from gel and cloned into the pCR-Blunt vector (Invitrogen, Carlsbad, CA) and were subcloned into both two-hybrid vectors. The nucleotide sequences of all inserts, including the cloning junctions, were verified by cycle sequencing.

*Yeast two-hybrid analysis*
The yeast strain L40 was transformed according to the LiAc/SS-DNA/PEG procedure (23) with different combinations of the pBTM116 and pVP16 plasmids containing MVP, VPARP and TEP1 inserts. Transformants were plated on MY plates lacking trp and leu. At least ten independent transformants were picked and screened for reporter gene activation by plating them on MY plates lacking trp, leu and his. The presence or absence of growth was assessed after three days at 30°C. The activity of the *LacZ* reporter was checked by a β-galactosidase plate assay (24). The plates were routinely examined after three hours of incubation at 30°C following the addition of 5-bromo-4-chloro-3-indolyl-β-D-galactopyranoside (X-gal). The overall results are presented in tables with '+' for interaction and '-' for no interaction. To validate the results the AD and BD were exchanged in all situations. This sometimes led to discrepancies, which is a known phenomenon of the two-hybrid approach (25).

*Purification of glutathione-S-transferase (GST) MVP fusion proteins*
A *Nco*I - *Eco*RV fragment of 2631 base pairs (encoding aa 1-871 of MVP) from pBSKSII-MVP was cloned between the *Nco*I and filled-in *Hind*III sites of the pGEX-KG polylinker (26). Likewise, a *Nco*I - *Sma*I fragment of 1264 base pairs (encoding aa 1-421 of MVP) was isolated and cloned between the *Nco*I and filled-in *Hind*III sites of the pGEX-KG polylinker. Both GST-MVP fusion proteins were expressed in *E. coli* DH5α as described by Guan and Dixon (26). After harvesting, the cells were lyzed by sonication in the presence of a protease inhibitor cocktail (Protease inhibitor cocktail tablets, Roche, Mannhein, FRG). Subsequently, the soluble fusion

proteins were bound to glutathione Sepharose 4B beads (Amersham Pharmacia Biotech, Uppsala, Sweden) after which the MVP part was released by a thrombin digest. The fractions containing MVP were concentrated by freeze-drying.

*Calcium overlay assay*
Proteins were subjected to SDS-PAGE (27) after which the size fractionated proteins were transferred to nitrocellulose (28). A calcium overlay assay was performed essentially as described by Maruyama *et al.* (29). In brief: The nitrocellulose membranes were washed 2 times for 15 minutes with 10 mM imidazole pH 6.8, 60 mM KCl and 5 mM MgCl. Then they were incubated for 10 minutes in the same buffer containing 1 μCi/ml of $^{45}$CaCl$_2$ (specific activity 2 mCi/ml). After a 5 minutes wash with water the membranes were dried and exposed to Kodak X-Omat™ AR film (Kodak, Rochester, NY) at -80°C. As a control, skeletal muscle tissue of BALB/c mice was used after homogenization by sonication in 25 mM sodium phosphate pH 7.4 containing 0.25% (v/v) Triton X-100 and a cocktail of protein inhibitors. Protein concentrations were determined by the BCA protein assay (Pierce, Rockford, IL).

**Results**

*Coiled coil domain mediates the interaction between MVP molecules*
The program COILS (http://www.ch.embnet.org/software/COILS_form.html) identified a coiled coil conformation in the C-terminal half of MVP (aa 648-800). Since coiled coil structures may be involved in protein-protein interactions, we focused on this particular domain of MVP. Next to the full-length MVP, N and C-terminal yeast two-hybrid constructs (MVP, MVPn and MVPc respectively), we prepared C-terminal deletion constructs sequentially removing the extreme C-terminal end but leaving the coiled coil intact (MVPcI), removing half of the coiled coil (MVPcII), deleting the complete coiled coil (MVPcIII) as well as a construct expressing only the coiled coil domain of MVP (MVPcIV) as is shown in figure 4.1. The results summarized in table 4.1 indicate the existence of two distinct interaction sites of MVP, an intermolecular and intramolecular binding site. First, full-length MVP interacts with itself and with the C-terminal part, as shown in the first row and first column of table 4.1. However, full-length MVP does not interact with the N-terminal part of MVP. It is clear that the interaction between full-length MVP and other parts of MVP can only be formed when the coiled coil domain is fully intact. When the coiled coil domain is deleted or partly deleted no interaction is possible. So, MVP interacts with itself via the coiled coil domain forming an intermolecular binding. Second, the second row and second column of table 4.1 show that the N-terminal part of MVP does not interact with full-length MVP or with itself. Interestingly, this part does interact with the C-terminal part. Even partial or complete deletion of the coiled coil domain does not affect this interaction. This intramolecular binding must be formed between the N-terminal part and aa 448-651 of the C-terminal part and may be important for the secondary structure of each MVP molecule. In a full-length MVP molecule this

interaction between MVPn and MVPc is already formed, which explains why full-length MVP does not interact with MVPn.

*MVP contains EF-hands capable of binding calcium*

The MOTIF search service on Genome Net (Bioinformatics Center at Kyoto University, http://motif.genome.ad.jp) reveals the presence of a putative EF-hand with the calcium-binding loop located at position 131-143. Careful analysis of the human MVP sequence revealed that this EF-hand is part of a degenerated repeat structure,

a

```
                        EF-hand loop
                     ‾‾‾‾‾‾‾‾‾‾‾‾‾‾‾‾
118  NTALHLKALLDFEDKDGDKVVAGDEWLFEGPG--TYIPRKEVEVVEIIQATI  167
171  NQALRLRARKECWDRDGKERVTGEEWLVTTVG--AYLPAVFEEVLDLVDAVI  220
224  KTALHLRARRNFRDFRGVSRRTGEEWLVTVQDTEAHVPDVHEEVLGVV--PI  273
```

b
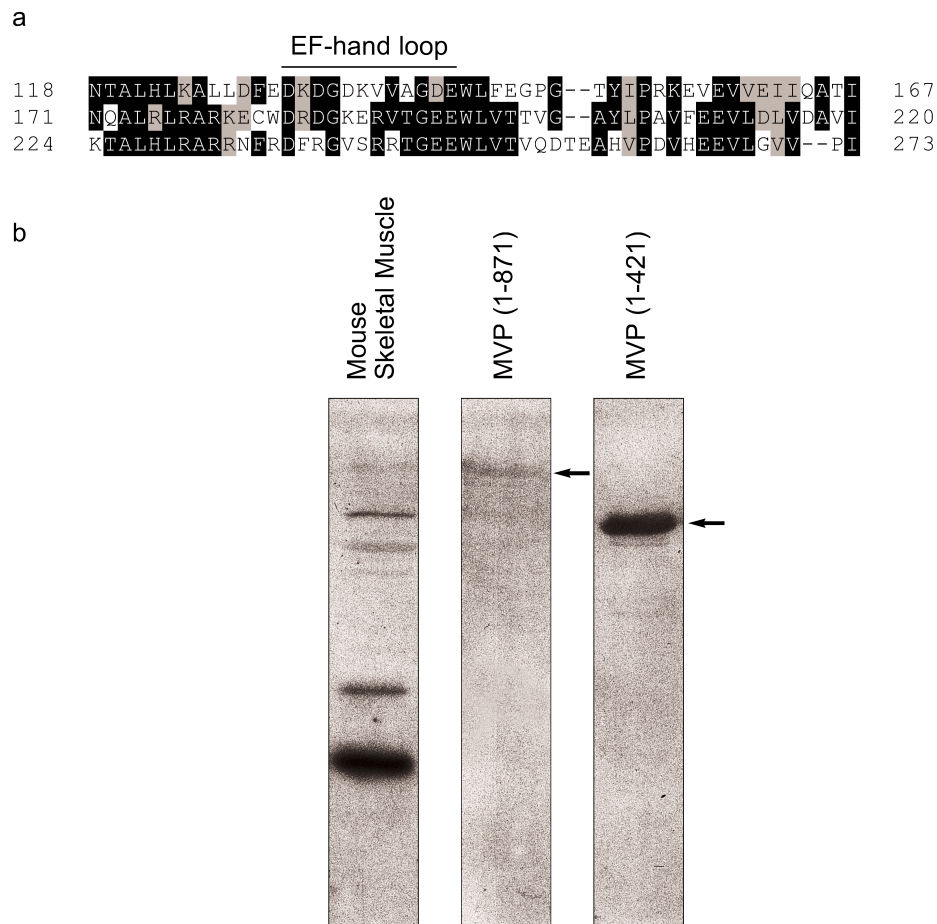


Figure 4.2. **EF-hands are present in the major vault protein.** A, alignment of the three most similar amino acid repeats of human MVP (aa 118-167, aa 171-220, aa 224-273), using the program CLUSTAL W (32). A solid line indicates three putative calcium-binding EF-hand loops. Blocks denote identical (black) or similar (grey) amino acid residues. B, 5 μg of GST purified MVP fragments as well as total mouse skeletal muscle lysate were loaded onto a 15% SDS-PAGE and blotted to nitrocellulose. The blot was used in a calcium overlay assay as described in the materials and methods section.

which consists of five stretches of approximately 50 amino acids. In at least three repeats putative EF-hands could be distinguished (Fig. 4.2A). EF-hands are composed of two alpha helices, separated by a loop structure that consists of about 12 amino acids. In general, amino acid residues at position 1, 3, 5, 7, 9 and 12 are involved in $Ca^{2+}$ binding by co-ordinating the ion directly with their oxygen containing side chains. The oxygen at position 7 comes from the backbone and can be supplied by any amino acid (Table 4.2). Comparison of the EF-hand loops of MVP shows that only the first two loops match the criteria for genuine EF-hand, i.e. contain six amino acid residues that can interact with calcium. In order to test whether human MVP is capable of binding calcium we performed a calcium-binding overlay (Fig. 4.2A). The principle being that even in denatured conditions the EF-hands can bind calcium. We noticed that both MVP (aa 1-871) and the N-terminal half of MVP (aa 1-421) were able to bind calcium. However, consistently more calcium was bound to the N-terminal half resulting in a darker band on the autoradiograph. Possibly the EF-hands of MVP (aa 1-871) are masked by the C-terminal part of MVP. Note that equal amounts of protein were loaded. This means that about two times more MVPn molecules were loaded compared to MVP molecules. However, the difference in intensity between the bands is clearly more then two times. A mouse skeletal muscle lysate, known to contain calcium-binding proteins among which calmodulin of 14 kDa, was used as control (29).

Table 4.2. **Comparison of MVP EF-hand loops with 165 other EF-hands**

| Amino acid | 1 | 2 | 3 | 4 | 5 | 6 | 7 | 8 | 9 | 10 | 11 | 12 |
|---|---|---|---|---|---|---|---|---|---|---|---|---|
| Consensus | X | * | Y | * | Z | G | # | I | x | * | * | z |
| EF1 | D | K | D | G | D | K | V | V | A | G | D | E |
|  | 98 | 28 | 73 | 51 | 56 | 2 | 4 | 13 | 1 | 4 | 27 | 86 |
| EF2 | D | R | D | G | K | E | R | V | T | G | E | E |
|  | 98 | 8 | 73 | 51 | 0 | 0 | 3 | 13 | 11 | 4 | 32 | 86 |
| EF3 | D | F | R | G | V | S | R | R | T | G | E | E |
|  | 98 | 2 | 0 | 51 | 0 | 1 | 3 | 0 | 11 | 4 | 32 | 86 |

Comparison of the three putative calcium-binding EF-hand loops in MVP. The consensus sequence presented is based on 165 other calcium-binding loops. Amino acid residues at positions X, Y, Z, #, x and z are important for calcium binding. G and I indicate conserved amino acid residues glycin and isoleucine, respectively. The numbers indicate the percentage of cases in which the same amino acid residue was found at this position in 165 other calcium-binding loops (31).

*Two-hybrid analysis of VPARP and TEP1*

The minor vault proteins VPARP and TEP1 contain several putative protein-protein interaction domains. Each of these domains could be involved in interactions with other vault components and hence contribute to the structural stability of the complex. As depicted in figure 4.1 we prepared several two-hybrid constructs either expressing the full-length VPARP, its N and C-terminal halves or the BCRT, inter-α-inhibitor and the Von Willebrand domains. We also included a construct expressing the extreme C-terminal amino acids of VPARP (aa 1562-1724; MVPint) that are supposed to interact with MVP (19). The constructs we generated of TEP1 either expressed the full-length TEP1, its N and C-terminal halves, the four repeats at the extreme N-terminal end or the WD40 repeat region. Analysis of the protein fragments in the two-hybrid setting reveals an interaction between the N and C-terminal half of VPARP (Table 4.3). This must be an intramolecular binding site, since full-length VPARP does not interact with either of the two VPARP halves. The intramolecular interaction of VPARP is formed between aa 295-615 of the N-terminal part and aa 1197-1561 of the C-terminal part of VPARP. No interactions of this sort could be observed within TEP1 (data not shown). Furthermore, no intermolecular interactions were detected between two VPARP or between two TEP1 molecules. Expression of the full-length VPARP gave rise to false activation of the reporter genes when expressed in the DNA binding domain vector (these results are indicated by dots in the table). This phenomenon was also observed when this plasmid was transformed to yeast without an activating domain construct (data not shown).

*Interactions between MVP, VPARP and TEP1 to make up the vault complex*

We tested all combinations of MVP, VPARP and TEP1 two-hybrid constructs with the exception of the MVP coiled coil constructs (MVPcI-IV). Only full-length VPARP and its C-terminal half were capable of interacting with MVP (Table 4.3). This interaction appears to be mediated by the previously identified MVP interaction domain (aa 1562-1724) of VPARP (19). Our results show that the N-terminal half of MVP is involved in this interaction. Surprisingly no interaction could be detected between TEP1 and the VPARP or MVP fragments (data not shown).

*Model of the identified interactions*

Figure 4.3 summarizes, in a schematic model, the interactions that were identified by the yeast two-hybrid system. Firstly, two intramolecular interactions could be found between the two halves of MVP and the two halves of VPARP (Fig. 4.3 numbers 1 and 2). Secondly, we identified the coiled coil domain as being responsible for the linking of at least two and possibly six MVP molecules forming a MVP-MVP unit (Fig. 4.3 number 3). This unit probably forms the basis for each of the vault petals. Thirdly, we confirmed earlier reports in which an interaction was described between VPARP and MVP. Our result show that this interaction is specifically mediated by the N-terminal part of MVP (Fig. 4.3 number 4).

**Discussion**

Vaults, the largest ribonucleoprotein particles known to date, were first described more than 15 years ago (4). Since then the individual vault components were identified, characterized and a high-resolution three-dimensional model of the complete vault complex was generated. However, little is known about the assembly of vault proteins into vault particles and the factors that mediate this process. In this study we identified and analyzed distinct structural domains within the vault proteins and in particular the ones involved in protein-protein interactions.

The program COILS predicts the presence of a coiled coil domain in the C-terminal half of all MVP molecules described to date. Our data clearly demonstrate that MVP molecules interact with each other via their coiled coil domain forming MVP-MVP units. Apparently the coiled coil structure of MVP is the main determinant for the vault structure. Interesting in this respect is the MVP sequence of *Ictalurus punctatus* (Genbank acc. nr. AF255664), which with a length of 549 amino acids is about 300 amino acids shorter than other MVP sequences in the database. However, alignment of the various MVP molecules reveals that the *I. punctatus* MVP contains a specific insertion of 32 amino acids (aa 350-381) that is identified as a coiled coil structure. Recently it was found that expression of rat MVP in vault-less Sf9 insect cells results in the formation of vault-like particles, independent of the presence of the two minor

Table 4.3. **Yeast two-hybrid analysis of VPARP and MVP**

| AD↓BD→ | VPARP | VPARPn | VPARPc | BRCT | IαI | vW | MVPint | MVP | MVPn | MVPc |
|---|---|---|---|---|---|---|---|---|---|---|
| VPARP | . | – | – | – | – | – | – | + | + | – |
| VPARPn | . | – | + | – | – | – | – | – | – | – |
| VPARPc | . | + | – | – | – | – | – | + | + | – |
| BRCT | . | – | – | – | – | – | – | – | – | – |
| IαI | . | – | – | – | – | – | – | – | – | – |
| vW | . | – | – | – | – | – | – | – | – | – |
| MVPint | . | – | – | – | – | – | – | + | + | – |

This table presents the observed interactions between various VPARP domains and the interactions between MVP and VPARP in a yeast two-hybrid screen. The '+' indicates an interaction and the '-' indicates combinations that did not interact. A binding site was found between the N-terminal and C-terminal part of VPARP. This must be an intramolecular binding, since full-length VPARP does not interact with either of these fragments. VPARP interacts with the N-terminal part of MVP by means of its MVP interaction domain (MVPint). The dots indicate false positive results.

vault proteins and vault RNA (30). This observation emphases the importance of the coiled coil domain in MVP molecules for the assembly of the total vault complex independent of the other vault proteins.
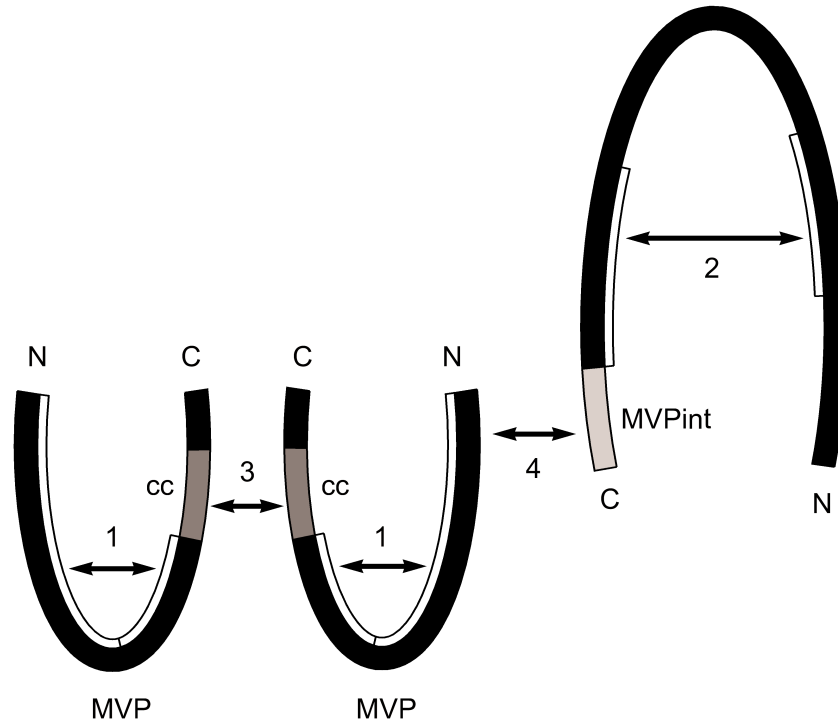


Figure 4.3. **Schematic view of the mapped protein-protein interactions within and between vault proteins.** Depicted are all interactions that were identified and mapped by means of the yeast two-hybrid system. 1, an intramolecular binding was identified between the N-terminal part (aa 1-447) and the C-terminal part (aa 448-651) of MVP. 2, an intramolecular binding site was identified for VPARP between the N-terminal part (aa 295-615) and the C-terminal part (aa 1197-1561). 3, MVP molecules interact with each other via their coiled coil domains (cc, aa 652-800). 4, there is an interaction between VPARP (MVPint, aa 1562-1724) and the N-terminal part of MVP. White blocks indicate the sites for intramolecular interactions.

Next to the coiled coil structure, MVP was found to contain three putative EF-hands in an N-terminal repeat structure. The EF-hand motif consists of approximately 40 amino acids arranged in a helix-loop-helix conformation with calcium ion binding in the loop region. The calcium-binding loops of the first two EF-hands of MVP are quite similar to 165 other EF-hand loops (31), but the third EF-hand loop diverged from the consensus sequence. If we consider the flanking regions of the EF-hand loops, the second EF-hand of MVP resembles most closely a classic EF-hand, whereas the first has an extra insertion between the two α-helices (data not shown). We discovered that full-length MVP indeed could bind calcium, however more calcium

was bound to the N-terminal half of MVP. A possible explanation for this observation might be that the EF-hands of full-length MVP are partly shielded by the C-terminal part of the protein, via the identified interaction between the N and C-terminal halves of MVP. The precise function of calcium binding for the vault complex is not known, but preliminary experiments are pointing to a role of calcium in the folding and assembly of MVP molecules into complete vault particles. Interestingly, particles with vault-like properties were formed after renaturation of guanidinium-HCl denatured purified MVP. This was only the case when calcium was added to the renaturation buffer (data not shown).

When we analyzed the minor vault protein constructs in our yeast two-hybrid setting, we found an interaction between the N-terminal part of MVP and aa 1564-1724 of VPARP, which was previously identified as the MVP interaction domain of VPARP (19). Apparently, in the intact vault complex the C-terminal part of MVP is bound to itself, leaving the N-terminal part accessible for VPARP binding. Furthermore, we found an interaction within the VPARP protein and located this intramolecular interaction between aa 295-615 of the N-terminal part and 1197-1561 of the C-terminal part. We did not find any interaction between TEP1 and the other vault proteins. Even when human vault RNA (hvg1 under control of a polymerase III promoter) was co-expressed in the yeast system, no interactions were found between TEP1/hvg1 and the other vault proteins (data not shown). This may indicate that the association of TEP1 to vaults needs a combination of vault proteins and/or other proteins. It was suggested that the repeat structure at the N-terminus of TEP1 would interact with VPARP (12). However, this was not the case in our two-hybrid screen.

In this study we found several domains that did not appear to be involved in the formation of vaults, e.g. BRCT and WD40 domains. The minor vault proteins, VPARP and TEP1, may need these structural domains to function elsewhere in the cell. For instance, certain domains of TEP1 may only be functional within the telomerase complex. Similarly, the VPARP protein that is also localized in the nucleus may need domains to perform separate functions there (19). Nevertheless, these domains may also play a role within the vault complex, like the binding of possible substrates for VPARP and/or the uptake of putative vault cargo. The identification of such a cargo or substrate may help to clarify the function of the vault complex.

**References**

1. Hamill, D. R. and Suprenant, K. A. Characterization of the sea urchin major vault protein: a possible role for vault ribonucleoprotein particles in nucleocytoplasmic transport. Dev Biol, 190: 117-128, 1997.

2. Abbondanza, C., Rossi, V., Roscigno, A., Gallo, L., Belsito, A., Piluso, G., Medici, N., Nigro, V., Molinari, A. M., Moncharmont, B., and Puca, G. A. Interaction of vault particles with estrogen receptor in the MCF-7 breast cancer cell. J Cell Biol, 141: 1301-1310, 1998.

3. Chugani, D. C., Rome, L. H., and Kedersha, N. L. Evidence that vault ribonucleoprotein particles localize to the nuclear pore complex. J Cell Sci, 106: 23-29, 1993.

4. Kedersha, N. L. and Rome, L. H. Isolation and characterization of a novel ribonucleoprotein particle: large structures contain a single species of small RNA. J Cell Biol, 103: 699-709, 1986.

5. Herrmann, C., Volknandt, W., Wittich, B., Kellner, R., and Zimmermann, H. The major vault protein (MVP100) is contained in cholinergic nerve terminals of electric ray electric organ. J Biol Chem, 271: 13908-13915, 1996.

6. Herrmann, C., Golkaramnay, E., Inman, E., Rome, L., and Volknandt, W. Recombinant major vault protein is targeted to neuritic tips of PC12 cells. J Cell Biol, 144: 1163-1172, 1999.

7. Li, J. Y., Volknandt, W., Dahlstrom, A., Herrmann, C., Blasi, J., Das, B., and Zimmermann, H. Axonal transport of ribonucleoprotein particles (vaults). Neuroscience, 91: 1055-1065, 1999.

8. Scheffer, G. L., Schroeijers, A. B., Izquierdo, M. A., Wiemer, E. A., and Scheper, R. J. Lung resistance-related protein/major vault protein and vaults in multidrug-resistant cancer [In Process Citation]. Curr Opin Oncol, 12: 550-556, 2000.

9. Kickhoefer, V. A., Vasu, S. K., and Rome, L. H. Vaults are the answer, what is the question? Trends in Cell Biol., 6: 174-178, 1996.

10. Kitazono, M., Okumura, H., Ikeda, R., Sumizawa, T., Furukawa, T., Nagayama, S., Seto, K., Aikou, T., and Akiyama, S. Reversal of LRP-associated drug resistance in colon carcinoma SW-620 cells. Int J Cancer, 91: 126-131, 2001.

11. Kitazono, M., Sumizawa, T., Takebayashi, Y., Chen, Z. S., Furukawa, T., Nagayama, S., Tani, A., Takao, S., Aikou, T., and Akiyama, S. Multidrug resistance and the lung resistance-related protein in human colon carcinoma SW-620 cells [see comments]. J Natl Cancer Inst, 91: 1647-1653, 1999.

12. Kong, L. B., Siva, A. C., Kickhoefer, V. A., Rome, L. H., and Stewart, P. L. RNA location and modeling of a WD40 repeat domain within the vault. Rna, 6: 890-900, 2000.

13. Kedersha, N. L., Heuser, J. E., Chugani, D. C., and Rome, L. H. Vaults. III. Vault ribonucleoprotein particles open into flower-like structures with octagonal symmetry. J Cell Biol, 112: 225-235, 1991.

14. Kong, L. B., Siva, A. C., Rome, L. H., and Stewart, P. L. Structure of the vault, a ubiquitous celular component. Structure Fold Des, 7: 371-379, 1999.

15. Kedersha, N. L., Miquel, M. C., Bittner, D., and Rome, L. H. Vaults. II. Ribonucleoprotein structures are highly conserved among higher and lower eukaryotes. J Cell Biol, 110: 895-901, 1990.

16. Kickhoefer, V. A., Stephen, A. G., Harrington, L., Robinson, M. O., and Rome, L. H. Vaults and telomerase share a common subunit, TEP1. J Biol Chem, 274: 32712-32717, 1999.

17. Kickhoefer, V. A., Liu, Y., Kong, L. B., Snow, B. E., Stewart, P. L., Harrington, L., and Rome, L. H. The Telomerase/Vault-associated Protein TEP1 Is Required for Vault RNA Stability and Its Association with the Vault Particle. J Cell Biol, 152: 157-164, 2001.

18. Harrington, L., McPhail, T., Mar, V., Zhou, W., Oulton, R., Bass, M. B., Arruda, I., and Robinson, M. O. A mammalian telomerase-associated protein [see comments]. Science, 275: 973-977, 1997.

19. Kickhoefer, V. A., Siva, A. C., Kedersha, N. L., Inman, E. M., Ruland, C., Streuli, M., and Rome, L. H. The 193-kD vault protein, VPARP, is a novel poly(ADP-ribose) polymerase. J Cell Biol, 146: 917-928, 1999.

20. Jean, L., Risler, J. L., Nagase, T., Coulouarn, C., Nomura, N., and Salier, J. P. The nuclear protein PH5P of the inter-alpha-inhibitor superfamily: a missing link between poly(ADP-ribose)polymerase and the inter-alpha- inhibitor family and a novel actor of DNA repair? FEBS Lett, 446: 6-8, 1999.

21. Faber, K. N., Heyman, J. A., and Subramani, S. Two AAA family peroxins, PpPex1p and PpPex6p, interact with each other in an ATP-dependent manner and are associated with different subcellular membranous structures distinct from peroxisomes. Mol Cell Biol, 18: 936-943, 1998.

22. Nagase, T., Kikuno, R., Ishikawa, K., Hirosawa, M., and Ohara, O. Prediction of the coding sequences of unidentified human genes. XVII. The complete sequences of 100 new cDNA clones from brain which code for large proteins *in vitro*. DNA Res, 7: 143-150, 2000.

23. Gietz, R. D., Schiestl, R. H., Willems, A. R., and Woods, R. A. Studies on the transformation of intact yeast cells by the LiAc/SS- DNA/PEG procedure. Yeast, 11: 355-360, 1995.

24. Duttweiler, H. M. A highly sensitive and non-lethal beta-galactosidase plate assay for yeast. Trends Genet, 12: 340-341, 1996.

25. Fields, S. and Sternglanz, R. The two-hybrid system: an assay for protein-protein interactions. Trends Genet, 10: 286-292, 1994.

26. Guan, K. L. and Dixon, J. E. Eukaryotic proteins expressed in Escherichia coli: an improved thrombin cleavage and purification procedure of fusion proteins with glutathione S-transferase. Anal Biochem, 192: 262-267, 1991.

27. Laemmli, U. K. and Favre, M. Maturation of the head of bacteriophage T4. I. DNA packaging events. J Mol Biol, 80: 575-599, 1973.

28. Towbin, H., Staehelin, T., and Gordon, J. Electrophoretic transfer of proteins

from polyacrylamide gels to nitrocellulose sheets: procedure and some applications. Proc Natl Acad Sci U S A, 76: 4350-4354, 1979.

29.  Maruyama, K., Mikawa, T., and Ebashi, S. Detection of calcium binding proteins by 45Ca autoradiography on nitrocellulose membrane after sodium dodecyl sulfate gel electrophoresis. J Biochem (Tokyo), 95: 511-519, 1984.

30.  Stephen, A. G., Raval-Fernandes, S., Huynh, T., Torres, M., Kickhoefer, V. A., and Rome, L. H. Assembly of vault-like particles in insect cells expressing only the major vault protein. J Biol Chem, 276: 23217-23220, 2001.

31.  Marsden, B. J., Shaw, G. S., and Sykes, B. D. Calcium binding proteins. Elucidating the contributions to calcium affinity from an analysis of species variants and peptide fragments. Biochem Cell Biol, 68: 587-601, 1990.

32.  Thompson, J. D., Higgins, D. G., and Gibson, T. J. CLUSTAL W: improving the sensitivity of progressive multiple sequence alignment through sequence weighting, position-specific gap penalties and weight matrix choice. Nucleic Acids Res, 22: 4673-4680, 1994.

CHAPTER 5

Multiple human vault RNAs:
Expression and association
with the vault complex

*Chapter 5*

**Abstract**

Human vaults are intracellular ribonucleoprotein particles believed to be involved in multidrug resistance. The complex consists of a major vault protein (MVP), two minor vault proteins (VPARP and TEP1) and several small untranslated RNA molecules. Three human vault RNA genes (*HVG1–3*) have been described and a fourth was found in a homology search (*HVG4*). In the literature only the association of hvg1 with vaults was shown *in vivo*. However, in a yeast three-hybrid screen the association of hvg1, hvg2 and hvg4 with TEP1 was demonstrated. In this study we investigated the expression and vault-association of different vault RNAs in a variety of cell lines, including pairs of drug sensitive and drug resistant cells. *HVG1–3* are expressed in all cell lines examined, however, none of the cell lines expressed *HVG4*. This probably is a consequence of the absence of essential external polymerase III promoter elements. The bulk of the vault RNA associated with vaults was hvg1. Interestingly, an increased amount of hvg3 was bound to vaults isolated from multidrug resistant cell lines. Our findings suggest that vaults bind the RNA molecules with different affinities in different situations. The ratio in which the vault RNAs are associated with vaults might be of functional importance.

**Introduction**

The vault complex, with a molecular mass of 13 MDa, is the largest intracellular ribonucleoprotein particle described to date. Fifteen years ago, vaults were first observed in preparations of clathrin-coated vesicles from rat liver as unusual ovoid particles that displayed highly regular dimensions possessing a complex barrel-shaped morphology. The structures were named 'vaults', a term that describes the morphology of the particles, which contain multiple arches reminiscent of vaulted ceilings in cathedrals. Since then vaults of nearly identical size and morphology have been reported to occur in phylogenetic groups as diverse as mammals, avians, amphibians, slime molds, echinoderms, mollusks and protozoa. The mammalian vault particle consists of multiple copies of a 100 KDa major vault protein (MVP), the minor vault proteins (MiVPs) of 193 and 240 kDa and small untranslated RNA molecules of 88 - 141 bases. The precise cellular function(s) of the vault complex are not yet completely clear (for reviews: 1-3).

The bulk of the vaults appear to reside in the cytoplasm. However, there are reports that describe vaults to be associated with the nucleus (4-6). Several groups reported on the involvement of vaults with intracellular transport (7-9) and nucleocytoplasmic transport (4-6). In addition, other lines of evidence suggest that vaults may function in intracellular detoxification processes and as a consequence function in multidrug resistance (MDR). Expression of MVP reflects the chemoresistance profile of many tumor cell lines and untreated cancers (3, 10-12). Furthermore, it was shown in several MDR cell lines that not only MVP was upregulated, but other vault components as well (13, 14). The most compelling data that link vaults to MDR comes from Kitazono *et al.* (15, 16). They used MVP-specific ribozymes in SW620 cells, which were induced by sodium butyrate to overexpress MVP. In this setting it was demonstrated that the reduction of MVP expression reverses the drug-resistant phenotype of the sodium butyrate treated cells. It is still unclear by which molecular mechanism vaults function in MDR. However, the experiments by Kitazono *et al.* suggest that vaults play a role in MDR by blocking or preventing the accumulation of the anthracycline doxorubicin in the nucleus.

The mammalian vault complex is assembled into a typical hollow barrel-like structure with an 8-2-2 symmetry. It has an invaginated waist and two protruding caps, which most likely consist of the minor vault proteins and the vault RNA (17-20). The major vault protein is believed to be the main structural determinant of the complex, comprising 70% of its molecular mass. Each vault particle is composed of 96 MVP molecules, eight molecules of p193, two molecules of p240 and at least six molecules of vRNA. The p193 subunit contains a distinct domain with similarity to the catalytic domain of poly (ADP-ribose) polymerase (PARP). It was subsequently demonstrated that p193 catalyses the ADP-ribosylation of itself and MVP (21). No other substrates for p193 have been described so far. Because of the PARP activity of p193 it was

renamed vault PARP (VPARP). The p240 subunit was found to be identical to a previously described component of the telomerase complex, the telomerase-associated protein (TEP1) (22, 23). The precise role of this subunit within the telomerase complex is not yet clear except that it is able to bind telomerase RNA. In a three-hybrid system TEP1 was shown to associate with vault RNA (22). Recently, it was found that TEP1 is required for a stable association of the vault RNA with the vault complex (20).

The role of the vault RNA is still an enigma. However, based on experiments in which degradation of the vault RNA by RNase treatment did not lead to morphological changes, the vault RNA is more likely to be a functional rather than a structural component (17, 19). Three related human vault RNA genes (*HVG1-3*; Genbank accession numbers: AF045143, AF045144 and AF045145) have been described; a fourth gene was found in a homology search (*HVG4*) (13, 22). It was estimated that about 20% of the expressed vault RNA is associated to the vault complex (13). In a three-hybrid analysis the association of hvg1, hvg2 and hvg4 to TEP1 was shown (22). However, the only vault RNA of which an association with vaults has been described *in vivo* is hvg1 (13). To study this discrepancy we have analyzed the expression and vault-association of vault RNA in 14 human cell lines, including various drug sensitive ones and their drug resistant counterparts. Furthermore, we examined which vault RNAs are present in the pool of free vault RNA and we have analyzed the polymerase III promoter elements of the vault RNA genes.

**Materials and methods**

*Cell lines and culture conditions*
The following human cell lines were used: the non-small cell lung carcinoma cell line SW1573, its doxorubucin (DOX) selected MDR variant SW1573/2R120 (24), the small cell lung carcinoma cell line GLC4 and its DOX-selected derivative GLC4/ADR (25); The multiple myeloma cell line 8226 S and its DOX-selected variant 8226 D40 (26); The epidermoid cell line KB 3-1 and two colchicine selected derivatives KB 8 and KB 8-5 (27); The colorectal adenocarcinoma cell line SW620, breast adenocarcinoma cell line MCF7 (28), cervix epitheloid carcinoma cell line HeLa, embryonal kidney cell line 293 transformed with adenovirus 5 DNA and the bone marrow stromal cell line L88/5 (29). All cell lines (except for MCF7 and L88/5) were maintained in DMEM (Life technologies, Paisley, Scotland) supplemented with 10% fetal calf serum, 1 mM pyruvate and 50 µg/ml gentamycin at 37°C under an atmosphere containing 5% $CO_2$. The cell lines MCF7 and L88/5 were maintained in RPMI (Life technologies, Paisley, Scotland) supplemented with 10% fetal calf serum and 50 µg/ml gentamycin and were cultured under the same conditions. Doxorubicin was added to SW1573/2R120, GLC4/ADR and 8226 S at concentrations of 120 nM, 240 nM and 375 nM, respectively. Colchicine was added to KB 8 and KB 8-5 at concentrations of 12.5 nM and 25 nM, respectively.
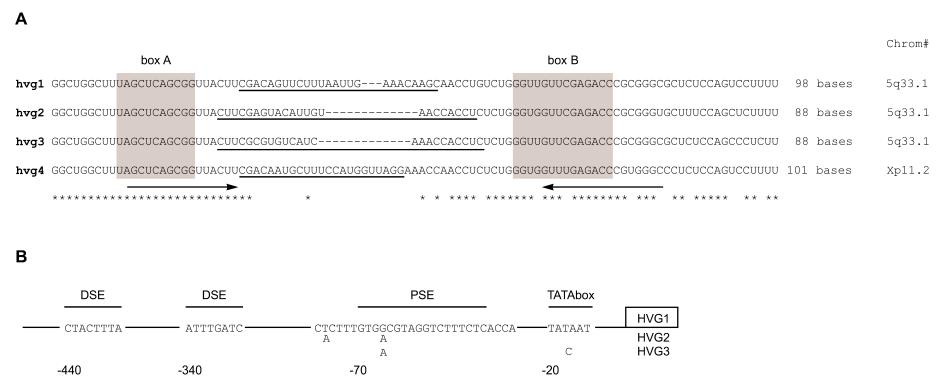
**A**



**B**



Figure 5.1. **Human vault RNA sequences: sequence alignment, chromosomal localization, primers and probes.** A PCR using oligonucleotides based on conserved regions in vault RNAs (arrows) identified four related but different vault RNA genes, corresponding to *HVG1-3* which are localized in a triple repeat on chromosome 5q33.1, but also a putative vault RNA gene on chromosome Xp11.2 designated *HVG4*. A, Depicted is a sequence alignment of the respective hvg sequences using the CLUSTAL program. Asterisks below the sequence indicate identical nucleotides. The gray boxes indicate internal RNA polymerase III promoter elements (box A and box B). The vault RNA species-specific oligonucleotide probes that were used are underlined. As universal probe the reverse primer was used. B, Summarizes the putative conserved external promoter elements found upstream of *HVG1-3*. None of these sequence elements could be detected upstream of *HVG4*.

*Antibodies*
Immunoblotting experiments were performed with the rabbit polyclonal anti-(MVP) and the mouse monoclonal anti-(p193) (mAb p193-4) (14). The mouse monoclonal anti-(β-tubulin) was purchased from the Sigma-Aldrich Corporation (St. Louis, MO). Species-specific anti-Ig antibodies conjugated to horseradish peroxidase (HRP) were obtained from Jackson ImmunoResearch Laboratories Inc. (West Grove, PA). In immunoprecipitation experiments the rabbit polyclonal anti-(MVP) and the mouse monoclonal anti-(MVP) (LRP-56; Monosan, Uden, The Netherlands) were used. The preimmune serum and the isotypic IgG2b were used as controls in these experiments.

*SDS-PAGE and Western analysis*
Cell lysates were subjected to SDS-PAGE after which the size-fractionated proteins were transferred to nitrocellulose. By incubating the membranes in TBST (50 mM Tris-Cl pH 7.5, 100 mM NaCl, 0.05% (vol/vol) Tween 20) containing 5% (wt/vol) non-fat dry milk (Bio-Rad Laboratories, Hercules, CA) the remaining protein binding sites were saturated. Subsequently the membranes were incubated with primary and secondary antibodies diluted in the same buffer. Immune-complexes were detected using the BM Chemiluminescence Blotting Substrate (POD) kit (Roche, Mannheim, FRG) and visualized on Hyperfilm™ ECL™ (Amersham Pharmacia Biotech, Uppsala, Sweden).

*Northern analysis*

RNA was isolated from freshly harvested cell pellets. The isolation was performed using RNAzol™ B according to recommendations from the manufacturer (Campro Scientific, Veenendaal, The Netherlands). About 15 μg of total RNA was dissolved in RNA loading buffer (45 mM Tris-borate, 1 mM EDTA, 90% (vol/vol) formamide). RNA samples were separated by electrophoresis on a 10% poly-acrylamide gel containing 8 M urea. The separated RNA was transferred to a Zeta-probe membrane (Bio-Rad Laboratories, Hercules, CA) using a semi-dry blotting method. In brief: RNAs were electroblotted at 10 Volts for 15 minutes followed by 30 Volts for 30 minutes in TAE buffer (40 mM Tris-acetate, 1 mM EDTA). Afterwards the membrane was cross-linked by UV (Bio-Rad GS gene linker) and prehybridized in Church buffer (30) at 55°C for at least two hours. The following oligonucleotide probes were used: HVG1: 5'-GCTTGTTTCAATTAAAGAACTGTCG; HVG2: 5'-AGGTGGTTACAATGTACTCGAAG; HVG3: 5'-GAGGTGGTTTGA-TGACACGCGAAG and HVG4; 5'-CCTAACCATGGAAAGCATTGTCG. Alternatively a universal probe (5'- GCCCGCGGGTYTCGAAC) was used, encompassing a region shared by all human vault RNAs. The probes were end-labeled with [γ$^{32}$P]-dATP. Hybridizations were performed at 55°C in Church buffer for 3 - 4 hours. Subsequently the membranes were washed twice at room temperature in 2 x SSC, 0.1% SDS (20 x SSC: 3 M sodium chloride, 0.3 M tri-sodium citrate dihydrate, pH 8) and once in 5 x SSC, 0.1% SDS for 5 minutes at 55°C. Blots were exposed to Kodak X-Omat™ AR film (Kodak, Rochester, NY) at -80°C or exposed to a Phosphorimager screen (Molecular Dynamics, Sunnyvale, CA) for quantitation. Afterwards the blots were stripped and re-probed with a 5S rRNA specific oligonucleotide (5'-TCTCCCATCCAAGTACTAACCAGGCC) as a control for equal loading.

*Cloning and sequencing of human vault RNA genes*

Putative human vault RNA genes were cloned by PCR using two primers, based on conserved regions in the rat and bullfrog vault RNA sequences (31). The forward primer was 5'-AGCTCAGCGGTTACTTC and the reverse primer was 5'-GCCCGCGGGTYTCGAAC. As template we used 300 ng human genomic DNA. The PCR was performed with *Pfu* polymerase (Stratagene, La Jolla, CA) using the following conditions: 95°C for 4 minutes, then 30 cycles of 94°C for 30 seconds, 50°C for 1 minute, 72°C for 2 minutes followed by 72°C for 8 minutes. The product of approximately 100 bp was excised from an agarose gel, cloned into pCR-Blunt (Invitrogen, Carlsbad, CA) and analyzed by sequencing. The plasmids formed (pCR-HVG1, pCR-HVG2, pCR-HVG3, pCR-HVG4) were used as a control for the specificity of the probes.

*Immunoprecipitation, RT-PCR and Southern analysis*

An IgG fraction of rabbit polyclonal anti-(MVP) was coupled to Protein A-Sepharose beads (Amersham Pharmacia Biotech, Uppsala, Sweden) according to the
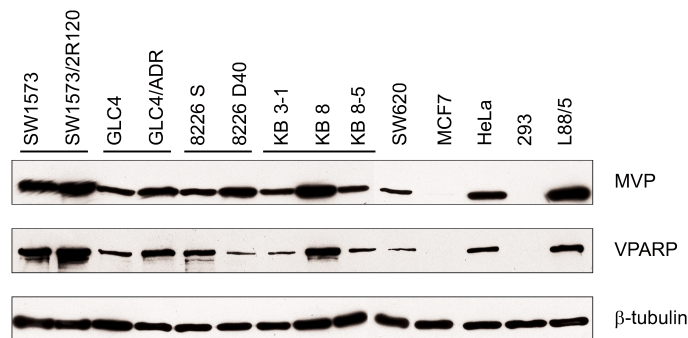
Figure 5.2. **Major vault protein (MVP) and VPARP in human cell lines.** Cell extracts were prepared from 14 human cell lines derived from different tissues, including drug sensitive and drug resistant pairs (indicated by the solid lines). 25 μg of total protein was subjected to SDS-PAGE and blotted onto nitrocellulose membranes. Identical blots were incubated with anti-(MVP), anti-(193 kDa) or anti-(β-tubulin) as a loading control.

recommendations of the manufacturer. Immunoprecipitations were carried out for 2 - 14 hours at 4°C in lysis buffer (PBS containing 0.2% (vol/vol) Triton-X100, 1% (wt/vol) BSA) supplemented with proteinase inhibitors cocktail (Complete™, Roche, Mannheim, FRG) and 0.1 U/μl RNAsin (Promega, Madison, WI). Subsequently the beads were washed two times with lysis buffer and three times with PBS containing 0.2% (vol/vol) Triton-X100. The beads were suspended in 0.5 ml RNAzol™ B (Campro Scientific, Veenendaal, The Netherlands) for RNA isolation or in protein sample buffer for Western analysis. When RNA was used for RT-PCR, the immunoprecipitated vaults were treated with DNase I (RNase free) prior to the addition of RNAzol. After treatment RNAzol™ B was added and RNA could be isolated. By using random hexameres, cDNA was generated in a reverse transcriptase reaction using Superscript™ RT (Life Technologies, Paisley, Scotland). On the generated cDNA, a PCR reaction using *Taq* polymerase (Promega, Madison, WI) was performed with the universal primers described above. The RT-PCR products were separated on a 2% agarose gel and were transferred to a Hybond™-N⁺ Nylon Transfer Membrane (Amersham Pharmacia Biotech, Uppsala, Sweden). The blots were cross-linked by UV and hybridized as described above (Northern Analysis).

*Immunoprecipitation for Northern analysis*
Mouse monoclonal anti-(MVP) (LRP-56) was coupled to Protein A-Sepharose beads (Amersham Pharmacia Biotech, Uppsala, Sweden) according to the manufacturer. The immunoprecipitations were carried out for two hours at 4°C in lysis buffer (50 mM Tris pH7.5, 1.5 mM MgCl₂, 75 mM NaCl, 0.5% (vol/vol) NP40) supplemented with proteinase inhibitors cocktail (Complete™, Roche, Mannheim, FRG) and 0.1 U/μl RNAsin (Promega, Madison, WI). The beads were washed three times with lysis buffer and RNAzol™ B was added to the beads. The supernatant of the first

immunoprecipitation was used for a second immunoprecipitation using the same conditions. The beads of the second immunoprecipitation were also dissolved in RNAzol™ B after the wash steps. RNA was isolated according to the manufacturer (Campro Scientific, Veenendaal, The Netherlands) RNA of the two immunoprecipitations of the same cell line were pooled, separated on a 10% poly-acrylamide gel containing 8 M urea, semi-dry blotted and detected as described before.

**Results**

*Cloning and analysis of human vault RNA genes*
To screen the human genome for genes encoding putative vault RNAs, a PCR was performed using primers based on the conserved parts of the rat and bullfrog vault RNA. The amplified fragments of approximately 100 bp were cloned and analyzed by sequencing. The analysis of 27 independent clones revealed the four previously described vault RNA genes (*HVG1-4*). No additional genes encoding vault RNAs were found. A BLAST search showed that *HVG1-3* are arranged in a triple repeat structure on chromosome 5q33.1 (BAC clone 119j3 (LBNL H175)) and *HVG4* is localized on chromosome Xp11.2 (PAC 339A18). The sequences spacing the *HVGs* on chromosome 5, about 7600 bp between *HVG1/HVG2* and 7200 bp between *HVG2/HVG3*, do not encode any open reading frames. The alignment of the four detected hvg species (Fig. 5.1A) clearly shows two conserved stretches at both ends, which contain polymerase III internal promoter elements (A and B boxes). In between these conserved regions there is a part of variable length with no significant homologous stretches. Notably, the *HVG1* gene contains a small duplication of 47 bp after the stop codon (TTTT). This repeat includes a second B box and ends with a genuine stop. This larger fragment was also amplified by PCR on genomic DNA with the universal primers, whereas a PCR performed on cDNA prepared from human mononuclear cells isolated from bone marrow did not give rise to this larger *HVG1* fragment implying it is not expressed (data not shown). Although the stop codon of *HVG3* is mutated to TCTT, it seems to be functional, since a *HVG3* expression product of the right size (88 bases) could be detected.

Comparison of upstream sequences of *HVG1-4* revealed a high degree of similarity between *HVG1*, *2* and *3*. Several external polymerase III promoter elements could be identified: a TATA box at position -20, a proximal sequence element (PSE) at position -70 and two distal sequence elements (DSE) at -340 and -440 (Fig. 5.1B). The upstream sequence of *HVG4* was totally different and did not contain any recognizable external promoter elements. The TATA box of *HVG3* is different from the other *HVGs*, TACAAT instead of TATAAT.

*Characterization of human cell lines for MVP and VPARP expression*
The major vault protein is expressed in all cell lines examined although expression levels vary considerably (Fig. 5.2). Low levels were found in the breast adenocarcinoma

cell line MCF7 and the embryonal kidney cell line 293. MVP could only be detected in these cell lines if vaults were concentrated by immunoprecipitation (data not shown). MVP is overexpressed in a number of drug resistant cancer cell lines such as the SW1573/2R120 and GLC4/ADR in which the drug resistance is not mediated by P-glycoprotein (10, 13). In general a 2 - 5 fold increase in MVP levels is detected by Western analysis in the resistant cell lines. Usually the difference in MVP levels between GLC4 and GLC4/ADR is more pronounced than the difference observed in the SW1573 and SW1573/2R120 combination. The reason why vault levels vary is not exactly clear and may be influenced by culture conditions. Interestingly, vaults are also overexpressed in the P-glycoprotein expressing resistant cell lines 8226 D40 and KB8. Generally, the expression levels of VPARP (p193) closely follow the MVP levels as would be expected, as they are both components of the same complex. However, this is not the case in the 8226 S and 8226 D40 cell lines.

*Three of the vault RNA molecules are expressed in cell lines*
Northern analysis was used to determine the expression levels of the four vault RNA species. Individual vault RNAs were detected by oligonucleotide probes (see Fig. 5.1A) that hybridize exclusively to specific vault RNAs. A universal probe, corresponding to the reverse primer, hybridizes to the conserved box B element that is present in all vault RNAs (Fig. 5.3A). Identical Northern blots were hybridized with these probes and with a 5S rRNA probe as a control for equal loading. There is expression of hvg1, 2 and 3 in all cell lines examined (Fig. 5.3B). Longer exposure times revealed low levels of hvg2 and hvg3 in the GLC4 and GLC4/ADR cells and hvg3 in the 8226 S and 8226 D40 cells. Note that two hybridizing bands were observed with the HVG3 probe. The RNAs migrate so close together in the gel system that they cannot differ more than a few bases in length. It is not clear whether these RNAs represent two true variants of hvg3 or whether they are the result of degradation during the procedure. In none of the cell lines hvg4 was detected. Hybridization of a Northern blot with the universal probe verified the results and showed two bands in most lanes. The top band corresponded to hvg1 of 98 bases and the lower band to the co-migrating hvg2 and 3, both 88 bases in length. Quantification of the signal in each lane and calculation of the ratio hvg1 versus hvg2/3 showed that the expression ratio is cell line dependent, the ratio being more or less equal in HeLa and the SW1573 and 8226 S cells. A slightly increased ratio was detected in the respective resistant derivatives, indicating a higher expression level of hvg1. The KB series and the L88/5 cells contained approximately twice as much hvg1 as hvg2/3, while the SW620, MCF7 and in particular 293 expressed more hvg2/3 than hvg1.

*Cytoplasmic pool of vault RNA consists of hvg1-3*
To check if the hvg species are present in a non-vault associated fraction, we performed three consecutive immunoprecipitations with rabbit polyclonal anti-(MVP) bound to protein A sepharose beads. On a Western blot equal portions of the precipitated proteins (1, 2 and 3) and the remaining supernatant (S) were loaded (Fig. 5.4A). No
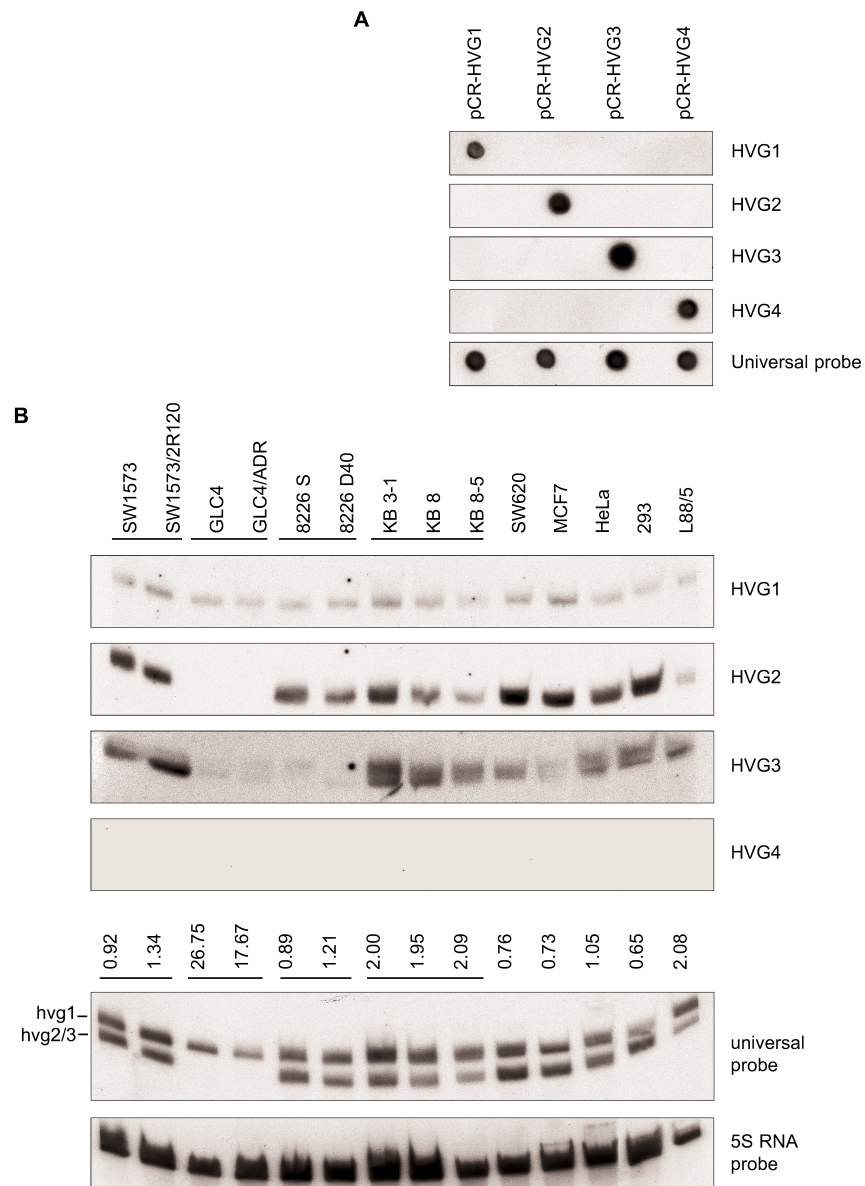
Figure 5.3. **Northern analysis of expressed vault RNAs. A,** To check the hybridization specificity of the various probes, plasmids containing one of the four putative *HVGs* were spotted on Zeta-probe (100 ng each), cross-linked and hybridized with the different probes as indicated. B, 15 μg of total RNA was size-fractionated on a polyacrylamide gel and blotted on Zeta-probe as described in the material and methods section. The blots were hybridized with the hvg specific probes, the universal probe and a 5S rRNA probe. The numbers on top of the universal probe panel indicate the hvg1:hvg2/3 ratio in each of the lanes as quantified using ImageQuant version 3.3 (Molecular Dynamics).
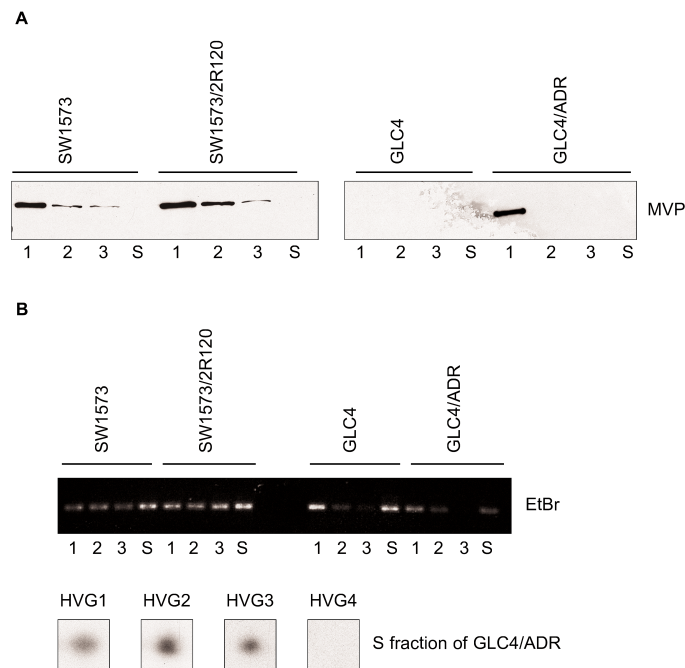
Figure 5.4. **Hvg1-3 are present in a pool not associated with the vault complex.** Vaults were cleared from cell lysates ($10^6$ cells) by three consecutive immunoprecipitations (1, 2 and 3). The cell lines used were the drug sensitive SW1573 and GLC4 and their drug resistant - vault overexpressing - counterparts. A, Western analysis shows the decrease in MVP signal in lanes 1, 2 and 3 respectively. Lane S contains an equal portion of the remaining supernatant, which is cleared from vaults. Note that the expression of MVP in GLC4 is below detection level. B, RNA isolated from the same fractions was used in a RT-PCR procedure. Equal portions of PCR product were loaded onto an agarose gel and stained with ethidium bromide. The vault-cleared supernatant still contains vault RNA. The pool of vault RNA (fraction S) from the drug resistant cell line GLC4/ADR was used for Southern analysis. The blots were hybridized using probes for hvg1, hvg2, hvg3 and hvg4.

residual MVP signal could be detected in the supernatant, indicating that it was cleared from vault particles. From the same samples RNA was isolated that was converted to cDNA and used in a PCR with a primer set capable of amplifying all vault RNA species. Equal portions of the PCR product were loaded onto an agarose gel, which was stained with ethidium bromide (Fig. 5.4B). The signal of the amplified vault RNAs decreased with each immunoprecipitation, which is clearly visible in the case of the GLC4 and GLC4/ADR cells. However, in all cell lines there was a strong signal in the supernatant fraction (S), indicating the presence of a pool of vault RNA. Southern analysis on the S fractions revealed that in all cases the pool consists of hvg1, 2 and 3 (only S fraction of GLC4/ADR is shown).

*All expressed vault RNA species associate with the vault complex*

When all vault RNA species have the same affinity for the vault complex, one would expect the expression ratio of hvg1-3 to be similar to the ratio found associated with the vault complex. Therefore we isolated RNA from immunoprecipitated vaults and dertermined the levels of the hvg species by Northern analysis using the universal probe (Fig. 5.5). In several parental cell lines we found that the bulk of the associated vault RNA is hvg1. On average, 50 percent of the expressed vault RNA is hvg1, however, about 80 percent of the vault RNA found bound to the vault complex is hvg1 (Table 5.1). Clearly the hvg expression ratio does not reflect the ratio in which hvgs are associated with the complex.

Table 5.1. **Percentage hvg1 expressed versus percentage hvg1 bound to vaults**

| Cell lines | % hvg1 expressed | % hvg1 associated |
|------------|------------------|-------------------|
| SW1573 | 48 | 67 |
| 8226 S | 47 | 90 |
| KB 3-1 | 67 | 81 |

This table represents the percentage of hvg1 that is expressed and the percentage of hvg1 that is associated to vaults in three parental cell lines. The percentages were calculated from the quantitation of Northern analysis shown in Fig. 5.3 and 5.5. Note that 100% = %hvg1 + %hvg2/3.

To further assess which vault RNA species are associated with the vault complex we immunoprecipitated vaults from each cell line. Subsequently, vault RNA was isolated and converted to cDNA. Vault RNA sequences were amplified by PCR, using the universal primers. Southern analysis using hvg specific probes demonstrated that hvg1 is associated with the vault complex in all cell lines (Fig. 5.6A). Association of hvg2 and hvg3 with the complex was observed as well. The hvg3 signal was consistently increased in the multidrug resistant cell lines when compared with the hvg3 level found in their drug sensitive parents. This phenomenon was not seen on the hvg1 and hvg2 blots indicating that this effect cannot be attributed to the overexpression of vaults. Using this sensitive RT-PCR assay we did not detect an hvg4 signal, which is in agreement with the absence of hvg4 expression.

To confirm these semi-quantitative PCR results, we isolated RNA from immunoprecipitated vaults from a large number of GLC4 and GLC4/ADR cells (Fig. 5.6B). Again the bulk of the vault RNA associated with vaults was hvg1, as was clearly shown when the blot was hybridized with the universal probe. In this exposure no signal of hvg2 and hvg3 could be detected. When the Northern blot, after stripping, was incubated with the HVG3 specific probe, a clear hvg3 signal was observed after a long exposure time. The hvg3 signal was increased in the drug resistant cell line.

**Discussion**

Degradation of vault RNA does not give rise to morphological alterations of the vault complex (17, 19). Therefore, it is believed that vault RNA is of functional importance to the complex. Since there are indications of vaults playing a role in multidrug resistance (MDR), we reasoned that this might be (partially) mediated by the vault RNAs expressed and associated with the vault complex.
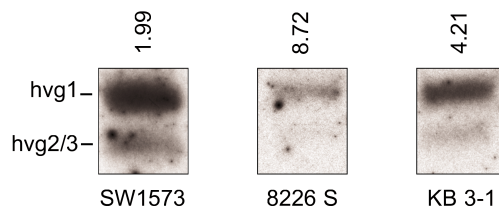


Figure 5.5. **Northern analysis of immunoprecipitated vaults.** RNA from vaults isolated by immunoprecipitation was subjected to PAGE in the presence of urea and transferred to Zeta-probe membrane. Hybridization with the universal probe revealed two bands. The numbers on top of the blot indicate the hvg1:hvg2/3 ratio as quantified using ImageQuant version 3.3.

We screened the human genome for all putative vault RNA genes by PCR using oligonucleotides that overlap conserved internal polymerase III promoter elements. After sequence analysis of 27 independent clones no other than the four previously described vault RNA species (*HVG1-4*) were found. We may conclude that in total there are four putative human vault RNA genes. Hvg1 was already shown to be associated with the vault complex *in vivo* (13). Hvg1, 2 and 4 were shown to be able to associate with TEP1 in a yeast-based three-hybrid system (22). TEP1 is also capable of binding telomerase RNA. However, telomerase RNA cannot be bound to TEP1 that is incorporated in the vault complex, since we were unable to detect telomerase RNA by RT-PCR in immunoprecipitated vaults (data not shown). It is not entirely clear whether vault RNA interacts with other vault components, but it was demonstrated by UV cross-linking that vault RNA primarily interacts with the minor vault proteins and not with MVP (13). The questions we focused on in this study are: Which vault RNA species are expressed in human cells and which are associated to the complex *in vivo*? And is there a relation between vault RNA association and the MDR phenotype of human cancer cell lines?

A Genbank search with the *HVG* sequences showed that the genes encoding *HVG1-3* are arranged in a triple repeat on the long arm of chromosome 5 at position 5q33.1 whereas the *HVG4* gene is located on the X chromosome at position Xp11.2. All four genes have the typical polymerase III internal type-2 A and B box elements, but only
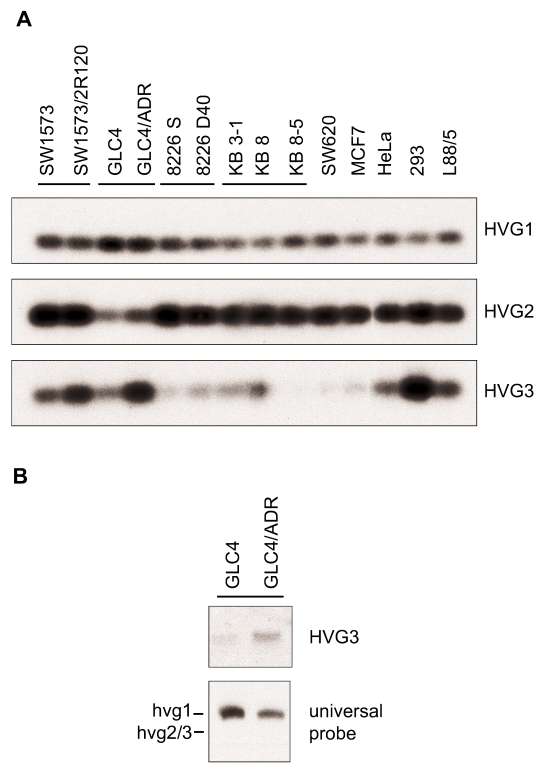
Figure 5.6. **Vault RNA species associated with the vault complex.** A, Vaults were purified by immunoprecipitation after which the associated vault RNAs were isolated and amplified in a RT-PCR procedure using the universal oligonucleotide primers. The PCR products were loaded onto an agarose gel and blotted to Hybond N⁺. The presence of the different vault RNA species was examined by hybridization using specific vault RNA oligonucleotide probes. B, Depicted is the result of a Northern analysis performed with vault RNA isolated from immunoprecipitated vault particles from GLC4 and its drug selected counterpart GLC4/ADR. The blot was hybridized with the universal probe and after stripping, hybridized with the hvg3 probe. Note that exposure time differ between the different blots.

the genes for hvg1-3 harbor external type-3 TATA, proximal and distal sequence elements. The hvg sequences diverge and are unique in the region between A and B box elements. The distance between these elements is 41 bases in *HVG1*, 31 bases in *HVG2* and *HVG3* and 44 bases in *HVG4*. These differences may have consequences for the transcription efficiency (32). Most likely the *HVGs* have originated through gene duplication. It is noteworthy that the bullfrog has two vault RNA genes whereas the genome of rat and mice have only a single gene. Because vault RNA genes of only a few organisms are available, it cannot be concluded whether there was ancestrally a single gene or multiple copies. Interesting in this respect is the fact that a repeat of the last 46 basepairs of the *HVG1* gene directly follows its stop sequence TTTT. If the first

stop would be absent this would result in a vault RNA containing one A box and two B boxes with a size very similar to the vault RNA found in rodents (31). This is not the case in the genes for hvg2 and 3.

We set out to determine the vault RNA expression levels in various human cell lines, including drug resistant ones that overexpress vaults and their drug sensitive parental cell lines. It was found that most cell lines express hvg1 as well as hvg2 and 3, although the latter two at a lower level. By contrast, no transcript of *HVG4* was found. Vilalta *et al.* (33) showed that transcription of rat vault RNA is dependent on both internal and external promoter elements. This is in agreement with the fact that we did not observe expression of *HVG4* in the 14 cell lines examined. Although the *HVG4* gene resembles the other HVGs closely and contains the type-2 internal promoter elements, the external promoter elements are lacking. When vaults were depleted from a cell lysate by subsequent immunoprecipitations a pool of free vault RNA remained in the vault-cleared lysate. This pool consists of all three vault RNA species.

When we investigated which hvg species were actually associated with the vault complex we found that all three expressed species were coimmunoprecipitated with intact vaults particles. Clearly the bulk of the vault RNA bound to the vault complex was hvg1, but also hvg2 and hvg3 were detected. The expression level of hvg2/3 is comparable in both sensitive and resistant cells. However, a sensitive RT-PCR procedure combined with Southern analysis suggested that the amount of associated hvg3 was increased in vaults complexes isolated from multidrug resistant cell lines. These results were confirmed in a more direct experiment in which levels of the various associated hvg species were determined by Northern analysis. In agreement with previous experiments, higher levels of hvg3 were associated with vaults in MDR cell lines. These results indicate that the enhanced level of associated hvg3 may be mediated by a change in affinity of the vault complex for the vault RNA species in response to certain functional cues.

In a recent study Siva *et al.* (34) describe that the ovarian carcinoma cell line A2780, when transfected with MVP (35), not only showed elevated MVP levels, but that VPARP and TEP1 were overexpressed as well. Since the hvgs are present in excess in a non-vault associated pool, they were supposed not to be rate limiting for vault assembly. These vault-component overexpressing cells did not appear to be more resistant to drugs than the parental cells. Consequently Siva *et al.* conclude that vaults may be necessary for MDR but are not sufficient and other mechanisms are underlying vault-mediated MDR. Our results suggest that the ratio of the vault-associated hvg species may mediate the role of vaults in MDR.

In patients suffering from myelodysplastic syndrome (MDS) and acute myeloid leukemia (AML) a loss of chromosome 5 and partial chromosome 5 deletions are associated with poor prognosis (36, 37). Notably the human vault RNA genes are

located in the region that is frequently involved in these chromosomal deletions (5q31-5q34). Breakpoints in this region might disregulate vault RNA expression and change vault RNA ratios, which may influence vault function in MDR and as such influence treatment outcome in these patients. Further studies are necessary to test this hypothesis.

The data presented in this study demonstrate that of the four putative *HVGs* described in literature only three are transcribed (*HVG1-3*). Furthermore we show that only a part of the expressed hvg species is associated with the vault complex at a ratio that does not reflect the expression ratio. The bulk of the vault RNA attached to vaults is hvg1 and a small amount is hvg2 and 3. The increased level of vault-attached hvg3 in MDR cell lines implies that the ratio in which hvg species are associated with the complex may determine its function.

*Chapter 5*

## References

1. Rome, L., Kedersha, N., and Chugani, D. Unlocking vaults: organelles in search of a function. Trends in Cell Biol., 1: 47-50, 1991.

2. Kickhoefer, V. A., Vasu, S. K., and Rome, L. H. Vaults are the answer, what is the question? Trends in Cell Biol., 6: 174-178, 1996.

3. Scheffer, G. L., Schroeijers, A. B., Izquierdo, M. A., Wiemer, E. A., and Scheper, R. J. Lung resistance-related protein/major vault protein and vaults in multidrug-resistant cancer. Curr Opin Oncol, 12: 550-556, 2000.

4. Abbondanza, C., Rossi, V., Roscigno, A., Gallo, L., Belsito, A., Piluso, G., Medici, N., Nigro, V., Molinari, A. M., Moncharmont, B., and Puca, G. A. Interaction of vault particles with estrogen receptor in the MCF-7 breast cancer cell. J Cell Biol, 141: 1301-1310, 1998.

5. Hamill, D. R. and Suprenant, K. A. Characterization of the sea urchin major vault protein: a possible role for vault ribonucleoprotein particles in nucleocytoplasmic transport. Dev Biol, 190: 117-128, 1997.

6. Chugani, D. C., Rome, L. H., and Kedersha, N. L. Evidence that vault ribonucleoprotein particles localize to the nuclear pore complex. J Cell Sci, 106: 23-29, 1993.

7. Herrmann, C., Golkaramnay, E., Inman, E., Rome, L., and Volknandt, W. Recombinant major vault protein is targeted to neuritic tips of PC12 cells. J Cell Biol, 144: 1163-1172, 1999.

8. Herrmann, C., Volknandt, W., Wittich, B., Kellner, R., and Zimmermann, H. The major vault protein (MVP100) is contained in cholinergic nerve terminals of electric ray electric organ. J Biol Chem, 271: 13908-13915, 1996.

9. Li, J. Y., Volknandt, W., Dahlstrom, A., Herrmann, C., Blasi, J., Das, B., and Zimmermann, H. Axonal transport of ribonucleoprotein particles (vaults). Neuroscience, 91: 1055-1065, 1999.

10. Scheper, R. J., Broxterman, H. J., Scheffer, G. L., Kaaijk, P., Dalton, W. S., van Heijningen, T. H., van Kalken, C. K., Slovak, M. L., de Vries, E. G., van der Valk, P., and *et al.* Overexpression of a M(r) 110,000 vesicular protein in non-P- glycoprotein-mediated multidrug resistance. Cancer Res, 53: 1475-1479, 1993.

11. Izquierdo, M. A., Scheffer, G. L., Flens, M. J., Giaccone, G., Broxterman, H. J., Meijer, C. J., van der Valk, P., and Scheper, R. J. Broad distribution of the multidrug resistance-related vault lung resistance protein in normal human tissues and tumors. Am J Pathol, 148: 877-887, 1996.

12. Izquierdo, M. A., Shoemaker, R. H., Flens, M. J., Scheffer, G. L., Wu, L., Prather, T. R., and Scheper, R. J. Overlapping phenotypes of multidrug resistance among panels of human cancer-cell lines. Int J Cancer, 65: 230-237, 1996.

13. Kickhoefer, V. A., Rajavel, K. S., Scheffer, G. L., Dalton, W. S., Scheper, R. J., and Rome, L. H. Vaults are up-regulated in multidrug-resistant cancer cell

lines. J Biol Chem, 273: 8971-8974, 1998.

14.	Schroeijers, A. B., Siva, A. C., Scheffer, G. L., de Jong, M. C., Bolick, S. C., Dukers, D. F., Slootstra, J. W., Meloen, R. H., Wiemer, E., Kickhoefer, V. A., Rome, L. H., and Scheper, R. J. The Mr 193,000 vault protein is up-regulated in multidrug-resistant cancer cell lines. Cancer Res, 60: 1104-1110, 2000.

15.	Kitazono, M., Sumizawa, T., Takebayashi, Y., Chen, Z. S., Furukawa, T., Nagayama, S., Tani, A., Takao, S., Aikou, T., and Akiyama, S. Multidrug resistance and the lung resistance-related protein in human colon carcinoma SW-620 cells [see comments]. J Natl Cancer Inst, 91: 1647-1653, 1999.

16.	Kitazono, M., Okumura, H., Ikeda, R., Sumizawa, T., Furukawa, T., Nagayama, S., Seto, K., Aikou, T., and Akiyama, S. Reversal of LRP-associated drug resistance in colon carcinoma SW-620 cells. Int J Cancer, 91: 126-131, 2001.

17.	Kedersha, N. L., Heuser, J. E., Chugani, D. C., and Rome, L. H. Vaults. III. Vault ribonucleoprotein particles open into flower-like structures with octagonal symmetry. J Cell Biol, 112: 225-235, 1991.

18.	Kong, L. B., Siva, A. C., Rome, L. H., and Stewart, P. L. Structure of the vault, a ubiquitous celular component. Structure Fold Des, 7: 371-379, 1999.

19.	Kong, L. B., Siva, A. C., Kickhoefer, V. A., Rome, L. H., and Stewart, P. L. RNA location and modeling of a WD40 repeat domain within the vault. Rna, 6: 890-900, 2000.

20.	Kickhoefer, V. A., Liu, Y., Kong, L. B., Snow, B. E., Stewart, P. L., Harrington, L., and Rome, L. H. The Telomerase/Vault-associated Protein TEP1 Is Required for Vault RNA Stability and Its Association with the Vault Particle. J Cell Biol, 152: 157-164, 2001.

21.	Kickhoefer, V. A., Siva, A. C., Kedersha, N. L., Inman, E. M., Ruland, C., Streuli, M., and Rome, L. H. The 193-kD vault protein, VPARP, is a novel poly(ADP-ribose) polymerase. J Cell Biol, 146: 917-928, 1999.

22.	Kickhoefer, V. A., Stephen, A. G., Harrington, L., Robinson, M. O., and Rome, L. H. Vaults and telomerase share a common subunit, TEP1. J Biol Chem, 274: 32712-32717, 1999.

23.	Harrington, L., McPhail, T., Mar, V., Zhou, W., Oulton, R., Bass, M. B., Arruda, I., and Robinson, M. O. A mammalian telomerase-associated protein [see comments]. Science, 275: 973-977, 1997.

24.	Kuiper, C. M., Broxterman, H. J., Baas, F., Schuurhuis, G. J., Haisma, H. J., Scheffer, G. L., Lankelma, J., and Pinedo, H. M. Drug transport variants without P-glycoprotein overexpression from a human squamous lung cancer cell line after selection with doxorubicin. J. Cell Pharmacol., 1: 35-41, 1990.

25.	Zijlstra, J. G., de Vries, E. G., and Mulder, N. H. Multifactorial drug resistance in an adriamycin-resistant human small cell lung carcinoma cell line. Cancer Res, 47: 1780-1784, 1987.

26.	Dalton, W. S., Grogan, T. M., Rybski, J. A., Scheper, R. J., Richter, L., Kailey, J., Broxterman, H. J., Pinedo, H. M., and Salmon, S. E. Immunohistochemical detection and quantitation of P-glycoprotein in multiple drug-resistant human

myeloma cells: association with level of drug resistance and drug accumulation. Blood, 73: 747-752, 1989.

27. Roninson, I. B., Chin, J. E., Choi, K. G., Gros, P., Housman, D. E., Fojo, A., Shen, D. W., Gottesman, M. M., and Pastan, I. Isolation of human mdr DNA sequences amplified in multidrug-resistant KB carcinoma cells. Proc Natl Acad Sci U S A, 83: 4538-4542, 1986.

28. Taylor, C. W., Dalton, W. S., Parrish, P. R., Gleason, M. C., Bellamy, W. T., Thompson, F. H., Roe, D. J., and Trent, J. M. Different mechanisms of decreased drug accumulation in doxorubicin and mitoxantrone resistant variants of the MCF7 human breast cancer cell line. Br J Cancer, 63: 923-929, 1991.

29. Thalmeier, K., Meissner, P., Reisbach, G., Falk, M., Brechtel, A., and Dormer, P. Establishment of two permanent human bone marrow stromal cell lines with long-term post irradiation feeder capacity. Blood, 83: 1799-1807, 1994.

30. Church, G. M. and Gilbert, W. Genomic sequencing. Proc Natl Acad Sci U S A, 81: 1991-1995, 1984.

31. Kickhoefer, V. A., Searles, R. P., Kedersha, N. L., Garber, M. E., Johnson, D. L., and Rome, L. H. Vault ribonucleoprotein particles from rat and bullfrog contain a related small RNA that is transcribed by RNA polymerase III. J Biol Chem, 268: 7868-7873, 1993.

32. Willis, I. M. RNA polymerase III. Genes, factors and transcriptional specificity. Eur J Biochem, 212: 1-11, 1993.

33. Vilalta, A., Kickhoefer, V. A., Rome, L. H., and Johnson, D. L. The rat vault RNA gene contains a unique RNA polymerase III promoter composed of both external and internal elements that function synergistically. J Biol Chem, 269: 29752-29759, 1994.

34. Siva, A. C., Raval-Fernandes, S., Stephen, A. G., LaFemina, M. J., Scheper, R. J., Kickhoefer, V. A., and Rome, L. H. Up-regulation of vaults may be necessary but not sufficient for multidrug resistance. Int J Cancer, 92: 195-202, 2001.

35. Scheffer, G. L., Wijngaard, P. L., Flens, M. J., Izquierdo, M. A., Slovak, M. L., Pinedo, H. M., Meijer, C. J., Clevers, H. C., and Scheper, R. J. The drug resistance-related protein LRP is the human major vault protein [see comments]. Nat Med, 1: 578-582, 1995.

36. Keating, M. J., Cork, A., Broach, Y., Smith, T., Walters, R. S., McCredie, K. B., Trujillo, J., and Freireich, E. J. Toward a clinically relevant cytogenetic classification of acute myelogenous leukemia. Leuk Res, 11: 119-133, 1987.

37. Le Beau, M. M., Albain, K. S., Larson, R. A., Vardiman, J. W., Davis, E. M., Blough, R. R., Golomb, H. M., and Rowley, J. D. Clinical and cytogenetic correlations in 63 patients with therapy- related myelodysplastic syndromes and acute nonlymphocytic leukemia: further evidence for characteristic abnormalities of chromosomes no. 5 and 7. J Clin Oncol, 4: 325-345, 1986.

CHAPTER 6

Loss of major vault protein severely affects
the stability of other vault components

*submitted*

*Chapter 6*

**Abstract**

Vaults are large ribonucleoprotein particles composed of multiple copies of three proteins, MVP, TEP1 and VPARP and small untranslated vault RNAs. MVP is the main structural component and responsible for the formation of the particles. *MVP* knockout mice are viable and show no clear abnormalities. In this paper we demonstrate that vault particles are absent in *MVP* knockout tissues. Moreover, immuno-blot analysis of *MVP$^{-/-}$* tissues, ES and MEF cells revealed that TEP1 and VPARP protein levels are severely decreased. The levels and half-life of vRNA were also found to be reduced, probably due to the diminished amounts of TEP1. Biochemical fractionation indicated that the residual VPARP in *MVP$^{-/-}$* MEFs is present in a cytosolic fraction. Northern blot analysis showed that TEP1 and VPARP mRNA levels and polysome formation are unaffected, suggesting that the reduction of TEP1 and VPARP are caused by protein instability. Re-introduction of GFP-tagged MVP in *MVP$^{-/-}$* MEF cells resulted in vault particle formation and increased levels of VPARP protein and vRNA. MVP molecules with a deleted coiled coil domain could not form vault particles, nor restore VPARP and vRNA levels. These data suggest that the formation of vault particles is mediated by the coiled coil domain of MVP and is essential for stabilization and subcellular distribution of the other vault components.

**Introduction**

Vaults are large ribonucleoprotein particles of unknown function, found in most eukaryotic cells. The majority of vaults reside in the cytoplasm, but a small fraction of around 5% is constitutively found associated with the nucleus (1-3). The complex consists of three different proteins and multiple copies of one or more small untranslated RNA molecules. The most abundant protein, the $M_r$ 100,000 major vault protein (MVP), makes up 70% of the total mass of the complex. The other protein constituents are the $M_r$ 193,000 vault poly-(ADP-ribosyl)polymerase (VPARP) and the $M_r$ 240,000 telomerase/vault associated protein 1 (TEP1) referred to as minor vault proteins. Not all TEP1 and VPARP in the cell are associated with the vault complex. It is not clear whether these proteins fulfil separate functions, unrelated to the function of vaults, in their non-vault associated state. VPARP has been detected in non-vault associated cytoplasmic clusters and is also present in the nucleus (4). TEP1 is shared with another ribonucleoprotein complex, namely the telomerase complex. The function of TEP1 in the telomerase complex is not yet known, but it has been shown that TEP1 is capable of binding the telomerase RNA and immuno-precipitates of TEP1 contain associated telomerase activity (5). Similarly, TEP1 can bind vault RNAs (6). The vault RNA (vRNA) differs in size and number between species. In human cells, three different, highly homologous vRNAs, hvg1, hvg2 and hvg3 are expressed, that are 98, 88 and 88 bases in size, respectively (7, Chapter 5). By contrast, rodents express a single larger vRNA, of 141 bases (7-9). The RNA component accounts for about 5% of the mass of the total particle and is not believed to be a structural component of the vault complex but rather a functional one, since degradation of vRNA does not alter vault morphology (10-12).

The vault complex is 35 x 65 nm in size and has an estimated molecular mass of 13 MDa (13), making it the largest ribonucleoprotein complex known, in fact three times the size of a ribosomal subunit. The vault proteins are arranged in a typical hollow barrel-like structure with an 8-2-2 symmetry, an invaginated waist and two protruding caps (10, 14). MVP has been shown to be responsible for the vault morphology, as in the absence of minor vault proteins it is capable of forming particles that closely resemble intact vault particles (15). TEP1, vRNA and probably VPARP are localized in the caps of the vault particle (10, 11). A model has been proposed in which an intact vault complex contains 96 copies of MVP, and two molecules of TEP1, eight molecules of VPARP and at least six copies of vRNA (10). The characteristic morphology of the vault particle is conserved between species, suggesting it is relevant for vault functioning (16). However, so far this function and the significance of each of the individual vault components remains an enigma. Based on vault morphology, subcellular localization and dynamics several groups have suggested a role for vaults in cellular transport (1-3, 17, 18). Since the lung resistance-related protein (LRP) was identified as the human major vault protein (19), studies have also focused on the

involvement of vaults in detoxification and multidrug resistance, possibly by the transport or sequestration of drugs (for a review see Scheffer *et al.* (20)).

*TEP1* knockout mice are viable and show no apparent abnormalities (11, 21). In these animals, telomerase activity and telomere length appear normal. In addition, the level of the telomerase RNA and its association with the telomerase complex are unaltered (11). However, the half-life of vRNA is severely reduced in the *TEP1* knockout mice and vRNA no longer stably associates with vaults. No major structural changes in purified vaults isolated from *TEP1$^{-/-}$* tissues are observed and the levels of MVP and VPARP are comparable in the *TEP1* knockout and wild-type mice .

One might predict that deletion of the *MVP* gene has grave consequences for the integrity and functional capability of the vault complex. Nevertheless, the *MVP* knockout mice are viable, fertile and have no apparent abnormalities or increased sensitivity to cytotoxic chemicals (22). This lack of phenotype could be explained if a redundancy for MVP would exist as was the case in *Dictyostelium discoideum* in which three homologues of *MVP* have been identified (23, 24). Although the murine genome does not seem to contain additional genes with high similarity to *MVP* (25), another more distantly related protein could be taking over the function of MVP or there could be functional redundancy with respect to vault function. Alternatively the remaining vault components TEP1, VPARP and vRNA might still be of functional significance.

Here we demonstrate that in the absence of MVP, vault particles are no longer formed and that the steady-state levels of TEP1, VPARP and vRNA are severely reduced in MVP-deficient mouse tissues and cells. In addition, the subcellular distribution of at least VPARP is changed dramatically. Furthermore, we show that TEP1 and VPARP mRNA levels and polysome formation are not affected upon loss of MVP suggesting that their reduced levels are due to a decrease in protein stability. Re-introduction of full-length MVP in knockout cells restored the levels of VPARP and vRNA, whereas truncated MVP, in which part of the coiled coil domain is deleted, could not restore VPARP nor vRNA levels. These data suggest that MVP and in particular its coiled coil domain, is required for vault particle formation and consequently the stabilization and subcellular distribution of VPARP, TEP1 and vRNA.

**Materials and methods**

*Generation of MVP-deficient mice and embryonic stem cells*
Homozygous *MVP$^{-/-}$* mice and MVP-deficient embryonic stem (ES) cells were generated as described previously (22). The mice used in this study are of a mixed genetic background (C57BL/6 and 129/OLA), backcrossed on C57BL/6 for three to five generations.

*Establishment of mouse embryonic fibroblast (MEF) lines and culture conditions*
MEF cell lines were derived essentially as described by Todaro and Green (26). 13.5 days old embryos were isolated from matings of $MVP^{+/-}$ mice after which extra-embryonic membranes and heads, hearts and livers were removed and used for genotyping. The remaining tissues were transferred to a 10 cm² dish, chopped into small pieces to which 2.5 ml of MEF medium (50% DMEM, 50% Ham's F10 supplemented with 10% FCS, 100 units/ml penicillin, 100 μg/ml streptomycin and 2 mM L-glutamin) was added. Every 24 hours, 2.5 ml of fresh medium was added till a maximum volume of 12.5 ml was reached. The cells were cultured at 37°C in a humidified atmosphere containing 5% $CO_2$. All cell lines were maintained at 20% confluency throughout the proliferative period. During crisis cells were maintained at near confluency and trypsinized weekly. Cell line establishment was evidenced by a marked increase in cellular proliferation.

*Vault purification and analysis*
Vaults were purified from ~7 grams of mouse liver as described previously (14), using a protocol adapted to the limited quantities of the mouse livers (11). In the final purification step, the vaults were purified over a single cesium chloride gradient to get rid of ferritin, which is the major contaminant during vault purification from liver. Vaults were recovered from several gradient fractions by dilution and pelleting at 100,000 x *g* using a Ti80 rotor (Beckman Coulter) and resuspension in 75 μl of 90 mM MES, pH 6.5 containing 1 mM DTT, 0.5 mM PMSF and a protease inhibitor cocktail. Of each fraction, 20 μl was subjected to SDS-PAGE, followed by either silver staining or immuno-blot analysis using anti-(MVP), anti-(VPARP) and anti-(TEP1) antibodies previously described (4, 6). Electron microscopical analysis of uranyl acetate stained vaults was performed as described (12).

*SDS-PAGE and immuno-blotting*
Fresh tissues from $MVP^{+/+}$, $MVP^{+/-}$ and $MVP^{-/-}$ littermate animals were homogenized in a 10 mM sodium phosphate buffer (pH 7.4) containing 0.25% (v/v) Triton X-100 and protease inhibitors (Complete™; Roche Applied Science, Mannheim, Germany), using an Ultra-Turrax T25 homogenizer (IKA-Labortechnik). The tissue lysates were spun briefly to pellet insoluble materials. Embryonic fibroblasts and ES cells were lysed in the same buffer solution. Protein concentrations were determined by the BCA method (Pierce, Rochford, IL). The protein lysates were subjected to SDS-polyacrylamide gelelectrophoresis (SDS-PAGE) on an 6-8% gel after which the size-fractionated proteins were transferred to nitrocellulose. The protein blots were blocked in TBST (50 mM Tris-Cl pH 7.5, 100 mM NaCl, 0.05% (v/v) Tween 20) containing 5% (w/v) non-fat dry milk (Bio-Rad, Laboratories, Hercules, CA). MVP was detected using a rabbit polyclonal antiserum raised against human MVP that cross-reacted with murine MVP (27). VPARP was detected using the mouse mAb p193-10 recognizing an epitope conserved between mouse and human (27). TEP1 was detected using an affinity purified rabbit anti-(TEP1) polyclonal antiserum obtained from Dr. L.

Harrington, (University of Toronto, Canada). Equal protein loading was demonstrated by incubating blots with a rabbit polyclonal anti-(catalase) (28). Species-specific anti-Ig antibodies conjugated to horseradish peroxidase (Jackson ImmunoResearch Laboratories, Westgrove, PA) were used as second antibody. Immune-complexes were detected using the BM chemiluminescence kit (Roche Molecular Biochemicals, Mannheim, Germany) and visualized on Hyperfilm ECL (Amersham-Pharmacia, Uppsala, Sweden). Western blotting results were quantified using ImageQuaNT, (Molecular Dynamics, Sunnyvale, CA).
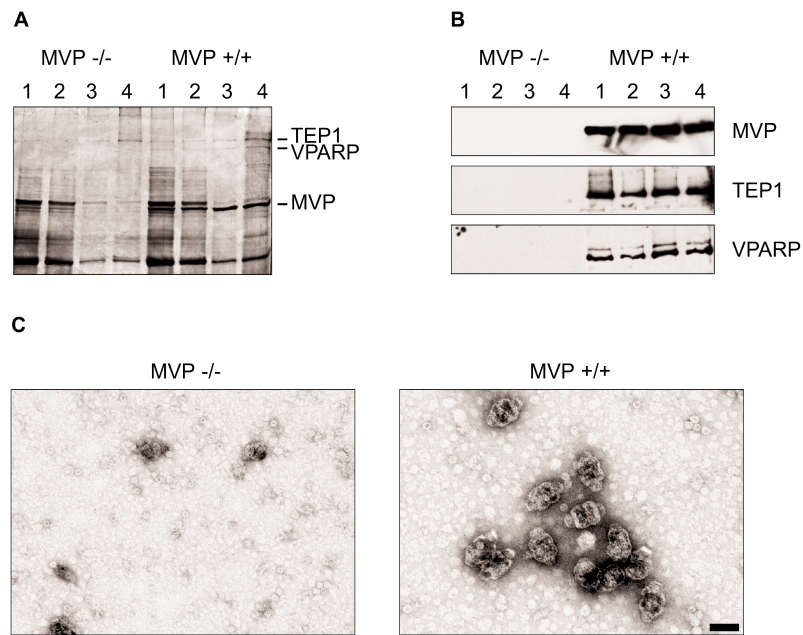


Figure 6.1. **Absence of vault particles in *MVP* knockout mice.** A, Livers from wild-type (MVP+/+) and *MVP* knockout (MVP-/-) mice were used to partially purify vault particles as described in the materials and methods section. In the final purification step, the vaults were purified over a cesium chloride gradient. Vaults were recovered from the gradient in four fractions by dilution and subsequent pelleting at 100,000 x *g*. The fractions (1-4) were analyzed by SDS-PAGE and the proteins present visualized by silver staining. Protein bands corresponding to vault proteins are marked in wild-type fractions and were not detected in *MVP*^{-/-} fractions, whereas contaminating proteins where present in both liver preparations in about equal amounts. B, The presence of vault proteins in the wild-type fractions and their absence in *MVP*^{-/-} fractions was confirmed by immuno-blotting. C, All wild-type and *MVP* knockout fractions were analyzed by electron microscopy. Vault particles with the typical barrel-shaped morphology could easily be detected in the wild-type liver fractions, but were completely absent in the corresponding fractions of the *MVP* knockout livers. Shown are electron micrographs of negatively stained vault preparations that were obtained from wild-type and knockout fraction 3. Scale bars correspond to 50 nm.

*Northern blot analysis*

Total RNA was purified from fresh tissues from $MVP^{+/+}$, $MVP^{+/-}$ and $MVP^{-/-}$ littermate animals using RNAzol™ B (Campro Scientific, Veenendaal, The Netherlands) following the recommendations of the manufacturer. Total RNA from cell lines was isolated using the RNAeasy kit (Qiagen, Hilden, Germany). 10 μg of total RNA was subjected to formaldehyde-agarose gel electrophoresis essentially as described (29). Subsequently the size fractionated RNA was blotted onto Hybond-N⁺ filters (Amersham, Little Chalfont, UK). ULTRAhyb™ (Ambion, Austin, Texas) was used as blocking and hybridization solution according to the protocol supplied by the manufacturer. Radiolabeled anti-sense RNA probes were prepared by *in vitro* transcription using T7 or Sp6 RNA polymerase from the following linearized templates: the murine MVP cDNA (nucleotide position 108 - 2589) cloned in pCR2.1 (Invitrogen, Carlsbad, CA); the *myc*-tagged murine TEP1 cDNA cloned in pCR3 (myc3-mTP1) obtained from Dr. L Harrington (University of Toronto, Canada) and a ~2000 bp fragment of the murine VPARP gene, which was PCR amplified from cDNA prepared from total murine liver RNA and cloned in pCR-Blunt (Invitrogen, Carlsbad, CA). The oligonucleotides used were based on mouse ESTs that displayed a high similarity with human VPARP cDNA; forward primer 5'-CTTGCAGATATTTAGAGTTGGCAGAGTG and reverse primer 5'-CCAGT-TGTCTTCTGAAGCTCAGTAG. After hybridization, the blots were washed 2 x 5 minutes in 2 x SSC; 0.1% SDS and 2 x 15 minutes in 0.1 x SCC; 0.1% SDS at 68˚C. As a loading control the blot was probed with a radiolabeled 18S rRNA oligonucleotide probe (5'-CTTTCGCTCTGGTCCGTCTTGCGCCGGTCC). Northern blot analysis of vRNA expression, using a universal vRNA probe, was performed as described before (7). Afterwards, the blots were stripped and reprobed with a 5S rRNA probe (5'-TCTCCCATCCAAGTACTAACCAGGCC) as a control for equal loading. For the half-life determination of vRNA, cells were incubated with 10 μg/ml actinomycin D. Samples for RNA isolation using RNAzol were taken at 0, 30 minutes, 1, 2, 3, 4, 6 and 8 hours. Northern blotting results were quantified using ImageQuaNT, (Molecular Dynamics, Sunnyvale, CA).

*Fractionation of polysomal bound RNA*

Sucrose gradients were prepared in 5 ml Ultraclear polystyrene ultracentrifuge tubes (Beckmann Coulter, Mijdrecht, The Netherlands) as follows: 1 ml 40% (w/v) sucrose, 1 ml 31.6% sucrose, 1 ml 23.3% sucrose and 1 ml 15% sucrose. Before adding each new layer, the tubes were snap frozen in liquid nitrogen. The gradients were stored at -80˚C and thawed slowly (overnight at 4˚C) before use. All sucrose solutions contained 10 mM DTT, 100 μg/ml cycloheximide and 500 μg/ml heparin. Around $25 \times 10^6$ wild-type and $MVP^{-/-}$ ES cells were harvested and resuspended in 400 μl NP-40 buffer (0.5% (v/v) NP-40 in 10 mM Tris-HCl pH 7.5, 140 mM NaCl, 1.5 mM $MgCl_2$, before use, 12 μl of 40 U/μl RNAsin, 15 μl of 10 mg/ml cycloheximide, 20 μl 1 M DTT and protease inhibitors were added to 943 μl NP-40 buffer). The cell lysates were resuspended by pippeting up and down 10 times and spun for 3 minutes at 3,300 x *g*

to remove the nuclei. The supernatants were transferred to a new RNase free tube and 30 µl heparin (50 mg/ml) was added. Mitochondria and membrane particles were removed by centrifugation at 13,000 x $g$ at 4°C for 10 minutes. The supernatants were loaded onto the sucrose gradients, which were centrifuged at 4°C for 1 hour at 42,000 rpm in a SW50Ti rotor (Beckmann). Afterwards, the gradient was aliquotted in 550-600 µl fractions that were transferred to tubes containing 58 µl 10% SDS, 12 µl 0.5 M EDTA pH 8.0 and 10 µl proteinase K (10 mg/ml) and mixed immediately. After an incubation of 30 minutes at 37°C, 750 µl phenol:chloroform (1:1) was added, the tubes were vortexed for 1 minutes and spun at 13,000 x $g$ for 5 minutes at room temperature. The water phase was transferred to a fresh tube and an equal volume of isopropanol was added and the RNA was allowed to precipitate for at least 1 hour at -20°C. After spinning at 13,000 x $g$ for 30 minutes, the pellets were washed with 75% ethanol and air dried for 10 minutes. The RNA pellet was dissolved in 15 µl DEPC-treated water, of which 2 µl was used in a Northern blot analysis to detect TEP1 and VPARP transcripts.

*Retroviral gene transfer*
The following N-terminal GFP-tagged constructs were cloned into the pBabePuro vector (30): human full-length MVP (GFP-MVP[1-893]) and a truncated human MVP deleting the coiled coil domain (GFP-ΔMVP[1-706]). For the production of virus, Phoenix E cells (Dr. G. Nolan, Stanford University, CA) were seeded at a density of 2.5 x 10^{6} cells/10 cm[2] dish in 10 ml DMEM medium supplemented with 10% FCS, 100 units/ml penicillin and 100 µg/ml streptomycin. After an overnight incubation at 37°C, in a humidified atmosphere containing 5% $CO_2$, the cells were transfected with 10 µg DNA of the appropriate constructs, by the $CaPO_4$ precipitation method. After 24 hours, the medium was replaced and again 24 hours later, the virus containing supernatant was harvested, filtered through a 0.45 µm filter, snap frozen in liquid nitrogen and stored at -80°C. For the infection of the MEFs, 3.5 cm[2] dishes were coated with 12 µg retronectine in 1 ml PBS for two hours. The retronectine solution was removed and the dishes were incubated with 1 ml 2% (w/v) BSA in PBS for 30 minutes. After washing the dishes twice with PBS, they were pre-treated with 1 ml virus supernatant, for one hour at 37°C. 0.2 x 10^{6} embryonic fibroblasts in 1 ml MEF medium were mixed with 1 ml virus supernatant and seeded in the pre-treated dishes. After 24 hours at 37°C, 1 ml medium was removed and replaced with fresh virus supernatant. After an additional 24 hours at 37°C, the cells were washed twice in PBS and incubated in selection medium containing 2.5 µg/ml puromycin. Surviving clones were amplified and the percentage of transfected cells expressing the GFP-tagged MVP constructs was estimated by FACS analysis.

*Subcellular fractionation*
Cell extracts were prepared from 30-60 x 10^{6} wild-type MEF cells, *MVP^{-/-}* MEF cells and/or *MVP^{-/-}* MEF cells expressing the GFP-tagged MVP constructs (see retroviral gene transfer, this section) in vault-buffer (50 mM Tris-Cl, pH 7.4, 1.5 mM $MgCl_2$,

75 mM NaCl and 0.5% (v/v) NP-40), supplemented with a cocktail of protease inhibitors (Complete™; Roche Applied Science, Mannheim, Germany). The cell extracts were incubated on ice for 5 minutes and centrifuged at 20,000 x $g$ for 20 minutes at 4°C removing the nuclei. The postnuclear supernatant was centrifuged at 100,000 x $g$ for 90 minutes at 4°C using a Beckman SW50.1 rotor. The resulting supernatant was designated the S-fraction. If it was necessary to obtain a more concentrated S-fraction the centrifuge tubes were topped off with mineral oil. The 100,000 x $g$ pellet (P) fraction and nuclei were resuspended in vault-buffer using a Dounce homogenizer. The nuclear fraction was made less viscous by shearing the DNA. Equal volume amounts the fractions were analyzed on by SDS-PAGE and Western blotting. The pellet fraction was applied to a 20-60% sucrose step gradient and centrifuged as described previously (9). After centrifugation, 10 fractions were collected from the gradients that were analyzed by SDS-PAGE and Western blotting.

*Fluorescence microscopy*
Cells were grown on poly-L-lysine coated coverslips, fixed with 3% (vol/vol) formaldehyde in PBS for 20 minutes at room temperature and permeabilized by a 5 minute incubation in a 1% (v/v) Triton-X100 solution in PBS. Coverslips were mounted on microscope slides in anti-fade (4% (w/v) n-propyl gallate in glycerol). The fluorescent pattern was examined using a Leica DMRXA microscope and pictures were created using Leica QFish version V 2.3e.

**Results**

*MVP disruption results in the absence of vault particles*
Since MVP is the main structural vault protein, we anticipated that its absence would result in disruption of the vault complex. To confirm this, we attempted to isolate vaults from livers of both wild-type and *MVP* knockout mice using the standard vault purification procedure involving differential centrifugation steps as well as velocity sucrose gradient centrifugation. In the final purification step, vaults were loaded on a cesium chloride gradient in order to separate vaults from ferritin, a major contaminant. Four fractions normally containing the partially purified vault particles were isolated from both wild-type and *MVP* knockout livers. Subsequently, these purified vault fractions were subjected to SDS-PAGE. Figure 6.1A shows the silver stained gel. In the wild-type fractions the vault proteins MVP, TEP1 and VPARP are clearly visible. In the corresponding *MVP*⁻/⁻ fractions, as expected no MVP was detected, however, TEP1 and VPARP were also undetectable. The fact that equal amounts and similar sized contaminating proteins were present in both wild-type and *MVP*⁻/⁻ fractions indicate that the fractions were indeed comparable. These results were confirmed in immuno-blotting experiments (Fig. 6.1B) and indicate the absence of a particle with the physical-chemical properties of vaults in *MVP* knockout livers and imply that there is no other protein substituting for MVP to make a vault particle. Electron micrographs of the wild-type fraction 3 show distinct particles with the typical lobular
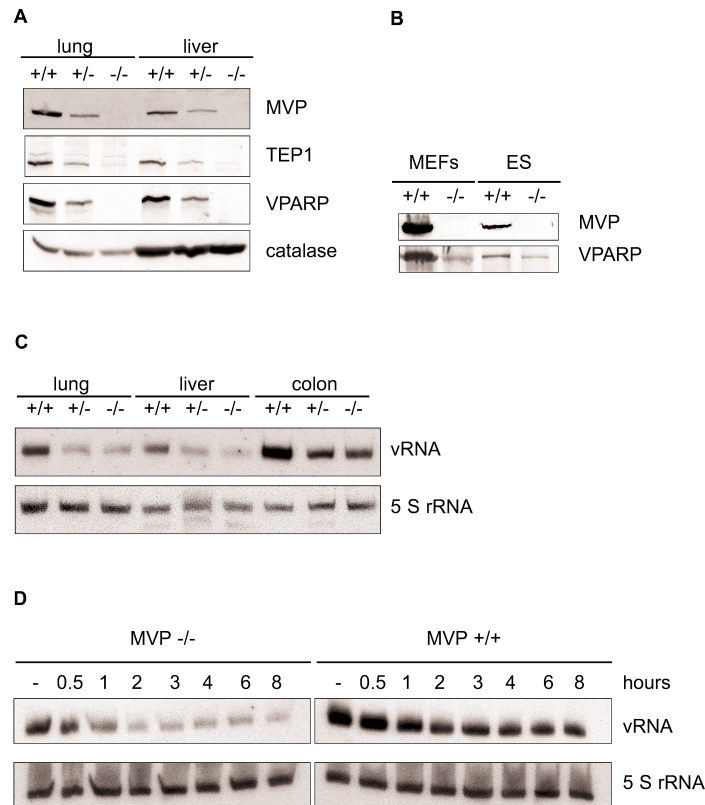
Figure 6.2. **Levels of TEP1, VPARP and vRNA are severely reduced in the absence of MVP.** A, Protein lysates, corresponding to 50 μg of total protein from *MVP^+/+^*, *MVP^+/-^* and *MVP^-/-^* tissues were subjected to SDS-PAGE and immuno-blotting to detect the steady-state levels of MVP, VPARP and TEP1. Lung and liver were investigated since these tissues normally contain relatively high levels of vaults. Upon disruption of *MVP*, the levels of both minor vault proteins are severely reduced. Loss of a single *MVP* allele, in the *MVP^+/-^* tissues already results in markedly reduced levels of TEP1 and VPARP. Equal loading and integrity of the protein samples was demonstrated by staining an identical blot with anti-(catalase). B, Protein lysates, corresponding to 50 μg of total protein from *MVP^+/+^* and *MVP^-/-^* MEF and ES cells were subjected to SDS-PAGE and immuno-blotting to detect MVP and VPARP levels. C, Northern blot analysis showing the levels of vRNA in wild-type, heterozygous and *MVP* knockout tissues. 15 μg of total RNA, isolated from various tissues was loaded in each lane. Levels of vRNA were determined by hybridization with a vRNA oligonucleotide probe as described in the materials and methods section. D, Determination of the half-life of vRNA in wild-type and *MVP* knockout MEFs. Cells were incubated with actinomycin D to inhibit transcription and RNA samples for Northern blot analysis were taken after 30 minutes, 1, 2, 3, 4, 6 and 8 hours. Northern blots were stripped and re-probed with a 5S rRNA probe as a loading control.

vault morphology, while the corresponding fraction, as well as the other fractions, derived from *MVP*^/- livers were devoid of these particles (Fig. 6.1C).

*The absence of MVP affects the levels of the other vault components*

Since in the absence of MVP no vault particles appear to be formed, potential vault functions that utilize the typical barrel-shaped morphology are most likely abolished in these cells. However, the minor vault proteins and/or vRNA may still be functional, either in the context of each other or in vault-independent processes. We therefore investigated the levels of TEP1, VPARP and vRNA in *MVP* knockout tissues and compared these with the levels observed in tissues from heterozygous and wild-type mice. Liver and lung were selected since vaults are highly expressed in these tissues. The absence of MVP appeared to have unexpectedly strong effects on the steady-state levels of the remaining vault proteins. Figure 6.2A indicates that the levels of both TEP1 and VPARP were severely reduced and could hardly be detected in both tissues examined. Interestingly, the disruption of a single *MVP* allele in the heterozygous tissues led to a 2-6 fold reduction in TEP1 and VPARP levels as compared to wild-type levels. We next investigated the levels of the vault proteins in *MVP* knockout cell lines, e.g. the embryonic stem (ES) cells and mouse embryonic fibroblasts (MEFs). We consistently observed a decrease of VPARP levels upon MVP disruption in protein lysates from ES and MEF cell lines (Fig. 6.2B). It was noted that the VPARP reduction in the cell lines is less pronounced (3-6 fold) than what we observed in the tissues. Unfortunately, the anti-(TEP1) antiserum cross-reacted with several high molecular weight proteins in the lysates of the ES and MEF cells obscuring the TEP1 signal, therefore no conclusion could be reached directly on TEP1 levels in these lines.
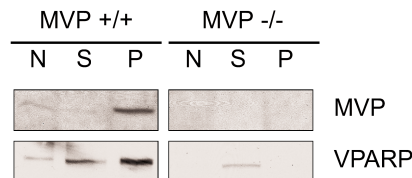


**Figure 6.3. Subcellular distribution of the residual VPARP in MVP-deficient MEFs.** Cell lysates of wild-type and *MVP*^/- MEFs were fractionated by differential centrifugation into a nuclear (N) and 100,000 x *g* supernatant (S) and pellet (P) fraction as described in the materials and methods section. Equal parts of the fractions were subjected to SDS-PAGE and immuno-blotting to examine the distribution of MVP and VPARP.

We next examined vRNA levels in the *MVP* knockout tissues. The Northern blot analysis is shown in Figure 6.2C. The vRNA levels were decreased 2- to 3-fold in these tissues upon MVP disruption, and more or less intermediate levels were observed in tissues from heterozygous mice. To determine the half-life of vRNA in the *MVP* knockout cells, MEFs were incubated with actinomycin D to inhibit transcription.

Total RNA was isolated before the addition of actinomycin D and at 30 minutes, 1, 2, 3, 4, 6 and 8 hours after addition (Fig. 6.2D). In the wild-type MEFs, the half-life of vRNA was calculated to be around 4 hours, whereas this was reduced to 1.5 - 2 hours in the MVP-deficient cells. Most probably, the decrease in vRNA stability is caused by the reduction of TEP1 protein levels. It has previously been shown that TEP1 is essential for the stabilization of vRNA and its association with the vault complex. In the absence of TEP1, vRNA levels are decreased 3- to 5-fold and vRNA half-life is reduced to 0.5-1 hour (11). The decreased vRNA levels and half-life in the MVP deficient MEFs suggest that TEP1 levels are also reduced in these cells.

*The absence of MVP affects the subcellular localisation of VPARP*
To examine the cellular distribution of the remaining VPARP present in *MVP* knockout cells we prepared cell lysates from wild-type and *MVP*$^{-/-}$ MEFs that were fractionated into a nuclear (N) fraction, a 100,000 x *g* supernatant (S) fraction representing the cytosol and the 100,000 x *g* crude vault pellet (P) fraction. In wild-type cells MVP is predominantly recovered in the P fraction with only a small amount found in the N fraction (Fig. 6.3). VPARP was found in all three fractions confirming the presence of a non-vault associated pool of VPARP in the nuclear matrix and cytoplasm (4). However, in *MVP* knockout cells VPARP was only detected in the S fraction. The absence of VPARP in the pellet fraction is due to the absence of vault particles and indicates that VPARP is not present in other complexes large enough to be pelleted under these conditions. The lack of detectable VPARP protein in the nuclear fraction suggests that MVP and/or intact vault particles are necessary for VPARP to reach the nuclear matrix.

*MVP determines the stability of the minor vault proteins*
The decreased levels of TEP1 and VPARP in *MVP* knockout cells and tissues can result from several causes, such as a reduction in transcription or translation rate. Alternatively, the absence of MVP might alter the stability of TEP1 and VPARP mRNA and/or proteins. Siva *et al.* presented evidence that over-expression of MVP in the transfected A2780 cell line AC16 resulted in increased levels of TEP1 and VPARP mRNA and proteins (31). To investigate whether the loss of MVP affects the steady state levels of TEP1 and VPARP mRNA, total RNA was isolated from the livers of wild-type and *MVP* knockout mice and wild-type and *MVP* knockout cell lines. As shown in Figure 6.4A, the mRNA levels of both TEP1 and VPARP were not reduced in the *MVP*$^{-/-}$ liver tissue. Similar results were obtained in cell lines (data not shown). This data indicates that the reduced protein levels of the minor vault proteins upon MVP disruption are not caused by a transcriptional downregulation, but must be either brought about at a translational or post-translational level. To distinguish between these two possibilities, total RNA from wild-type and *MVP*$^{-/-}$ ES cells was isolated and fractionated into a subpolysomal and polysomal-bound fraction, using sedimentation centrifugation on a sucrose gradient (32, 33). Northern blot analysis was used to determine the localization of TEP1 and VPARP transcripts in the gradient and to

calculate the percentage of transcripts that are polysome bound, i.e. being translated. Almost all the message from both TEP1 and VPARP appeared to be in the fractions containing polysomal bound mRNA (fraction 5 to 8), as is seen in Figure 6.4B. In the wild-type cells, the percentages of polysomal bound RNA were found to be 96% for TEP1 and 91% for VPARP. These percentages were similar in the MVP-deficient cells (95% for TEP1 and 88% for VPARP). The high percentages of polysomal bound TEP1 and VPARP transcripts suggest that the proteins are constitutively produced. Loss of MVP does not seem to influence the rate of translation of TEP1 and VPARP messages. Thus, the observed differences in minor vault protein levels seem to be caused by an increased protein instability.
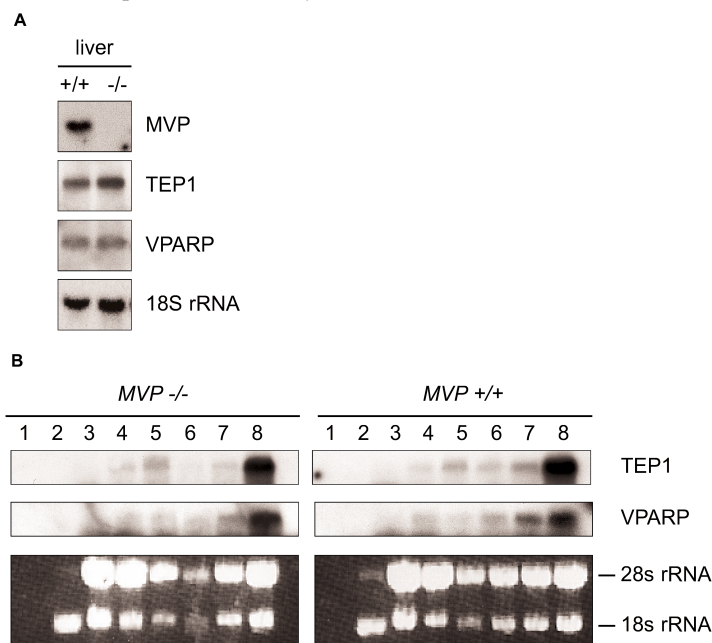


Figure 6.4. **TEP1 and VPARP mRNA levels and polysome formation are unaffected by the loss of MVP.** A, Total RNA was isolated from wild-type and *MVP* knockout liver tissues. 10 μg of RNA was subjected to Northern blot analysis and the blots were hybridized with MVP, TEP1 and VPARP probes and an 18S rRNA probe as a control for equal loading. B, To determine the percentage of TEP1 and VPARP transcripts being translated, total RNA from $MVP^{+/+}$ and $MVP^{-/-}$ ES cells was fractionated on a sucrose gradient into subpolysomal and polysomal bound mRNA. The sucrose gradients were fractionated into 8 equal portions. RNA in each fraction was isolated and analyzed by Northern blotting to detect the TEP1 and VPARP mRNAs. Fractions 1-3 of the sucrose gradients correspond to subpolysomal RNA, and fractions 5-8 contain the polysomal bound RNAs. Fraction 4, containing a mixture of subpolysomal and polysomal RNA is not taken into account when calculating the distribution of the TEP1 and VPARP transcripts across the gradient. The lower panel depicts the ethidium bromide staining pattern showing the 28S and 18S rRNA bands indicating the presence of ribosomes in the respective fractions.

To investigate whether re-introduction of MVP into *MVP* knockout cells could restore the minor vault protein and vRNA levels to wild-type amounts, we cloned an N-terminal GFP-tagged (human) MVP construct (GFP-MVP[1-893]) into a retroviral expression vector pBabe. A construct expressing GFP only was used as a negative control. After retroviral transduction and selection for transduced cells on puromycin, the percentage of GFP or GFP-MVP[1-893] expressing cells was determined by FACS analysis (85% for GFP-MVP[1-893] and 95% for GFP, results not shown). The intracellular localization of the GFP-MVP[1-893] construct was determined by microscopical analysis and appears to be identical to the typical granular cytoplasmic staining that has been described for intact vault particles (Fig. 6.5A). This suggests that these GFP-MVP molecules are assembled into vault particles. To confirm these results, a 100,000 x *g* pellet from wild-type and GFP-MVP[1-893] expressing knockout cells was size-fractionated on a sucrose gradient (Fig. 6.5B). Although the gradients are not completely identical, the GFP-tagged MVP molecules were detected in comparable gradient fractions (peaking at 40-45% sucrose) as the murine MVP in the wild-type cells, indicating that the GFP-tagged MVP molecules are incorporated into complexes with a mass and size similar to vault particles. Moreover, in addition to GFP-MVP[1-893], these fractions also contained TEP1 and VPARP, implying the formation of genuine vaults in the GFP-MVP transfected knockout cells. In Figure 6.5C, the levels of VPARP and vRNA in the GFP-MVP[1-893] expressing cells are compared with the levels in the wild-type and MVP-deficient cells. Expression of GFP-MVP[1-893] restored the VPARP level, which was found to be 12-fold increased compared to the level detected in the MVP-deficient cells. The restored levels exceeded the levels observed in the wild-type cells, which may be explained by the relatively high expression level of the GFP-MVP[1-893] construct, calculated to be around eight times as high as the level of the wild-type MVP. The vRNA levels were also determined in the *MVP* knockout cells expressing the full-length GFP-tagged MVP construct. vRNA, after correction for loading using the same blot stained for 5S rRNA, was found to be 2-fold increased compared to the MVP-deficient cells, indicating that the TEP1 levels are also (partly) restored in these cells. Apparently, in the formation of the vault complex, MVP is the limiting factor.

*Complete vault particles are necessary for stabilization of minor vault proteins*
Finally, we examined whether VPARP is stabilized and protected from degradation through its interaction with either single MVP molecules or whole vault particles. To this purpose, we generated a GFP-tagged truncated (human) MVP construct with a partial deletion in the coiled coil domain (GFP-ΔMVP[1-706]). This domain is responsible for the interaction between MVP molecules and hence the assembly of the vault particles (34, Chapter 4). Fluorescence microscopy showed that the subcellular distribution of GFP-ΔMVP[1-706] is less granular and more diffuse then the full length GFP-tagged MVP construct (Fig. 6.5A). The GFP-ΔMVP[1-706] could not be pelleted at 100,000 x *g*, indicating that these molecules, lacking the coiled coil domain, are not incorporated into vault particles. Hence, no vault proteins could be detected in the

sucrose gradient fractions from the GFP-ΔMVP$^{1-706}$ expressing cells (data not shown). Note that the region interacting with VPARP was mapped to the N-terminal part of MVP and is still present in the GFP-ΔMVP$^{1-706}$ molecules (34). However, the expression of GFP-ΔMVP$^{1-706}$ in the *MVP$^{-/-}$* MEFs does not lead to an increase in the level of VPARP nor vRNA (Fig. 6.5C). These results suggest that the binding of VPARP to MVP, if it occurs, is not sufficient to stabilize VPARP. Therefore, incorporation into whole vault particles seems to be essential to stabilize VPARP, TEP1 and vRNA.

**Discussion**

Although recently much has been learned about the structure and components of vaults, the function of this elusive ribonucleoprotein particle remains unknown. Previously, we reported on the generation of a *MVP* knockout mouse model (22). These mice are viable and show no apparent abnormalities. Here we show that loss of MVP, the main structural component of vaults, has major consequences for the integrity of the vault particle. In addition, we investigated the effects of the absence of MVP on the other components of the vault complex.

As expected, the typical barrel-shaped vault particles are absent when MVP is disrupted. We have reported that the murine genome, in contrast to *Dictyostelium discoideum*, contains only a single copy of the *MVP* gene (25). The absence of TEP1 and VPARP from 'vault' fractions purified from *MVP* knockout livers indicates that no other protein(s) are substituting for MVP to form an alternate vault complex. It is possible that TEP1 and VPARP form a separate complex in the absence of MVP however, no interaction between these proteins was observed in a yeast two-hybrid setting (34, Chapter 4).

Besides the disruption of the vault complex, loss of MVP strongly affects the levels of TEP1, VPARP and vRNA. However, in *MVP* knockout tissues and cell lines the mRNA levels encoding TEP1 and VPARP remain constant, suggesting that the transcription and mRNA stability are unaffected. Moreover, since the polysome profile appears similar in MVP-deficient and wild-type cell lines, these results suggest that the decreased levels of TEP1 and VPARP result from protein instability. As a consequence of the decreased levels of TEP1 in the MVP knockout tissues, the level of vRNA is also reduced. Previously it has been shown that TEP1 is necessary for vRNA stability (11). The remaining vRNA molecules might also be stabilized by binding to other factors, such as the La protein, that was recently found to be associated with vRNA and vaults (35), explaining the still clearly detectable levels of vRNA even though the level of TEP1 protein is severely reduced. The reduction of VPARP in cell lines was less dramatic than what we observed in *MVP* knockout tissues. This difference may be caused by inherent differences between various *in vitro* cell lines and tissues where one might expect that protein degradation pathways are
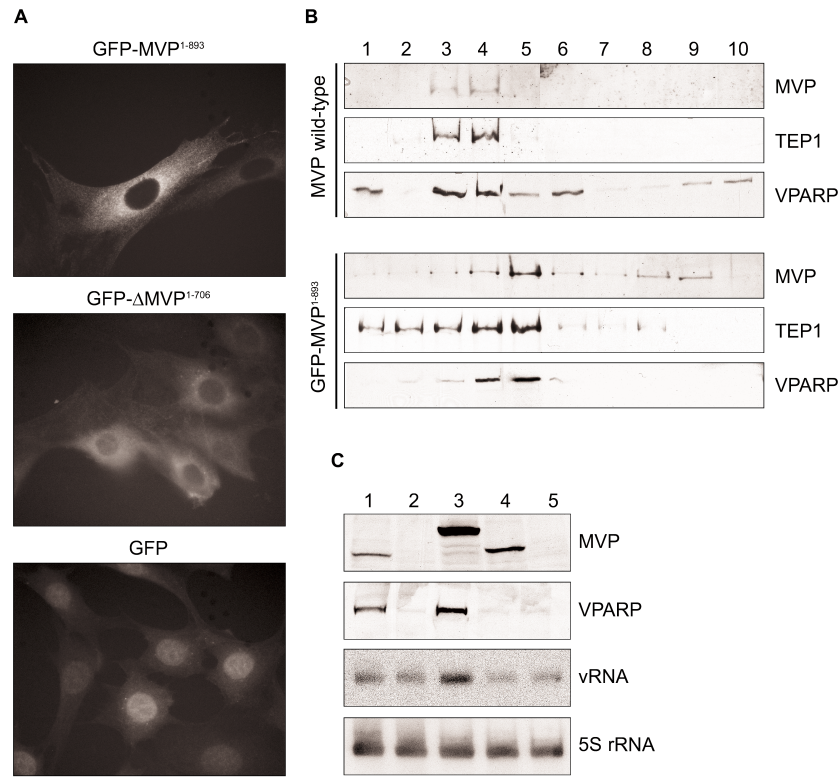
**Figure 6.5. Expression of GFP-MVP in *MVP⁻ᐟ⁻* cells stabilizes VPARP and vRNA through the formation of vault particles.** A, GFP-tagged full length human MVP (GFP-MVP^1-893) and GFP-tagged MVP with a partial deletion in the coiled coil domain (GFP-ΔMVP^1-706) were expressed in *MVP* knockout MEF cells by retroviral gene transfer, as described in the materials and methods section. The subcellular localization of the GFP-tagged constructs was examined by fluorescence microscopy. B, To examine whether the GFP-tagged constructs are assembled into vault particles, cell lysates from wild-type and GFP-MVP^1-893 expressing knockout MEFs were prepared and vaults pelleted at 100,000 x *g*. The pellet was carefully resuspended and fractionated onto a sucrose step gradient, which was aliquotted into 10 fractions of 1 ml. The density of the gradient increases from fraction 10 to fraction 1. The presence of MVP, TEP1 and VPARP in these fractions was determined by subjecting 40 µl of each fraction to Western blot analysis. Vault protein levels were peaking in wild-type fractions 3 and 4 and in GFP-MVP^1-893 fractions 4 and 5, corresponding to 40-45% sucrose. Note that the TEP1 antibody is useful for detection of TEP1 in the fractions of the sucrose gradients, whereas the presence of cross-reacting proteins prevent the use of this antibody to detect TEP1 in total MEF lysates. C, The expression levels of MVP and VPARP protein and vRNA were determined in whole cell lysates from wild-type MEFs (lane 1), *MVP* knockout MEFs (lane 2), *MVP* knockout MEFs expressing GFP-MVP^1-893 (lane 3) and *MVP* knockout MEFs expressing GFP-ΔMVP^1-706 (lane 4). As a negative control, *MVP* knockout cell expressing GFP were used (lane 5). The bottom panel depicts the 5S rRNA signal obtained after stripping and reprobing of the vRNA blot.

125

more active in tissues than in cell lines. Unfortunately, we were not able determine the TEP1 levels in cell lines due to cross-contaminating proteins obscuring the TEP1 signal, but the reduced vRNA levels and half-life of vRNA in the *MVP* knockout MEFs strongly suggest that TEP1 is also reduced.

In conclusion, in wild-type cells, MVP is required for vault particle formation and for stabilizing the other vault components. Indeed, when GFP-MVP is expressed in the knockout MEFs, the VPARP levels are rescued to near wild-type levels. Interestingly, expression of a truncation mutant lacking the coiled coil domain in the C-terminal part of MVP does not rescue VPARP levels. The coiled coil is thought to have a role in vault particle assembly (34). Therefore it seems likely that whole vault particles are necessary to prevent degradation of VPARP and probably TEP1. The resistance of the vault complex against breakdown has been demonstrated before. Herrmann and colleagues reported that MVP, incorporated in the complex, is resistant to proteolytic attack (36). Apparently, assembly into the vault complex is an efficient way of stabilizing the individual components. Based on the present data one could hypothesize that vaults act to sequester and protect factors that may interact in a more transient manner. Recently, the tumor suppressor PTEN has been shown to interact with vaults (37) and several studies have suggested that vaults play a role as transporters (1-3).

Another possibility is that vaults serve as a storing, stabilizing and/or transport compartment for the minor vault proteins, which are otherwise rapidly degraded as determined in this study. Like the vault particle, the function of the minor vault proteins is not yet known. Their normal cellular function could be carried out by the non-vault associated fractions where their activity might be modulated by interaction with vaults. However, the extreme reduction of TEP1 and VPARP levels in the MVP-deficient mice must also affect the non-vault associated levels of these proteins. This is indicated by the absence of VPARP in the nuclear fraction obtained from *MVP* knockout MEFs. This observation questions the proposed presence of three nuclear localization signals (4) but instead suggests that MVP or vault particles are essential for VPARP localization to the nucleus. The decrease in TEP1 and VPARP levels in these mice points out the importance of MVP in the formation of vault particles and in the stabilization of the individual components. Investigation of the subcellular localization of the remaining TEP1 and VPARP might shed more light on the function of the vault proteins and the vault particle.

By disruption of the *MVP* gene, we have generated the first knockout mouse model in which genuine vault particles are physically and functionally absent. From our data we conclude that possible vault functions, utilizing the hollow, barrel-shaped vault morphology, such as vault-mediated transport, are apparently not essential for embryonic development, tissue specialization, reproduction or basic essential cellular functions.

## References

1.  Abbondanza, C., Rossi, V., Roscigno, A., Gallo, L., Belsito, A., Piluso, G., Medici, N., Nigro, V., Molinari, A. M., Moncharmont, B., and Puca, G. A. Interaction of vault particles with estrogen receptor in the MCF-7 breast cancer cell. J Cell Biol, 141: 1301-1310, 1998.

2.  Chugani, D. C., Rome, L. H., and Kedersha, N. L. Evidence that vault ribonucleoprotein particles localize to the nuclear pore complex. J Cell Sci, 106: 23-29, 1993.

3.  Hamill, D. R. and Suprenant, K. A. Characterization of the sea urchin major vault protein: a possible role for vault ribonucleoprotein particles in nucleocytoplasmic transport. Dev Biol, 190: 117-128, 1997.

4.  Kickhoefer, V. A., Siva, A. C., Kedersha, N. L., Inman, E. M., Ruland, C., Streuli, M., and Rome, L. H. The 193-kD vault protein, VPARP, is a novel poly(ADP-ribose) polymerase. J Cell Biol, 146: 917-928, 1999.

5.  Harrington, L., McPhail, T., Mar, V., Zhou, W., Oulton, R., Bass, M. B., Arruda, I., and Robinson, M. O. A mammalian telomerase-associated protein [see comments]. Science, 275: 973-977, 1997.

6.  Kickhoefer, V. A., Stephen, A. G., Harrington, L., Robinson, M. O., and Rome, L. H. Vaults and telomerase share a common subunit, TEP1. J Biol Chem, 274: 32712-32717, 1999.

7.  van Zon, A., Mossink, M. H., Schoester, M., Scheffer, G. L., Scheper, R. J., Sonneveld, P., and Wiemer, E. A. Multiple human vault RNAs. Expression and association with the vault complex. J Biol Chem, 276: 37715-37721, 2001.

8.  Kickhoefer, V. A., Searles, R. P., Kedersha, N. L., Garber, M. E., Johnson, D. L., and Rome, L. H. Vault ribonucleoprotein particles from rat and bullfrog contain a related small RNA that is transcribed by RNA polymerase III. J Biol Chem, 268: 7868-7873, 1993.

9.  Kickhoefer, V. A., Rajavel, K. S., Scheffer, G. L., Dalton, W. S., Scheper, R. J., and Rome, L. H. Vaults are up-regulated in multidrug-resistant cancer cell lines. J Biol Chem, 273: 8971-8974, 1998.

10. Kong, L. B., Siva, A. C., Kickhoefer, V. A., Rome, L. H., and Stewart, P. L. RNA location and modeling of a WD40 repeat domain within the vault. Rna, 6: 890-900, 2000.

11. Kickhoefer, V. A., Liu, Y., Kong, L. B., Snow, B. E., Stewart, P. L., Harrington, L., and Rome, L. H. The telomerase/vault-associated protein TEP1 is required for vault RNA stability and its association with the vault particle. J Cell Biol, 152: 157-164, 2001.

12. Kedersha, N. L. and Rome, L. H. Isolation and characterization of a novel ribonucleoprotein particle: large structures contain a single species of small RNA. J Cell Biol, 103: 699-709, 1986.

13. Kedersha, N. L., Heuser, J. E., Chugani, D. C., and Rome, L. H. Vaults. III. Vault ribonucleoprotein particles open into flower-like structures with octagonal symmetry. J Cell Biol, 112: 225-235, 1991.

14. Kong, L. B., Siva, A. C., Rome, L. H., and Stewart, P. L. Structure of the vault, a ubiquitous celular component. Structure Fold Des, 7: 371-379, 1999.

15. Stephen, A. G., Raval-Fernandes, S., Huynh, T., Torres, M., Kickhoefer, V. A., and Rome, L. H. Assembly of vault-like particles in insect cells expressing only the major vault protein. J Biol Chem, 276: 23217-23220, 2001.

16. Kedersha, N. L., Miquel, M. C., Bittner, D., and Rome, L. H. Vaults. II. Ribonucleoprotein structures are highly conserved among higher and lower eukaryotes. J Cell Biol, 110: 895-901, 1990.

17. Herrmann, C., Golkaramnay, E., Inman, E., Rome, L., and Volknandt, W. Recombinant major vault protein is targeted to neuritic tips of PC12 cells. J Cell Biol, 144: 1163-1172, 1999.

18. Li, J. Y., Volknandt, W., Dahlstrom, A., Herrmann, C., Blasi, J., Das, B., and Zimmermann, H. Axonal transport of ribonucleoprotein particles (vaults). Neuroscience, 91: 1055-1065, 1999.

19. Scheffer, G. L., Wijngaard, P. L., Flens, M. J., Izquierdo, M. A., Slovak, M. L., Pinedo, H. M., Meijer, C. J., Clevers, H. C., and Scheper, R. J. The drug resistance-related protein LRP is the human major vault protein. Nat Med, 1: 578-582, 1995.

20. Scheffer, G. L., Schroeijers, A. B., Izquierdo, M. A., Wiemer, E. A., and Scheper, R. J. Lung resistance-related protein/major vault protein and vaults in multidrug-resistant cancer [In Process Citation]. Curr Opin Oncol, 12: 550-556, 2000.

21. Liu, Y., Snow, B. E., Hande, M. P., Baerlocher, G., Kickhoefer, V. A., Yeung, D., Wakeham, A., Itie, A., Siderovski, D. P., Lansdorp, P. M., Robinson, M. O., and Harrington, L. Telomerase-associated protein TEP1 is not essential for telomerase activity or telomere length maintenance *in vivo*. Mol Cell Biol, 20: 8178-8184, 2000.

22. Mossink, M. H., Van Zon, A., Fränzel-Luiten, E., Schoester, M., Kickhoefer, V. A., Scheffer, G. L., Scheper, R. J., Sonneveld, P., and Wiemer, E. A. Disruption of the murine major vault protein (MVP/LRP) gene does not induce hypersensitivity to cytostatics. Cancer Res, 62: 7298-7304, 2002.

23. Vasu, S. K., Kedersha, N. L., and Rome, L. H. cDNA cloning and disruption of the major vault protein alpha gene (mvpA) in Dictyostelium discoideum. J Biol Chem, 268: 15356-15360, 1993.

24. Vasu, S. K. and Rome, L. H. Dictyostelium vaults: disruption of the major proteins reveals growth and morphological defects and uncovers a new associated protein. J Biol Chem, 270: 16588-16594, 1995.

25. Mossink, M., van Zon, A., Fränzel-Luiten, E., Schoester, M., Scheffer, G., Scheper, R., Sonneveld, P., and Wiemer, E. The genomic sequence of the murine major vault protein and its promoter. Gene, 294: 225, 2002.

26. Todaro, G. and Green, H. Quantitative studies of the growth of mouse embryo cells in culture and their development into established lines. J Cell Biol, 17: 299-313, 1963.

27. Schroeijers, A. B., Siva, A. C., Scheffer, G. L., de Jong, M. C., Bolick, S. C., Dukers, D. F., Slootstra, J. W., Meloen, R. H., Wiemer, E., Kickhoefer, V. A., Rome, L. H., and Scheper, R. J. The Mr 193,000 vault protein is up-regulated in multidrug-resistant cancer cell lines. Cancer Res, 60: 1104-1110, 2000.

28. Tager, J. M., Van der Beek, W. A., Wanders, R. J., Hashimoto, T., Heymans, H. S., Van den Bosch, H., Schutgens, R. B., and Schram, A. W. Peroxisomal beta-oxidation enzyme proteins in the Zellweger syndrome. Biochem Biophys Res Commun, 126: 1269-1275, 1985.

29. Sambrook, J., Fritsch, E. F., and Maniatis, T. Molecular Cloning, A Laboratory Manual, 1989.

30. Morgenstern, J. P. and Land, H. Advanced mammalian gene transfer: high titre retroviral vectors with multiple drug selection markers and a complementary helper-free packaging cell line. Nucleic Acids Res, 18: 3587-3596, 1990.

31. Siva, A. C., Raval-Fernandes, S., Stephen, A. G., LaFemina, M. J., Scheper, R. J., Kickhoefer, V. A., and Rome, L. H. Up-regulation of vaults may be necessary but not sufficient for multidrug resistance. Int J Cancer, 92: 195-202, 2001.

32. Mullner, E. W. and Garcia-Sanz, J. A. Polysome gradients, Vol. 1, p. 457-462: Academic press, 1997.

33. Garcia-Sanz, J. A., Mikulits, W., Livingstone, A., Lefkovits, I., and Mullner, E. W. Translational control: a general mechanism for gene regulation during T cell activation. Faseb J, 12: 299-306, 1998.

34. van Zon, A., Mossink, M. H., Schoester, M., Scheffer, G. L., Scheper, R. J., Sonneveld, P., and Wiemer, E. A. Structural domains of vault proteins: a role for the coiled coil domain in vault assembly. Biochem Biophys Res Commun, 291: 535-541, 2002.

35. Kickhoefer, V. A., Poderycki, M. J., Chan, E. K., and Rome, L. H. The La RNA binding protein interacts with the vault RNA and is a vault- associated protein. J Biol Chem, 277:41282-41286, 2002.

36. Herrmann, C., Volknandt, W., Wittich, B., Kellner, R., and Zimmermann, H. The major vault protein (MVP100) is contained in cholinergic nerve terminals of electric ray electric organ. J Biol Chem, 271: 13908-13915, 1996.

37. Yu, Z., Fotouhi-Aroakani, N., Wu, L., Maoui, M., Wang, S., Banville, D., and Shen, S. H. PTEN Associates with the vault particles in Hela cells. J Biol Chem, 277:40247-40252, 2002.

The efflux kinetics and intracellular distribution
of daunorubicin are not affected by vault expression

*submitted*

*Chapter 7*

**Abstract**

Vaults may contribute to multidrug resistance by transporting drugs away from their subcellular targets. In particular the extrusion of anthracyclines from the nucleus has been reported to be a vault-mediated process. To study the involvement of vaults in this process, we investigated the handling of the anthracycline daunorubicin by drug sensitive and drug resistant - vault overexpressing - non-small lung cancer cells including a GFP-tagged MVP overexpressing transfectant (SW1573/MVP-GFP). Cells were exposed to 1 μM of daunorubicin for 60 minutes after which the cells were allowed to efflux the accumulated drug. No significant differences in daunorubicin efflux kinetics were observed between the sensitive SW1573 and SW1573/MVP-GFP transfectant, whereas the drug resistant SW1573/2R120 cells clearly demonstrated an increased efflux rate. The intracellular distribution was monitored by fluorescence microscopy and showed that daunorubicin initially accumulated in the nuclei in all cell lines, after which it appeared in distinct vesicular structures in the cytoplasm. This process occurs more rapid and efficiently in SW1573/2R120 cells. It was noted that the redistribution of daunorubicin was not accompanied by changes in the intracellular localization of vaults. Similar experiments were performed using mouse embryonic fibroblasts (MEFs) derived from wild-type and *MVP* knockout mice, which were previously shown to be devoid of vault particles. Both cell lines showed comparable drug efflux rates and the intracellular distribution of daunorubicin in time was identical. Reintroduction of a human MVP tagged with GFP in the *MVP*$^{-/-}$ results in the formation of vault particles. Nevertheless, the expression of GFP-tagged MVP in these cells did not give rise to extra or an altered daunorubicin handling as compared to *MVP*$^{-/-}$ cells expressing GFP. Our results indicate that vaults are not directly involved in the sequestration of anthracyclines in vesicles, nor in their efflux from the nucleus.

**Introduction**

The vault complex is an evolutionarily conserved ribonucleoprotein particle that is composed of multiple copies of three high molecular weight proteins and small untranslated RNA molecules of 88-141 bases (vRNAs) (see for reviews: 1, 2). The main component is the $M_r$ 100,000 major vault protein (MVP), also referred to as lung resistance-related protein (LRP), which determines the vault structure. A $M_r$ 193,000 vault poly(ADP-ribose) polymerase (VPARP) together with the $M_r$ 240,000 telomerase-associated protein (TEP1) constitute the minor vault proteins (3, 4). The term 'vaults' describes the morphology of the particles, which contain multiple arches reminiscent of vaulted ceilings in cathedrals. The vault components are arranged into a hollow barrel-like structure measuring approximately 35 x 65 nm, with eight-fold symmetry, an invaginated waist and two protruding caps (5, 6). Mammalian vaults are predominantly localized in the cytoplasm; a small fraction (~5%) of vaults is found associated with the nucleus (7, 8). The precise cellular function of the complex is still unknown, but there is some evidence that vaults play a role in cellular detoxification processes and consequently contribute to the multidrug resistance (MDR) phenotype frequently observed in cancer cells.

A link between vaults and MDR was first suggested when the lung resistance-related protein (LRP), was identified as the human major vault protein (9). Previously, LRP had been found overexpressed in several non-Pgp multidrug resistant cell lines (10). It was proposed that vaults function in MDR by mediating the extrusion of drugs from the nucleus and/or the sequestration of drugs into exocytotic vesicles. In subsequent studies it was established that MVP/LRP (vault) expression correlated with a chemoresistant phenotype in several cancer cell lines and primary tumor samples (11-14). In addition, several clinical studies indicated that MVP/LRP expression at diagnosis was an independent adverse prognostic factor for response to chemotherapy (for a review see Scheffer *et al.* (2)). Up till now few studies have attempted to directly assess the contribution of vaults to drug resistance. Stable expression of MVP in the ovarian carcinoma cell line A2780, led to increased numbers of vault particles, but failed to confer drug resistance to etoposide, vincristine and doxorubicin (9, 15). By contrast, experiments by the group of Akiyama provide support for a role of vaults in the extrusion of anthracyclines from the nucleus (16-18). Kitazono *et al.* demonstrated that treatment of the human colorectal carcinoma SW-620 cells with sodium butyrate resulted in a strong induction of MVP and made the cells less sensitive to doxorubicin, etoposide (VP-16), vincristine and paclitaxel (18). The expression of MVP-specific ribozymes reversed the observed drug-resistant phenotype. Focusing on the molecular mechanism of vault-mediated resistance against anthracyclines they showed that doxorubicin was effluxed more rapidly from the nuclei of sodium butyrate treated - vault overexpressing - cells compared to non-treated cells. Moreover, the nuclear doxorubicin efflux could be inhibited by the addition of polyclonal anti-(MVP) antibodies (18). Recently, we generated an *MVP* knockout mouse model in which vault

particles are absent (19). We tested the sensitivity of MVP deficient cells to a panel of cytostatic agents and found that both embryonic stem cells and bone marrow cells did not show an increased sensitivity to these drugs as compared to wild-type cells. It was concluded that disruption of the murine *MVP* gene did not induce hypersensitivity to cytostatics.

To study how drugs are handled in the cell in the presence and absence of vaults, we examined the influx and efflux kinetics and subcellular distribution of the fluorescent anthracycline daunorubicin. To study how drugs are handled in the cell in the presence and absence of vaults, we examined the influx and efflux kinetics and subcellular distribution of the fluorescent anthracycline daunorubicin. We compared mouse embryonic fibroblasts derived from wild type and *MVP*$^{-/-}$ mice and the drug sensitive human non-small cell lung cancer cell line SW1573 and its drug resistant - vault overexpressing - derivative SW1573/2R120. We also examined the drug handling abilities of transfectants stably expressing a green fluorescent protein (GFP) labeled MVP, which was previously shown to be incorporated into intact vault particles, thereby enabling us to monitor vault distribution in the challenged cell.

**Materials and methods**

*Cell lines and culture conditions*
The cell lines SW1573, its doxorubicin selected multidrug resistant variant SW1573/2R120 (20) and the transfectant SW1573/MVP-GFP (Chapter 2) were maintained in DMEM (Life Technologies, Paisley, Scotland), supplemented with 10% (vol/vol) fetal calf serum, 1 mM pyruvate, 100 U/ml penicillin and 100 μg/ml streptomycin (Life Technologies, Paisley, Scotland) at 37°C under an atmosphere containing 5% $CO_2$. The SW1573/MVP-GFP and SW1573/2R120 were routinely cultured in the presence of 200 μg/ml G-418 (Geneticin, Life Technologies, Paisley, Scotland) and 120 nM doxorubicin, respectively.

*Mouse embryonic fibroblasts*
Mouse embryonic fibroblasts (MEFs) of *MVP*$^{-/-}$ and wild-type littermates were isolated as follows: 13.5 days old embryos were isolated from extra-embryonic membranes and heads, hearts and livers were removed. The remaining parts of the embryos were transferred to a 10 cm$^2$ dish, chopped into small pieces to which 2.5 ml of MEF medium (50% DMEM, 50% Ham's F10 supplemented with 10% (vol/vol) fetal calf serum, 100 units/ml penicillin, 100 μg/ml streptomycin and 2 mM L-glutamine) was added. Every 24 hours, 2.5 ml of fresh medium was added till a maximum volume of 12.5 ml was reached. The cells were cultured at 37°C in a humidified atmosphere containing 5% $CO_2$. Established MEF cell lines were obtained by keeping the cells nearly confluent and trypsinizing weekly, until spontaneously immortalized cells, overcoming senescence, could be expanded. *MVP* knockout MEFs stably expressing human GFP-MVP and GFP alone were generated (Chapter 6).
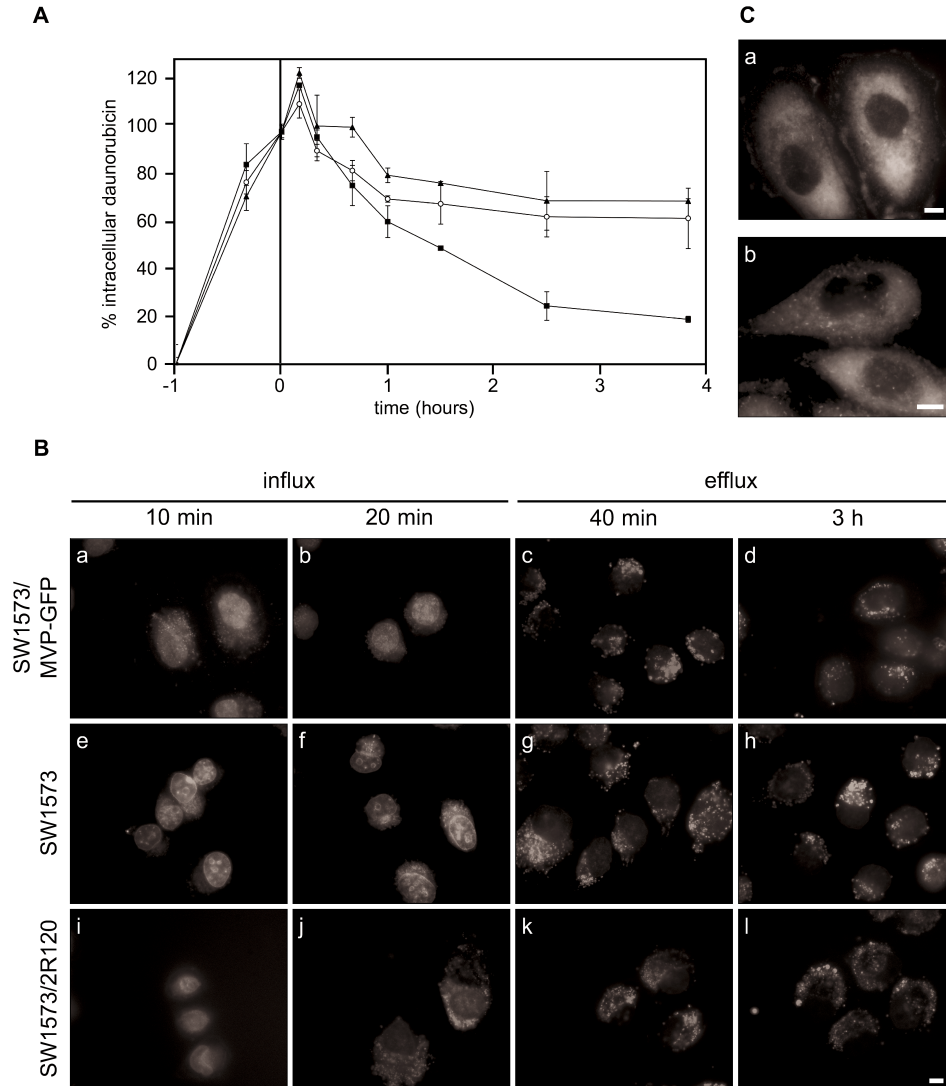
Figure 7.1. **Daunorubicin in- and efflux kinetics and intracellular distribution in SW1573, the SW1573/MVP-GFP transfectant and SW1573/2R120.** The drug sensitive SW1573 cell line, SW1573 stably expressing MVP-GFP and the drug resistant - vault overexpressing - derivative SW1573/2R120 were incubated in the presence of 1 μM daunorubicin. After one hour the cells were washed and fresh medium was added. A, Both the influx and efflux of daunorubicin were monitored by measuring the total intracellular fluorescence in time by FACS. Depicted is the fluorescence present inside SW1573 (O), the MVP-GFP transfectants (▲) and SW1573/2R120 (■) as a percentage of the amount of fluorescence present in the cells at the end of the influx period (t=0 hours), which is arbitrarily set at 100%. B, The intracellular daunorubicin

distribution was examined in time by fluorescence microscopy in the SW1573 transfected with MVP-GFP (*a-d*), SW1573 (*e-h*) and SW1573/2R120 (*i-l*). The fluorescent drug initially accumulates in the nucleus (N) in all cell lines examined, after which the drug appears in distinct cytoplasmic structures. These vesicles become visible early during the influx phase in the resistant SW1573/2R120 cell line (*j*), whereas in the other cell lines the fluorescent vesicles only appear during the efflux phase (*c, g*). Also note that the nucleus of the resistant cell line is virtually cleared from daunorubicin during the efflux time (*k* and *l*). Bar corresponds to 10 μm. C, The subcellular distribution of GFP-tagged vaults does not change upon daunorubicin treatment as is visualized by fluorescence microscopy of living cells at 20 minutes of drug-influx (*a*) and 3 hours of drug-efflux (*b*). Note that the particulate fluorescent pattern, which is characteristic for the vault compartment in immunofluorescence experiments on fixed cells, is not clearly visible due to the rapidly moving vault particles. Bar corresponds to 10 μm.

*Intracellular distribution and in- and efflux kinetics of daunorubicin*
Cells were grown on poly-L-lysine coated coverslips in the absence of drugs for at least two days prior to the experiment. The fluorescent drug daunorubicin (Sigma-Aldrich, Zwijndrecht, The Netherlands) was added to the culture medium in a final concentration of 1 μM after which the uptake of the drug was allowed to proceed for one hour. Subsequently, the cells were washed twice with phosphate buffered saline (PBS) and drug-free medium was added allowing the cells to efflux the drug. At regular intervals coverslips were removed from the culture dish after which the intracellular distribution of daunorubicin and/or the GFP-tagged vault compartment, was examined by fluorescence microscopy using a Leica DMRXA microscope. Images were created using Leica QFish version V 2.3e. Cellular accumulation of the fluorescent daunorubicin during the in- and efflux experiment was assayed by flowcytometry. In short: the cells were cultured in 6 well plates and treated with 1 μM daunorubicin for one hour. At regular intervals the cells were washed with PBS, harvested by trypsinisation and immediately analyzed by FACScan (Becton Dickinson) for daunorubicin fluorescence (488 nm excitation, 575 nm emission). A minimum of 10,000 cells was counted per sample in 2-4 independent experiments. The mean fluorescence distribution was calculated at each time point and corrected for background fluorescence. Data analysis was performed with CellQuest (Becton Dickinson) software.

**Results**

*Efflux rates and intracellular distribution of daunorubicin in non-small cell lung cancer cells*
The drug sensitive non-small cell lung cancer cell line SW1573 and its drug resistant derivative SW1573/2R120 were cultured in the presence of 1 μM of the anthracycline daunorubicin for one hour after which the drug was washed away and the cells were allowed to efflux the drug. At regular intervals we monitored the intracellular daunorubicin fluorescence by FACScan (Fig. 7.1A). It is clear that the extrusion of

daunorubicin from the drug resistant SW1573/2R120 occurs far more efficient than in the drug sensitive parental cells, resulting in a reduction of the intracellular fluorescence after a 4-hour efflux period to 20% of the fluorescence present in the cells after the influx period. By contrast, 70% of the initial fluorescence was still detected in the SW1573 cells after an efflux of four hours. Figure 7.1A shows that the initial clearance rate of daunorubicin appears to be rapid after which it levels off, suggesting the involvement of different mechanisms. The intrinsic fluorescence of daunorubicin also enabled us to examine its intracellular distribution in time. Daunorubicin was initially directed to the nucleus in both cell lines (Fig. 7.1B, *e* and *i*). Interestingly, in the resistant cell line SW1573/2R120 there was a rapid shift of daunorubicin fluorescence from the nucleus to the cytoplasm, where it appeared in typical vesicular structures in the perinuclear region (Fig. 7.1B, *j*). After 40 minutes of drug efflux the nuclei of SW1573/2R120 cells were almost cleared from drug, whereas daunorubicin was still clearly detectable in the nuclei of the drug sensitive parental SW1573 even after four hours of efflux time. At least two possible drug resistance mechanisms seem to be operational in the SW1573/2R120 that may contribute to drug efflux. The cells express significant levels the multidrug resistant associated protein (MRP1) and show a 2-4 fold overexpression of vaults compared to the drug sensitive parent (10, 21).

*Expression of a GFP-tagged MVP in SW1573 does not alter the efflux kinetics and intracellular distribution of daunorubicin*

To investigate if an overexpression of vaults is responsible for the observed drug handling differences, the SW1573 cell line was stable transfected with a construct encoding a C-terminal GFP-tagged MVP (SW1573/MVP-GFP). We previously demonstrated that expression of MVP-GFP in SW1573 resulted in a four-fold increase in MVP levels and that the GFP-tagged MVP molecules were incorporated into vault particles (Chapter 2). Furthermore, MVP has been identified as the vault subunit whose levels are limiting in the formation of vaults (14, 15), implying that expression of MVP-GFP results in increased levels of vault particles. When challenged with daunorubicin the behavior of the SW1573/MVP-GFP transfectant was indistinguishable from that of the drug sensitive SW1573 cells (Fig. 7.1A, 1B *a-d*) indicating that a raised level of vaults is not sufficient to give rise to an increased daunorubicin efflux or an intracellular redistribution of the fluorescent drug, as observed in SW1573/2R120 cells. The expression of the GFP-tagged MVP allowed us to assess the effects of daunorubicin on the vault compartment. As is shown in figure 7.1C the subcellular distribution of the vaults did not change during the drug treatment. Particularly, vaults were never found to accumulate at or in the daunorubicin filled vesicles.

*Daunorubicin handling of mouse embryonic fibroblasts lacking the major vault protein*

We examined the redistribution and efflux of daunorubicin in mouse embryonic fibroblast cells derived from wild-type and $MVP^{-/-}$ littermates. Previously, it was shown that vault particles were absent in *MVP* knockout tissues and cells (19). Furthermore,
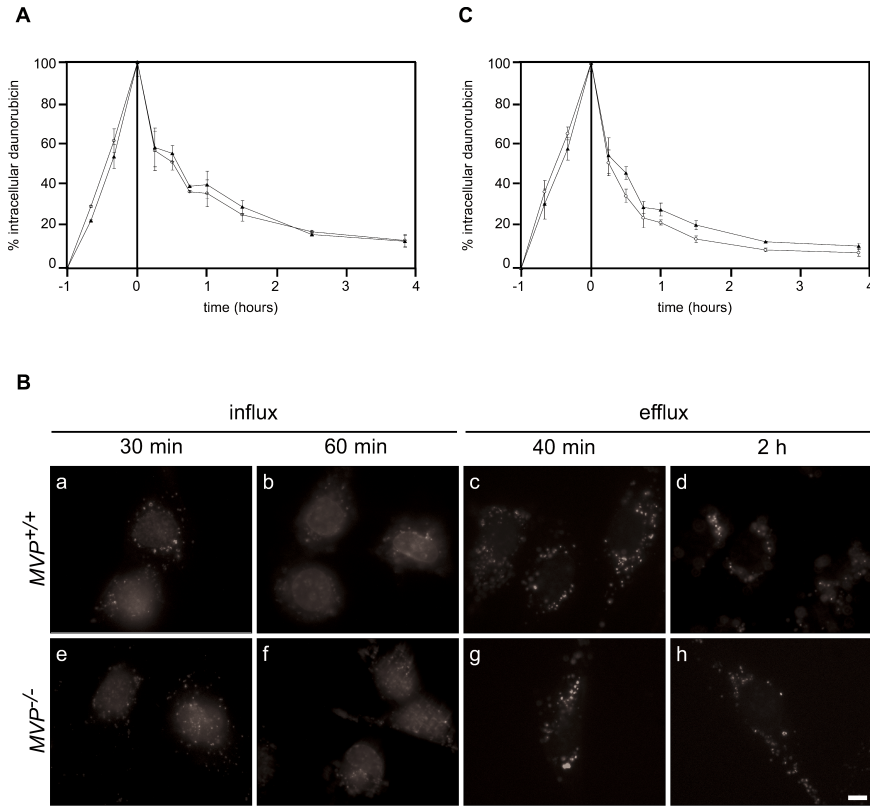
Figure 7.2. **Daunorubicin in- and efflux kinetics and intracellular distribution in $MVP^{-/-}$ and wild-type mouse embryonic fibroblasts.** Mouse embryonic fibroblasts derived from wild-type mice and $MVP$ knockout littermates were cultured in the presence of 1 μM daunorubicin for one hour after which the cells were washed, incubated in fresh medium and allowed to efflux the drug. A. The total amount of intracellular fluorescence was determined in wild-type (▲) and $MVP^{-/-}$ (O) cells as described in the legend of figure 7.1A. B, The intracellular distribution of daunorubicin during influx and efflux was found to be similar in $MVP^{-/-}$ and wild-type cells. Bar corresponds to 10 μm. C, The stable expression of a GFP-tagged MVP (O) in the $MVP^{-/-}$ MEFs, did not alter the drug kinetics as compared to $MVP^{-/-}$ MEFs transfected with GFP (▲) alone.

it was reported that the absence of MVP directly affected the stability of the other vault components, making the presence of a rudimentary vault complex highly unlikely (19, Chapter 6). Figure 7.2A shows the intracellular daunorubicin fluorescence of the MEFs during the daunorubicin uptake and subsequent efflux. No differences were observed between wild-type cells and the cells lacking vaults. Comparison of the daunorubicin efflux rates in the MEFs with the rates observed in non-small cell lung cancer cells (Fig. 7.1A) reveals that MEFs are more efficient in the removal of

daunorubicin. This is also reflected by the rapid redistribution of daunorubicin from the nucleus to the vesicles in the cytoplasm (Fig. 7.2B). As we did not observe a significant difference between wild-type and vault deficient cells, we conclude that vaults do not play a role in either the extrusion of daunorubicin from the cells or in the intracellular redistribution of the drug. Reintroduction of an expression construct encoding human MVP tagged at its N-terminus with GFP in *MVP*$^{-/-}$ cells results in the formation vault particles and concomitant stabilization of the minor vault proteins TEP1 and VPARP and vRNA (Chapter 6). However, expression of the GFP-tagged MVP in these cells did not give rise to extra daunorubicin extrusion as compared to *MVP*$^{-/-}$ MEFs transfected with a GFP expression construct (Fig. 7.2C). Taken together our results suggest that vaults are not directly involved in the sequestration of daunorubicin in cytoplasmic vesicles and/or the extrusion of drugs from the nucleus.

**Discussion**

Multidrug resistance (MDR) in tumor cells is a significant clinical issue as it directly affects the efficacy of chemotherapy. MDR cells are characterized by a decreased accumulation of various drugs, which can be caused by the expression of drug transporters like P-glycoprotein, MRP1 and BCRP1 (22). However, changes in drug accumulation cannot fully account for the anthracycline resistance in many MDR cells and other mechanisms have to contribute to the MDR phenotype. Vaults have been associated with intracellular drug transport and drug sequestration. There is experimental evidence that vaults are directly involved in the removal of anthracyclines from the nucleus (16-18). The mechanistic model that is postulated involves vaults in the nuclear membrane and/or nuclear pore complex where they function as drug efflux pumps. To test whether vaults function in the handling of anthracyclines, we investigated drug influx and efflux kinetics and its subcellular localization using a non-small cell lung cancer cell line overexpressing the major vault protein and mouse embryonic fibroblasts derived from wild type and *MVP* knockout mice as well as drug sensitive and resistant human non-small cell lung cancer cells.

We studied the daunorubicin efflux from a known drug resistant - vault overexpressing - cell line SW1573/2R120 and its drug sensitive parent SW1573. Furthermore, we included a stable transfected SW1573 cell line expressing a GFP-tagged MVP in our studies. Comparison of the non-small cell lung carcinoma cell line SW1573 with its MVP overexpressing transfectant (SW1573/MVP-GFP) revealed no changes in daunorubicin efflux rate and intracellular distribution. By contrast, the resistant derivative SW1573/2R120 clearly displayed a higher drug efflux rate resulting in a reduced drug accumulation in agreement with reports in the literature (23, 24). We observed that daunorubicin is directed to the nucleus and subsequently transferred from the nucleus to cytoplasmic vesicles. This process occurs earlier and more efficient in the resistant cells.

The sequestration of anthracyclines in cytoplasmic structures/vesicles has been described in several drug resistant cell lines and has been associated with the expression of P-gp, MRP1 and/or MVP (25-33). However, much is still unclear about the sequestration process and its role in MDR. It is believed that the cytoplasmic structures that sequester anthracyclines are acidic in nature, like lysosomes, trans-Golgi network and endosomes (29-31, 33, 34). Anthracyclines, being weak bases, accumulate in these acidic compartments where they are retained because they are protonated, becoming membrane-impermeable. Nevertheless, if the acidic nature of the anthracyclines were the only driving force for the sequestration in the cytoplasmic vesicles, one would expect this to occur during the influx phase as well. However, this is in contrast with our observation of the initial accumulation of the drug in the nucleus in all cell lines tested. Reports as to whether sequestration itself contributes to MDR are conflicting as is the evidence that the vesicles that accumulate anthracyclines are exocytotic in nature (28-31, 33-37). Nevertheless, treatment of resistant cells with carboxylic ionophores (like monensin and nigericin), brefeldin A and chloroquine, which disrupt intracellular vesicular transport and raise intracellular pH, results in increased anthracycline accumulation and redistribution of drug to the nucleus (29, 31, 34). Like our results, these observations suggest that the sequestration of drug in cytoplasmic vesicles reduces the amount of drug in the nucleus.

On the basis of our findings the role of vaults in the processes mentioned above, particularly the drug sequestration and the removal of drugs from the nucleus, is little or non-existent. Especially our experiments with mouse embryonic fibroblasts devoid of vault particles clearly indicate that vaults are not essential for the sequestration of daunorubicin and its efflux.

*Chapter 7*

**References**

1.   Suprenant K. A. Vault ribonucleoprotein particles: sarcophagi, gondolas, or safety deposit boxes? Biochemistry, 41(49):14447-14454, 2002.

2.   Scheffer, G. L., Schroeijers, A. B., Izquierdo, M. A., Wiemer, E. A., and Scheper, R. J. Lung resistance-related protein/major vault protein and vaults in multidrug-resistant cancer. Curr Opin Oncol, 12: 550-556, 2000.

3.   Kickhoefer, V. A., Siva, A. C., Kedersha, N. L., Inman, E. M., Ruland, C., Streuli, M., and Rome, L. H. The 193-kD vault protein, VPARP, is a novel poly(ADP-ribose) polymerase. J Cell Biol, 146: 917-928, 1999.

4.   Kickhoefer, V. A., Liu, Y., Kong, L. B., Snow, B. E., Stewart, P. L., Harrington, L., and Rome, L. H. The Telomerase/Vault-associated Protein TEP1 Is Required for Vault RNA Stability and Its Association with the Vault Particle. J Cell Biol, 152: 157-164, 2001.

5.   Kedersha, N. L., Heuser, J. E., Chugani, D. C., and Rome, L. H. Vaults. III. Vault ribonucleoprotein particles open into flower-like structures with octagonal symmetry. J Cell Biol, 112: 225-235, 1991.

6.   Kong, L. B., Siva, A. C., Rome, L. H., and Stewart, P. L. Structure of the vault, a ubiquitous celular component. Structure Fold Des, 7: 371-379, 1999.

7.   Abbondanza, C., Rossi, V., Roscigno, A., Gallo, L., Belsito, A., Piluso, G., Medici, N., Nigro, V., Molinari, A. M., Moncharmont, B., and Puca, G. A. Interaction of vault particles with estrogen receptor in the MCF-7 breast cancer cell. J Cell Biol, 141: 1301-1310, 1998.

8.   Chugani, D. C., Rome, L. H., and Kedersha, N. L. Evidence that vault ribonucleoprotein particles localize to the nuclear pore complex. J Cell Sci, 106: 23-29, 1993.

9.   Scheffer, G. L., Wijngaard, P. L., Flens, M. J., Izquierdo, M. A., Slovak, M. L., Pinedo, H. M., Meijer, C. J., Clevers, H. C., and Scheper, R. J. The drug resistance-related protein LRP is the human major vault protein. Nat Med, 1: 578-582, 1995.

10.  Scheper, R. J., Broxterman, H. J., Scheffer, G. L., Kaaijk, P., Dalton, W. S., van Heijningen, T. H., van Kalken, C. K., Slovak, M. L., de Vries, E. G., van der Valk, P., and *et al.* Overexpression of a M(r) 110,000 vesicular protein in non-P- glycoprotein-mediated multidrug resistance. Cancer Res, 53: 1475-1479, 1993.

11.  Schroeijers, A. B., Siva, A. C., Scheffer, G. L., de Jong, M. C., Bolick, S. C., Dukers, D. F., Slootstra, J. W., Meloen, R. H., Wiemer, E., Kickhoefer, V. A., Rome, L. H., and Scheper, R. J. The Mr 193,000 vault protein is up-regulated in multidrug-resistant cancer cell lines. Cancer Res, 60: 1104-1110, 2000.

12.  Izquierdo, M. A., Shoemaker, R. H., Flens, M. J., Scheffer, G. L., Wu, L., Prather, T. R., and Scheper, R. J. Overlapping phenotypes of multidrug resistance among panels of human cancer-cell lines. Int J Cancer, 65: 230-237, 1996.

13. Izquierdo, M. A., Scheffer, G. L., Flens, M. J., Giaccone, G., Broxterman, H. J., Meijer, C. J., van der Valk, P., and Scheper, R. J. Broad distribution of the multidrug resistance-related vault lung resistance protein in normal human tissues and tumors. Am J Pathol, 148: 877-887, 1996.

14. Kickhoefer, V. A., Rajavel, K. S., Scheffer, G. L., Dalton, W. S., Scheper, R. J., and Rome, L. H. Vaults are up-regulated in multidrug-resistant cancer cell lines. J Biol Chem, 273: 8971-8974, 1998.

15. Siva, A. C., Raval-Fernandes, S., Stephen, A. G., LaFemina, M. J., Scheper, R. J., Kickhoefer, V. A., and Rome, L. H. Up-regulation of vaults may be necessary but not sufficient for multidrug resistance. Int J Cancer, 92: 195-202, 2001.

16. Ohno, N., Tani, A., Uozumi, K., Hanada, S., Furukawa, T., Akiba, S., Sumizawa, T., Utsunomiya, A., Arima, T., and Akiyama, S. Expression of functional lung resistance--related protein predicts poor outcome in adult T-cell leukemia. Blood, 98: 1160-1165, 2001.

17. Kitazono, M., Okumura, H., Ikeda, R., Sumizawa, T., Furukawa, T., Nagayama, S., Seto, K., Aikou, T., and Akiyama, S. Reversal of LRP-associated drug resistance in colon carcinoma SW-620 cells. Int J Cancer, 91: 126-131, 2001.

18. Kitazono, M., Sumizawa, T., Takebayashi, Y., Chen, Z. S., Furukawa, T., Nagayama, S., Tani, A., Takao, S., Aikou, T., and Akiyama, S. Multidrug resistance and the lung resistance-related protein in human colon carcinoma SW-620 cells [see comments]. J Natl Cancer Inst, 91: 1647-1653, 1999.

19. Mossink, M. H., Van Zon, A., Fränzel-Luiten, E., Schoester, M., Kickhoefer, V. A., Scheffer, G. L., Scheper, R. J., Sonneveld, P., and Wiemer, E. A. Disruption of the Murine Major Vault Protein (MVP/LRP) Gene Does Not Induce Hypersensitivity to Cytostatics. Cancer Res, 62: 7298-7304, 2002.

20. Kuiper, C. M., Broxterman, H. J., Baas, F., Schuurhuis, G. J., Haisma, H. J., Scheffer, G. L., Lankelma, J., and Pinedo, H. M. Drug transport variants without P-glycoprotein overexpression from a human squamous lung cancer cell line after selection with doxorubicin. J. Cell Pharmacol., 1: 35-41, 1990.

21. Flens, M. J., Scheffer, G. L., van der Valk, P., Broxterman, H. J., Eijdems, E. W., Huysmans, A. C., Izquierdo, M. A., and Scheper, R. J. Identification of novel drug resistance-associated proteins by a panel of rat monoclonal antibodies. Int J Cancer, 73: 249-257, 1997.

22. Borst, P. and Elferink, R. O. Mammalian ABC transporters in health and disease. Annu Rev Biochem, 71: 537-592, 2002.

23. de Lange, J. H., Schipper, N. W., Schuurhuis, G. J., ten Kate, T. K., van Heijningen, T. H., Pinedo, H. M., Lankelma, J., and Baak, J. P. Quantification by laser scan microscopy of intracellular doxorubicin distribution. Cytometry, 13: 571-576, 1992.

24. Versantvoort, C. H., Broxterman, H. J., Pinedo, H. M., de Vries, E. G., Feller, N., Kuiper, C. M., and Lankelma, J. Energy-dependent processes involved in reduced drug accumulation in multidrug-resistant human lung cancer cell lines without P-glycoprotein expression. Cancer Res, 52: 17-23, 1992.

25. Gervasoni, J. E., Jr., Fields, S. Z., Krishna, S., Baker, M. A., Rosado, M., Thuraisamy, K., Hindenburg, A. A., and Taub, R. N. Subcellular distribution of daunorubicin in P-glycoprotein-positive and -negative drug-resistant cell lines using laser-assisted confocal microscopy. Cancer Res, 51: 4955-4963, 1991.

26. Sognier, M. A., Zhang, Y., Eberle, R. L., Sweet, K. M., Altenberg, G. A., and Belli, J. A. Sequestration of doxorubicin in vesicles in a multidrug-resistant cell line (LZ-100). Biochem Pharmacol, 48: 391-401, 1994.

27. Breuninger, L. M., Paul, S., Gaughan, K., Miki, T., Chan, A., Aaronson, S. A., and Kruh, G. D. Expression of multidrug resistance-associated protein in NIH/3T3 cells confers multidrug resistance associated with increased drug efflux and altered intracellular drug distribution. Cancer Res, 55: 5342-5347, 1995.

28. Verovski, V. N., Van den Berge, D. L., Delvaeye, M. M., Scheper, R. J., De Neve, W. J., and Storme, G. A. Low-level doxorubicin resistance in P-glycoprotein-negative human pancreatic tumour PSN1/ADR cells implicates a brefeldin A-sensitive mechanism of drug extrusion. Br J Cancer, 73: 596-602, 1996.

29. Cleary, I., Doherty, G., Moran, E., and Clynes, M. The multidrug-resistant human lung tumour cell line, DLKP-A10, expresses novel drug accumulation and sequestration systems. Biochem Pharmacol, 53: 1493-1502, 1997.

30. Hurwitz, S. J., Terashima, M., Mizunuma, N., and Slapak, C. A. Vesicular anthracycline accumulation in doxorubicin-selected U-937 cells: participation of lysosomes. Blood, 89: 3745-3754, 1997.

31. Altan, N., Chen, Y., Schindler, M., and Simon, S. M. Defective acidification in human breast tumor cells and implications for chemotherapy. J Exp Med, 187: 1583-1598, 1998.

32. Schuurhuis, G. J., van Heijningen, T. H., Cervantes, A., Pinedo, H. M., de Lange, J. H., Keizer, H. G., Broxterman, H. J., Baak, J. P., and Lankelma, J. Changes in subcellular doxorubicin distribution and cellular accumulation alone can largely account for doxorubicin resistance in SW- 1573 lung cancer and MCF-7 breast cancer multidrug resistant tumour cells. Br J Cancer, 68: 898-908, 1993.

33. Loetchutinat, C., Priebe, W., and Garnier-Suillerot, A. Drug sequestration in cytoplasmic organelles does not contribute to the diminished sensitivity of anthracyclines in multidrug resistant K562 cells. Eur J Biochem, 268: 4459-4467, 2001.

34. Sehested, M., Skovsgaard, T., and Roed, H. The carboxylic ionophore monensin inhibits active drug efflux and modulates *in vitro* resistance in daunorubicin resistant Ehrlich ascites tumor cells. Biochem Pharmacol, 37: 3305-3310, 1988.

35. Vichi, P. J. and Tritton, T. R. Protection from adriamycin cytotoxicity in L1210 cells by brefeldin A. Cancer Res, 53: 5237-5243, 1993.

36. Wood, D. J., Rumsby, M. G., and Warr, J. R. Monensin and verapamil do not alter intracellular localisation of daunorubicin in multidrug resistant human KB cells. Cancer Lett, 108: 41-47, 1996.

37.  Seidel, A., Hasmann, M., Loser, R., Bunge, A., Schaefer, B., Herzig, I., Steidtmann, K., and Dietel, M. Intracellular localization, vesicular accumulation and kinetics of daunorubicin in sensitive and multidrug-resistant gastric carcinoma EPG85-257 cells. Virchows Arch, 426: 249-256, 1995.

CHAPTER 8

General discussion

*Chapter 8*

**Introduction**

Vaults were first described in the mid-eighties as contaminants of preparations of clathrin-coated vesicles isolated from rat liver (1). The typical ovoid structures that were observed are in fact ribonucleoprotein particles composed of multiple copies of a $M_r$ 100,000 major vault protein (MVP) and two minor vault proteins of $M_r$ 193,000 (VPARP) and $M_r$ 240,000 (TEP1) as well as small untranslated RNA molecules of 88-141 bases. The components are assembled into hollow barrel-shaped structures that are found in eukaryotic species. Although the precise cellular and physiological function of vaults is not elucidated several functions have been proposed usually envisaging a role for vaults in intracellular transport processes, notably the transport of xenobiotics or drugs. However, direct evidence for a role of vaults as intracellular transport module is scarce or lacking all together.

The studies presented in this thesis were performed to address the following questions:
1. What does vault structure, biogenesis, subcellular localization and dynamics tell us about function of the mammalian vault complex?
2. Are vaults involved in the intracellular transport and/or sequestration of toxic agents?

*Approach*
To address the questions raised above, we generated cell line transfectants stably expressing a green fluorescent protein tagged major vault protein. The tagged MVP molecules are incorporated into genuine vault particles, which enable us to examine the intracellular distribution and *in vivo* dynamics of fluorescent vaults. To study vault structure and biogenesis we mapped and characterized protein domains in the three vault protein components. The protein-protein interactions were examined by yeast two-hybrid analysis. As the RNA component of the vault complex is believed to be of functional significance, we investigated the expression and association with the vault complex of human vault RNAs in various cancer cell lines in relation to drug resistance. The dependence of vault structure and vault biogenesis on MVP was examined in tissues and cells derived from *MVP* knockout mice that were previously generated in our group. The direct involvement of vaults in drug transport, particularly the nuclear extrusion and sequestration of anthracyclines, was studied by analyzing the daunorubicin distribution and efflux in wild-type and *MVP* knockout cell lines.

**Subcellular localization and dynamics of the vault complex**

Vaults are detectable in most mammalian cells and tissues; however, their absolute expression level differs. A relatively high expression of vaults is encountered in the gastro-intestinal tract epithelia, lung, keratinocytes, adrenal cortex and macrophages. A low vault expression is seen in tissues like brain, smooth and skeletal muscle and various other tissues (2, 3). Probably all mammalian cells and cell lines express vaults to a certain extent or at least are able to induce the expression of vaults when challenged in the appropriate manner (4-6). We studied the subcellular distribution

and dynamics of vaults in the non-small cell lung carcinoma cell line SW1573 using a transfectant stably expressing MVP-GFP or GFP-MVP. The 26 kDa green fluorescent protein (GFP) or its enhanced multi-color variants are widely used to visualize proteins, protein complexes or organelles in living cells (see for review Tsien (7)). In Chapter 2 we show in various ways that both the MVP-GFP and GFP-MVP fusion proteins are incorporated into genuine vault particles. However, our data imply that vaults containing these GFP-tagged MVP molecules may be less stable than regular vault particles particularly during biochemical fractionation. Although we cannot test whether the GFP-tag is interfering with vault function due to the absence of an assay for vault function, we have several indications to believe that the tagged vault particles are functioning similar to regular vaults. First, both the C-terminal and N-terminal tagged MVP molecules behaved similarly in all our experiments, indicating that the actual position of the GFP-tag is of no relevance for incorporation into vaults and vault behaviour. Second, the tagged MVP molecules behaved similar to endogenous MVP; i.e. the subcellular localization and reaction to certain stimuli are comparable. Finally, as described in Chapter 6, expression of GFP-MVP in *MVP^-/-* mouse embryonic fibroblasts resulted in the formation of vault particles with similar physico-chemical properties as regular vaults, which resulted in the stabilization of the minor vault proteins (VPARP and TEP1).

In SW1573 cells cultured under standard conditions vaults were found evenly dispersed though the cytoplasm where the majority is freely mobile and moves by diffusion. It was noted that selective permeabilisation of the plasma membrane by the cholesterol complexing agent digitonin leads to a rapid release of vaults from the cells with vaults behaving like the soluble cytosolic protein marker lactate dehydrogenase (Van Zon *et al.*, unpublished data). Furthermore, co-localization studies demonstrated no distinct accumulation of GFP-tagged vaults at or on any of the main cellular compartments like the endoplasmic reticulum, Golgi apparatus or endosomes. However, using biochemical fractionation studies and immunofluorescence studies some vaults were found to be associated with the nucleus and nuclear membrane (Van Zon *et al.*, unpublished data). Others have also observed this phenomenon and in the literature it is estimated that approximately 5% of the total amount of vaults in mammalian cells is associated with the nucleus (8, 9). If the large vault particles are present in the nuclear matrix, individual components should be imported and assembled into vaults within the nucleus. As far as we know only VPARP has putative nuclear import signals and is clearly detected in the nuclear matrix in immunofluorescent experiments or in nuclear fractions. Chugani *et al.* (9) suggested that vaults form the elusive central plug in the nuclear pore complex, a hypothesis that has not yet been confirmed by others. It was shown that vaults dock or bind close to nuclear pores on the cytoplasmic face of the nuclear membrane. We found that vaults accumulate at the nuclear membrane after inhibiting protein synthesis by a treatment of the cells with cycloheximide (Van Zon *et al.*, unpublished data). This treatment results in an increased functional nuclear pore size by approximately 60 Å (10). It is unclear whether the protein synthesis inhibition or the increased pore size itself is

responsible for the accumulation of vaults at the nuclear membrane. Close examination of SW1573 cells expressing GFP-tagged vaults revealed that a fraction of the vault particles was in close proximity of microtubules. The interaction between vaults and microtubules was further substantiated when β-tubulin could be immunoprecipitated together with vaults. Furthermore, it was shown that vault movement that for a large part occurs by diffusion was affected by disintegration of the microtubules by nocodazole treatment i.e. vaults seem to be partly dependent upon intact microtubules for their movement.

An intriguing aspect of vaults is described in Chapter 2 namely their ability to assemble into highly ordered tube-like structures under certain conditions like the lowering of the temperature from 37°C to 21°C. The vault-tube formation is completely reversible. We have noticed that a number of other conditions, such as the treatment of the cells with hydrogen peroxide, sodium azide or ADP-ribosylation inhibitors, also gave rise to the formation of vault-tubes, although usually less and smaller tubes are formed. The question arises what the functional significance is of these tubes and whether they also occur under normal physiological conditions in mammalian tissues. Interestingly, the tubes seem to originate at non-vault associated VPARP clusters (VPARP-rods), which are predominantly present in the perinuclear region of the cytoplasm. We show the existence of a dynamic relationship between vault particles and the VPARP-rods. It may be that at lower temperature certain processes that occur normally are slowed down, giving rise to an accumulation of vault particles that then form the highly regular tubes. Also the cytoskeleton appears to participate in vault-tube formation. Destabilisation of microtubules by nocodazole stimulates vault-tube formation when the temperature is lowered and microtubule stabilization by taxol prevents or severely inhibits tube formation.

What have we learned from these studies? First, vaults are able to arrange themselves into higher order structures: the vault-tubes. The physiological significance of this process is still unclear. Second, vault particles dynamically interact with the cytoplasmic non-vault associated VPARP-rods. Third, the interaction between vaults and microtubules affects vault movement and apparently also the vault organization within the cell.

**Structural and functional relationship of the vault components**

Although the main vault components have been identified and characterized, little is known about the assembly of the largest ribonucleoprotein and which factors play a role in this process. Furthermore, it is unknown whether the complex is stably present in cells or going through multiple cycles of disassembly and reassembly. Also the function of each individual vault protein within or outside the vault complex it not, or at least not exactly, understood. To begin addressing these questions, we used a yeast two-hybrid approach to delineate domains within the three vault proteins. Most importantly, we identified that the evolutionarily conserved coiled coil domain in the

C-terminal half of MVP is essential for MVP-MVP interactions and as a direct consequence for vault assembly. Furthermore, we identified that the association between VPARP and MVP is mediated by the N-terminal part of MVP and the C-terminus of VPARP. We demonstrated that isolated MVP was able to bind calcium most likely through the calcium binding EF-hands present in the N-terminal half of the protein. Recently, it was shown that the calcium binding has functional significance as it was reported that the tumor suppressor PTEN was capable of interacting with intact vaults a binding mediated by calcium (11).

The vault RNA is believed to fulfil a functional role within the complex rather than a structural role. This remark is based on the observation that degradation of the vault RNA does not affect the overall morphology of the vault complex (1, 12). Although this is a rather circumstantial argument not backed up by hard evidence, it is not unreasonable if we consider the role of the RNA component of known eukaryotic ribonucleoproteins like the ribosome, the telomerase complex, the signal recognition particle and snRNPs. Furthermore, the recent discovery of novel small non-coding RNAs in various organisms with important roles in gene regulation like micro RNAs (miRNAs) and small interfering RNAs (siRNAs) shows that RNAs are suitable for a diverse range of functions (13-15). Therefore, the relatively small RNA component of vaults might be the key to a functional understanding of the vault complex. In rodents only one vault RNA of 141 bases is expressed whereas humans express three related vault RNAs of 88 - 98 bases (hvg1 -3). Our own findings do support a functional role for the RNA component of vaults, as it was found that the ratio in which the various human vault RNAs associate with the vault complex differs. Consistently, we observed more hvg3 bound to vaults isolated from drug resistant cell lines suggesting the ratio at which vault RNAs are bound determines human vault function.

It was observed that not all VPARP and TEP1 expressed in cells are associated with the vault complex. TEP1 is associated with the telomerase complex, whereas VPARP is present in cytoplasmic clusters (VPARP-rods) and in the nuclear matrix. The question is whether VPARP and TEP1 have a separate function outside the context of the vault complex or whether these proteins are still functionally dependent on the vaults. A first clue comes from our studies towards the effects of loss of MVP on the remaining vault components. As described in Chapter 6, the absence of MVP severely affects levels of VPARP and TEP1. In *MVP* knockout tissues hardly any VPARP and TEP1 could be detected. The same is observed in *MVP*$^{-/-}$ embryonic stem cells and mouse embryonic fibroblasts (MEFs) from *MVP*$^{-/-}$ mice, however the phenotype in these cell lines is less severe. Interestingly, biochemical fractionation reveals that VPARP is not present in a nuclear fraction of *MVP*$^{-/-}$ MEFs. This suggests that MVP also determines the subcellular localization of VPARP. Taken together our data indicate that the non-vault associated VPARP and TEP1 are linked to the vault complex.

**Vaults and multidrug resistance**

The first observation linking vaults to multidrug resistance was reported by Scheffer *et al.* (16), who demonstrated that the lung resistance related protein (LRP) was in fact the human major vault protein. Lung resistance related protein was found to be overexpressed in drug resistant cancer cell lines that did not express P-glycoprotein (17). Based on the putative transport function of vaults and the cellular distribution of fluorescent anthracyclines in vault-expressing resistant cell lines, it was proposed that vaults act by transporting drugs away from their subcellular targets. There is a considerable amount of literature dealing with a putative role of vaults in multidrug resistance (reviewed by Scheffer *et al.* (18) and Mossink *et al.* (19)). It was observed that the expression of vault proteins closely reflected the chemoresistance profile of many tumor cell lines and untreated cancers. In addition, elevated MVP levels were observed in cell lines resistant to various classes of cytotoxic agents including doxorubicin, mitoxantrone, methotrexate, etoposide, vincristine, cytarabine and cisplatin. However, very few studies directly assessed the role of vaults in drug resistance. In transfection experiments, the ovarian carcinoma cell line A2780 was stably expressing MVP; the elevated level of MVP led to an increased number of vaults, but it did not confer drug resistance against doxorubicin, vincristine and etoposide (VP-16) (16, 20). It was concluded from these studies that vaults may be necessary but are not sufficient to confer drug resistance. By contrast, experiments by Kitazono *et al.* provide experimental support for a role of vaults in the extrusion of anthracyclines from the nuclei of resistant cells (5, 21, 22). Treatment of the colon carcinoma cell line SW620 with sodium butyrate led to a strong induction of MVP and made the cells significantly less sensitive to doxorubicin, etoposide (VP-16), vincristine, paclitaxel and the transport antibiotic gramicidin D. The stable expression of two unrelated MVP-specific ribozymes reversed the observed resistant phenotype. Furthermore, the efflux of doxorubicin from the nuclei in intact cells or even isolated nuclei could be inhibited by the expression of the ribozymes or the addition of polyclonal anti-(MVP) antibodies (5). More insight is needed in the biochemical requirements of this efflux process, which apparently takes place in a relatively simple buffer without ATP or any cytosolic factors. The molecular mechanism for vault-mediated drug resistance as sketched by the authors may hold true for anthracyclines and perhaps etoposide, but most likely not for resistance against cytotoxic drugs that target the cytoskeleton (like taxol and vincristine). Recently, our group showed that *MVP*$^{-/-}$ embryonic stem cells as well as bone marrow cells derived from *MVP* knockout mice were not hypersensitive to cytotoxic drugs with different modes of action (23). In these initial experiments, however, intracellular drug distribution and drug handling were not examined. Therefore we studied the distribution and intracellular localization of the anthracycline daunorubicin in SW1573 cells overexpressing a GFP-tagged MVP and in MEFs derived from *MVP* knockout mice. No differences in drug handling were observed in the cell lines tested. We therefore conclude that vaults do not have a direct role in multidrug resistance, not ruling out that cells overexpressing vaults may have an advantage in surviving the cellular stress.

**Future directions**

Although our knowledge about the vault complex increased considerably over the years, we still lack insight into its cellular functions. For future studies the developed knockout models will be highly instrumental to reveal the full significance of vaults. They provide investigators with model systems in which the effects of the absence of vaults or individual vault proteins on cellular and organ functioning can be directly studied. It might be worthwhile to intercross the various knockout mice available in order to generate a knockout in which all vault components are absent. At least such a mouse model would resolve the discussion about possible active remnants of the vault complex in the various single knockouts. In this respect one could even think of disrupting the vRNA gene as well.

Another important line for future research is the identification of vault interacting proteins. The vault components that have been identified, which are present in fixed stoichiometric amounts in highly purified vault preparations, can be considered the core of the complex. *In vivo* additional proteins may associate with the vault complex in a stable or transient manner depending on the cell-type and/or specific conditions. These interactions may be weak and some of them may be lost during vault purification. Two examples of such vault-associated proteins have recently been described; the La RNA-binding protein (24) and the tumor suppressor PTEN (11). Particularly the significance of the vault-PTEN interaction is not yet clear. It is proposed that the interaction with MVP might modulate PTEN activity. Clearly, vaults are not essential for PTEN function, as MVP deficient animals are viable and show no apparent abnormalities, whereas PTEN disruption leads to embryonic lethality (11). The activation of PI3 kinase/AKT signaling pathway or tumorigenesis can be studied in the available knockout models. Furthermore, if vaults truly function as intracellular transport modules then the identification of its cargo and the characterization of additional VPARP substrates may help to pinpoint its function. Equally interesting are more detailed studies into a possible cross-talk and cooperation between vaults and the telomerase complex, particularly because it was recently reported that both VPARP and vRNA are also associated with the telomerase complex (25).

In coming years, as vault research progresses fully exploiting the various knockout models that have been developed, vaults will continue to surprise and offer novel cell biological insights. After all, one can hardly imagine a unique organelle as the vault complex having a solely ornamental role.

## References

1.    Kedersha, N. L. and Rome, L. H. Isolation and characterization of a novel ribonucleoprotein particle: large structures contain a single species of small RNA. J Cell Biol, 103: 699-709, 1986.
2.    Mossink, M. H., van Zon, A., Schoester, M., Scheffer, G. L., Scheper, R. J., Sonneveld, P., and Wiemer, E. A. Isolation and characterization of the murine vRNA and the cDNA encoding the major vault protein: Vault expression patterns in normal tissues. Abstract AACR, 42: 919, 2001.
3.    Izquierdo, M. A., Shoemaker, R. H., Flens, M. J., Scheffer, G. L., Wu, L., Prather, T. R., and Scheper, R. J. Overlapping phenotypes of multidrug resistance among panels of human cancer-cell lines. Int J Cancer, 65: 230-237, 1996.
4.    Mossink, M. H., Van Zon, A., Schoester, M., Fränzel-Luiten, E., Scheffer, G. L., Scheper, R. J., Sonneveld, P., and Wiemer, E. A. Vaults are not induced by short-term exposure to sublethal doses of cytostatics but are strongly upregulated by differentiating agents and oxidative stress in HL-60 cells. Abstract AACR, 43: 1105, 2002.
5.    Kitazono, M., Sumizawa, T., Takebayashi, Y., Chen, Z. S., Furukawa, T., Nagayama, S., Tani, A., Takao, S., Aikou, T., and Akiyama, S. Multidrug resistance and the lung resistance-related protein in human colon carcinoma SW-620 cells [see comments]. J Natl Cancer Inst, 91: 1647-1653, 1999.
6.    Berger, W., Elbling, L., and Micksche, M. Expression of the major vault protein LRP in human non-small-cell lung cancer cells: activation by short-term exposure to antineoplastic drugs. Int J Cancer, 88: 293-300, 2000.
7.    Tsien, R. Y. The green fluorescent protein. Annu Rev Biochem, 67: 509-544, 1998.
8.    Hamill, D. R. and Suprenant, K. A. Characterization of the sea urchin major vault protein: a possible role for vault ribonucleoprotein particles in nucleocytoplasmic transport. Dev Biol, 190: 117-128, 1997.
9.    Chugani, D. C., Rome, L. H., and Kedersha, N. L. Evidence that vault ribonucleoprotein particles localize to the nuclear pore complex. J Cell Sci, 106: 23-29, 1993.
10.   Feldherr, C. M., Akin, D., and Cohen, R. J. Regulation of functional nuclear pore size in fibroblasts. J Cell Sci, 114: 4621-4627, 2001.
11.   Yu, Z., Fotouhi-Aroakani, N., Wu, L., Maoui, M., Wang, S., Banville, D., and Shen, S. H. PTEN Associates with the vault particles in Hela cells. J Biol Chem, 277:40247-40252, 2002.
12.   Kong, L. B., Siva, A. C., Kickhoefer, V. A., Rome, L. H., and Stewart, P. L. RNA location and modeling of a WD40 repeat domain within the vault. Rna, 6: 890-900, 2000.
13.   Steinberg, D. MicroRNA shows macro potential. The Scientist 22-24, 2003.
14.   Mattick, J. S. Non-coding RNAs: the architects of eukaryotic complexity.

EMBO Rep, 2: 986-991, 2001.

15.    Pickford, A. S. and Cogoni, C. RNA-mediated gene silencing. Cell Mol Life Sci, 60: 871-882, 2003.

16.    Scheffer, G. L., Wijngaard, P. L., Flens, M. J., Izquierdo, M. A., Slovak, M. L., Pinedo, H. M., Meijer, C. J., Clevers, H. C., and Scheper, R. J. The drug resistance-related protein LRP is the human major vault protein. Nat Med, 1: 578-582, 1995.

17.    Scheper, R. J., Broxterman, H. J., Scheffer, G. L., Kaaijk, P., Dalton, W. S., van Heijningen, T. H., van Kalken, C. K., Slovak, M. L., de Vries, E. G., van der Valk, P., and *et al.* Overexpression of a M(r) 110,000 vesicular protein in non-P- glycoprotein-mediated multidrug resistance. Cancer Res, 53: 1475-1479, 1993.

18.    Scheffer, G. L., Schroeijers, A. B., Izquierdo, M. A., Wiemer, E. A., and Scheper, R. J. Lung resistance-related protein/major vault protein and vaults in multidrug-resistant cancer [In Process Citation]. Curr Opin Oncol, 12: 550-556, 2000.

19.    Mossink, M. H., van Zon, A., Scheper, R. J., Sonneveld, P., and Wiemer, E. A. Vaults: A ribonucleoprotein particle involved in drug resistance? Oncogene reviews, in press, 2003.

20.    Siva, A. C., Raval-Fernandes, S., Stephen, A. G., LaFemina, M. J., Scheper, R. J., Kickhoefer, V. A., and Rome, L. H. Up-regulation of vaults may be necessary but not sufficient for multidrug resistance. Int J Cancer, 92: 195-202, 2001.

21.    Kitazono, M., Okumura, H., Ikeda, R., Sumizawa, T., Furukawa, T., Nagayama, S., Seto, K., Aikou, T., and Akiyama, S. Reversal of LRP-associated drug resistance in colon carcinoma SW-620 cells. Int J Cancer, 91: 126-131, 2001.

22.    Ohno, N., Tani, A., Uozumi, K., Hanada, S., Furukawa, T., Akiba, S., Sumizawa, T., Utsunomiya, A., Arima, T., and Akiyama, S. Expression of functional lung resistance--related protein predicts poor outcome in adult T-cell leukemia. Blood, 98: 1160-1165, 2001.

23.    Mossink, M. H., Van Zon, A., Fränzel-Luiten, E., Schoester, M., Kickhoefer, V. A., Scheffer, G. L., Scheper, R. J., Sonneveld, P., and Wiemer, E. A. Disruption of the Murine Major Vault Protein (MVP/LRP) Gene Does Not Induce Hypersensitivity to Cytostatics. Cancer Res, 62: 7298-7304, 2002.

24.    Kickhoefer, V. A., Poderycki, M. J., Chan, E. K., and Rome, L. H. The La RNA binding protein interacts with the vault RNA and is a vault- associated protein. J Biol Chem, 277:40247-40252 2002.

25.    Shall, S. Poly (ADP-ribosylation)--a common control process? Bioessays, 24: 197-201, 2002.

*Summary*
and
SAMENVATTING

## Summary

Vaults are the largest ribonucleoprotein particles found in eukaryotic cells. The main component of these 13 MDa structures is the $M_r$ 100,000 major vault protein (MVP). In mammalian cells, about 96 copies of this protein are necessary to form one vault particle. Two additional proteins are associated with the complex, the so-called minor vault proteins of $M_r$ 193,000 (VPARP) and $M_r$ 240,000 (TEP1), as well as several untranslated RNA molecules of 86-141 bases. The components are arranged into a hollow barrel-like structure with each half representing eight arches, which are reminiscent to the arched vaulted ceilings of cathedrals. Therefore, when vaults were first observed as contaminants in a preparation of clathrin coated vesicles form rat liver, the large complexes were named 'vaults'. The typical morphology and the individual vault constituents appear conserved throughout evolution, implying an important role for vaults in cellular metabolism. A number of functions have been suggested for these unique particles, but the general idea is that vaults function in intracellular transport processes. Nevertheless, the precise cellular function of the vault complex has not yet been elucidated. In this study we attempted to gain insight in vault biogenesis, dynamics and their interaction with other cellular components in order to unravel the physiological significance of vaults. **Chapter 1** gives an overview of the vault components, the vault structure and subcellular localization and reviews the proposed functions of vault particles.

In **Chapter 2** we studied the subcellular localization and dynamics of the vault complex in a non-small cell lung cancer cell line (SW1573) expressing a green fluorescent protein (GFP) tagged MVP (SW1573/MVP-GFP). Most of the tagged proteins were incorporated into vault particles that behaved similar to endogenous vaults, enabling us to study vault dynamics *in vivo* by fluorescence recovery after photobleaching (FRAP). The results indicated that the majority of the vault particles are freely mobile and move by diffusion. Dramatic rearrangements in vault localization were observed when the cells were incubated at 21°C (room temperature). In about 50 to 80% of the cells large elongated fluorescent structures appeared, the vault-tubes. These vault-tubes were ordered structures from which MVP molecules were exchanged in time. Vault-tube formation reduced the non-vault associated fraction of VPARP, which was present in small-elongated structures in the cytoplasm (VPARP-rods) as well as in the nuclear matrix. Furthermore, the formation of the vault-tubes was reversible and depended on a coiled coil structure present in MVP. Moreover, vault-tube formation was influenced by the stability of microtubules. The relation between vaults and the microtubules was investigated in **Chapter 3**. In SW1573/MVP-GFP transfectants we observed co-localization of vault particles with microtubules, but not with actin filaments. An interaction between vaults and microtubules had already been suggested in literature, when sea-urchin vaults were found to co-purify with microtubules in several cycles of polymerization and depolymerization. We confirmed and extended these results showing a co-immunoprecipitation of vaults and β-tubulin. Moreover,

using quantitative fluorescence-recovery after photobleaching (FRAP) we demonstrated that disassembly of microtubules influenced vault mobility (vaults move slower), but not the mobility of GFP molecules in a control experiment. Although we are just beginning to explore the relation between vaults and microtubules, the microtubules appear to influence general vault movement as well as the assembly of vaults into vault-tubes.

**Chapter 4** described several distinct domains of the three vault proteins: MVP, VPARP and TEP1. Using a yeast two-hybrid system we demonstrated the presence of an intramolecular binding site within MVP and showed that MVP molecules interact with each other via their coiled coil domain. Next to the conserved coiled coil domain, MVP contained three putative EF-hands that were capable of binding calcium. The binding of calcium seemed important for the interaction of MVP with other proteins (e.g. PTEN) and may be involved in vault biogenesis. Within VPARP intramolecular binding sites were detected and it was found that the C-terminus of VPARP interacts with the N-terminal part of MVP. No interactions were found between TEP1 and the other vault components. Because TEP1 is known to bind the vault RNA (vRNA), we tested whether co-expression of vRNA in the two-hybrid system resulted in binding of TEP1 to the other vault proteins; However, this was not the case.

The expression and vault-association of the human vRNAs was investigated in **Chapter 5**. In humans three genes had been described that encode different vault RNAs (*HVG1–3*) and a fourth was found in a homology search (*HVG4*). Only *HVG1–3* were expressed and present in excess in a non-vault bound pool in all cell lines tested. The genes were located in a tandem repeat structure on chromosome 5q33.1. All expressed hvgs associate with vaults, but the expression ratio did not reflect the ratio in which the hvgs were associated with the complex. The bulk of the vRNA that was associated with vaults was hvg1. Interestingly, an increased amount of hvg3 was bound to vaults that were isolated from multidrug resistant cell lines. This implied that the ratio in which the hvg species were associated with the vault complex might influence or determine its function and points to a functional role for vRNA within the vault complex.

The observation that vault-tube formation results in a decrease of the non-vault bound VPARP, suggested that the proteins of the vault complex (at least MVP and VPARP), whether incorporated into vaults or not, were somehow functionally related and comprised a single integrated system. This hypothesis was corroborated by the results described in **Chapter 6**, in which the consequences of the disruption of *MVP* for the integrity of the vault complex and the stability of the other vault components were investigated. For this study we used an *MVP* knockout mouse model, which had been generated previously in our group. As expected, the *MVP* knockout tissues no longer contained vaults or vault-like particles. Moreover, the loss of MVP resulted in dramatically decreased levels of the minor vault proteins (TEP1 and VPARP) and a

clear reduction of the vRNA levels. The decrease in TEP1 and VPARP protein levels was not caused by reduced transcription rates, mRNA instability or a translational down regulation. The minor vault proteins were less stable in the absence of the core of the vault complex. The reduction in vRNA levels probably was a direct result of the decrease in TEP1 protein. The effect of the loss of MVP was reversible, as re-introduction of full length human MVP in knockout cells restored the levels of VPARP and vRNA.

Experiments performed previously revealed that the disruption of *MVP* did not affect the sensitivity of embryonic stem cells or bone marrow cells to cytostatics; however, intracellular drug handling was not investigated in those experiments. Therefore, in **Chapter 7** we analyzed the intracellular distribution and influx/efflux kinetics of fluorescent anthracyclines in mouse embryonic fibroblasts (MEFs) derived from wild-type and *MVP* knockout mice and compared these results with the drug handling of the non-small cell lung cancer cell line (SW1573), its drug resistant - vault overexpressing - counterpart (SW1573/2R120) and the MVP-GFP overexpressing cell line (SW1573/MVP-GFP). No significant differences were observed between the sensitive SW1573 and the MVP-GFP overexpressing SW1573 cells. In all cell lines, including the drug resistant SW1573/2R1320, daunorubicin initially accumulated in the nucleus after which it was transferred to cytoplasmic vesicles. The efflux of drugs from the nucleus appeared more rapid and efficient in the drug resistant cell line. We did not observe a significant difference in drug-handling between wild-type and vault deficient cells and between vault deficient and deficient cells in which we re-introduced a full length human MVP tagged with GFP. Both systems showed that vaults do not directly play a role in the extrusion of daunorubicin from cells or in the intracellular redistribution of the drug from the nucleus to cytoplasmic vesicles.

Finally, in **Chapter 8**, the results of this thesis were summarized and their significance was discussed.

## Samenvatting

Vaults zijn de grootste ribonucleoproteine deeltjes die tot nu toe gevonden zijn in eukaryote cellen. De belangrijkste component van deze 13 MDa structuren is het $M_r$ 100.000 major vault eiwit (major vault protein ofwel MVP). In zoogdiercellen zijn er ongeveer 96 kopieën van dit eiwit nodig om een vault partikel te vormen. Er zijn nog twee andere eiwitten onderdeel van het complex, de zogenaamde minor vault eiwitten van $M_r$ 193.000 (VPARP) en $M_r$ 240.000 (TEP1). Verder zitten er nog een aantal niet getransleerde RNA moleculen van ongeveer 86 tot 141 nucleotiden aan het vault complex vast. De verschillende componenten zijn gerangschikt in een holle ton-vormige structuur waarvan elke helft bestaat uit acht bogen die lijken op de bogen in de gewelven (in het engels: vaults) van een kathedraal. Daarom werden de complexen, die als eerste gevonden werden als contaminatie van gezuiverde 'clathrin coated vesicles' uit rattenlevers, 'vaults' genoemd. Hun typische morfologie en de individuele componenten bleken evolutionair geconserveerd. Dit kan duiden op een belangrijke rol voor vaults in het metabolisme van de cel. Een aantal functies zijn al gesuggereerd voor de vaults. Het algemene idee is dat vaults een functie hebben in transportprocessen binnen de cel. Toch is de precieze functie van het vault complex nog niet bekend. In deze studie proberen we inzicht te krijgen in de biogenese van vaults, hun dynamiek en de interactie van vaults met andere cellulaire componenten om op deze manier de fysiologische betekenis van de vaults te achterhalen. **Hoofdstuk 1** geeft een overzicht van de vault componenten, de vault structuur en de subcellulaire lokalisatie en geeft een overzicht van de veronderstelde functies van het vault partikel.

In **Hoofdstuk 2** bestudeerden we de subcellulaire lokalisatie en dynamiek van het vault complex in een 'non-small cell' longkanker cellijn (SW1573) die een MVP molecuul tot expressie brengt waaraan een groen fluorescerend eiwit (green fluorescent protein ofwel GFP) hangt (SW1573/MVP-GFP). De meeste van de GFP gelabelde eiwitten werden ingebouwd in vault partikels die een zelfde gedrag vertonen als de endogene vaults. Hierdoor waren we in staat om de dynamiek van vaults in levende cellen te bestuderen met behulp van een techniek die 'fluorescence recovery after photobleaching' (FRAP) heet. De resultaten lieten zien dat het grootste gedeelte van de vault partikels vrij kan bewegen door middel van diffusie. Niettemin zagen we een dramatische herschikking van de vaults wanneer we de cellen incubeerden bij 21°C (kamertemperatuur). In ongeveer 50 tot 80% van de cellen ontstonden grote langwerpige fluorescerende structuren die we vault-tubes (vault-buizen) noemden. Deze vault-tubes waren geordende structuren waarbinnen de MVP moleculen werden uitgewisseld in de tijd. De vorming van de vault-tubes leidde tot een vermindering van de niet-vault gebonden fractie van VPARP, die normaal aanwezig is in kleine langwerpige structuren in het cytoplasma (de VPARP-rods ofwel VPARP-staafjes) en in de kern matrix. De vorming van de vault-tubes was reversibel en afhankelijk van een coiled coil structuur die in het MVP eiwit zit. Verder bleek dat de vorming van de vault-tubes werd beïnvloed door de stabiliteit van de microtubuli. De relatie tussen

vaults en de microtubuli werd onderzocht in **Hoofdstuk 3**. In SW1573/MVP-GFP transfectanten zagen we een co-lokalisatie van vault partikels met microtubuli, maar niet met actine filamenten. Een interactie tussen vaults en microtubuli was al eerder gesuggereerd in de literatuur. Vaults werden meegezuiverd tijdens de isolatie van microtubuli uit een zee-egel, zelfs na meerdere rondes van polymerisatie en depolymerisatie. Co-immunoprecipitatie experimenten bevestigden dat er een interactie bestaat tussen vault partikels en microtubili (β-tubulin). Verder lieten we met behulp van kwantitatieve FRAP zien dat het afbreken van microtubuli de mobiliteit van de vaults beïnvloedt (vaults bewegen langzamer). Als controle hadden we GFP meegenomen, waarvan de mobiliteit niet veranderde na de afbraak van de microtubuli. We zijn nog maar net begonnen met het bestuderen van de relatie tussen vaults en microtubuli, maar het lijkt erop dat de algemene beweeglijkheid van vaults en de opbouw van de vault-tubes in meer of mindere mate afhankelijk zijn van deze cytoskelet elementen.

**Hoofdstuk 4** beschrijft verschillende domeinen van de drie vault eiwitten: MVP, VPARP en TEP1. Met behulp van een gist twee-hybriden systeem toonde we aan dat er een intramoleculaire binding is binnen het MVP eiwit. Verder lieten we zien dat MVP moleculen met elkaar een interactie aangaan via hun coiled coil domein. Naast dit coiled coil domein had MVP ook drie EF-hands die in staat waren om calcium te binden. De binding van calcium lijkt belangrijk voor de interactie tussen MVP en andere eiwitten (zoals bijvoorbeeld PTEN) en zou een rol kunnen spelen bij de opbouw van het vault complex. Binnen VPARP werd een intramoleculaire binding gevonden en we ontdekten dat het C-terminale uiteinde van VPARP een interactie aangaat met het N-terminale deel van MVP. Er werden geen interacties waargenomen tussen TEP1 en de andere vault componenten. Omdat het bekend was dat TEP1 het vault RNA (vRNA) bindt hebben we onderzocht of een co-expressie van vRNA in het twee-hybriden systeem een effect zou hebben op de binding van TEP1 met de andere vault proteïnen. Dit was niet het geval.

De expressie en vault-binding van de humane vRNAs werd onderzocht in **Hoofdstuk 5**. In de mens werden eerder drie genen beschreven die coderen voor drie verschillende vault RNAs (*HVG1-3*) en een vierde werd gevonden tijdens het zoeken naar homologen (*HVG4*). Alleen *HVG1-3* kwamen tot expressie en waren aanwezig in een niet-vault gebonden fractie in alle cellijnen die we getest hebben. De genen (*HVG1-3*) lagen in tandem in een herhalende structuur op chromosoom 5q33.1. Alle hvgs die tot expressie kwamen waren in staat te binden aan vaults, maar de verhouding waarin ze bonden was niet gelijk aan de verhouding waarin ze tot expressie kwamen. Het grootste deel van het vRNA dat gebonden was aan vaults was hvg1. Opmerkelijk was dat er steeds een verhoogde hoeveelheid hvg3 gebonden was aan de vaults geïsoleerd uit drug-resistente cellijnen. Dit kan betekenen dat de verhouding waarin de hvg soorten gebonden zijn met vaults de functie van het complex beïnvloedt of bepaalt. Dit alles duidde op een functionele rol voor het vRNA.

De observatie dat de vault-tube vorming resulteerde in een vermindering van de hoeveelheid niet-gebonden VPARP suggereerde dat de eiwitten (in ieder geval MVP en VPARP), of ze nu ingebouwd zijn in vaults of niet, op de een of andere manier functioneel gerelateerd zijn en een enkel geïntegreerd systeem vormen. Deze hypothese werd ondersteund door de resultaten die in **Hoofdstuk 6** beschreven worden. In dit hoofdstuk werden de gevolgen bestudeerd van de verwijdering van het *MVP* gen op de integriteit van het vault complex en de stabiliteit van de andere vault componenten. In deze studie maakten we gebruik van de *MVP* knockout muis die eerder binnen onze groep gemaakt was. Zoals verwacht bevatte de *MVP* knockout weefsels geen vaults of vaultachtige partikels. Verder had het verlies van MVP een dramatisch effect op de niveaus van de TEP1 en VPARP eiwitten en was er een duidelijke reductie in de niveaus van vRNA. De afname van de hoeveelheid TEP1 en VPARP eiwit was niet het gevolg van een verminderde transcriptie, mRNA instabiliteit of een verlaging van de translatie. De minor vault eiwitten waren minder stabiel bij afwezigheid van de belangrijkste structurele component van het complex. De reductie in de vRNA niveaus was waarschijnlijk een direct gevolg van de verlaagde hoeveelheid TEP1 eiwit. De effecten van het afwezige MVP konden worden gecompenseerd door de introductie van het volledige humane MVP in de knockout cellen, wat leidde tot een herstel van de niveaus aan VPARP en vRNA.

Experimenten die eerder waren gedaan toonden aan dat de verwijdering van *MVP* geen effect had op de gevoeligheid van embryonale stamcellen of beenmergcellen voor verschillende cytostatica. In deze experimenten werd niet gekeken naar de intracellulaire verwerking van de drugs. Daarom analyseerden we in **Hoofdstuk 7** de intracellulaire distributie en de in- en efflux kinetiek van fluorescente anthracyclines in muizen embryonale fibroblasten (MEFs) afkomstig van wild-type en *MVP* knockout muizen en vergeleken we de resultaten met de verwerking van drugs in de 'non-small cell' longkanker cellijn (SW1573), zijn drugresistente tegenhanger (SW1573/2R120) en de MVP-GFP overexpresserende cellijn (SW1573/MVP-GFP). Er werden geen significante verschillen gevonden tussen de gevoelige SW1573 en de MVP-GFP overexpresserende SW1573 cellen. In alle cellijnen die getest werden, ook in de drugresistente SW1573/2R120, was er een opeenhoping van daunorubicine in de kern waarna het fluorescente daunorubicine signaal zich verplaatste naar cytoplasmatische blaasjes. De efflux van drug uit de kern was veel sneller en meer efficiënt in de drugresistente cellijn. Er werden geen significante verschillen in de drugsverwerking gevonden tussen de wild-type en de vault deficiënte cellen en tussen de vault deficiënte cellen waar het volledige humane *MVP* (gemarkeerd met GFP) was teruggezet. Beide systemen lieten zien dat vaults niet direct betrokken zijn bij de verwijdering van daunorubicine uit de cellen of in de intracellulaire distributie van de drugs van de kern naar cytoplasmatische blaasjes.

Tot slot werden de resultaten in **Hoofdstuk 8** opgesomd en het belang ervan bediscussieerd.

**List of abbreviations**

| | |
|---|---|
| aa | amino acid |
| AD | transactivation domain |
| ADP | adenosine diphosphate |
| BD | DNA-binding domain |
| bp | base pair |
| BRCT | BRCA1 C-terminus |
| BSA | bovine serum albumin |
| cDNA | complementary DNA |
| DMEM | Dulbecco's modified Eagle's medium |
| DSE | distal sequence element |
| FITC | fluorescein isothiocyanate |
| FRAP | fluorescence recovery after photobleaching |
| GFP | green fluorescent protein |
| GST | glutathione-S-transferase |
| HRP | horseradish peroxidase |
| hvg | human vault RNA gene |
| Ig | immunoglobulin |
| LRP | lung resistance-related protein |
| mAb | monoclonal antibody |
| MDR | multidrug resistance |
| MEF | mouse embryonic fibroblast |
| MiVP | minor vault protein |
| $M_r$ | relative molecular weight |
| MRP | multidrug resistance protein |
| MVP | major vault protein |
| NES | nuclear export signal |
| NLS | nuclear localization signal |
| NPC | nuclear pore complex |
| PARP | poly(ADP-ribose) polymerase |
| PBS | phosphate-buffered saline |
| PCR | polymerase chain reaction |
| Pgp | p-glycoprotein |
| PSE | proximal sequence element |
| PTEN | phosphatase and tensin homologue deleted on chromosome 10 |
| RPMI | Rosswell park memorial institute medium |
| TEP1 | telomerase-associated protein 1 |
| TRITC | tetramethyl rhodamine isothiocyanate |
| VPARP | vault poly(ADP-ribose) polymerase |
| vRNA | vault RNA |

**Curriculum vitae**

De auteur van dit proefschrift werd geboren op 14 januari 1975 te Gouda. In 1993 behaalde hij het HAVO diploma aan het Monseigneur Frencken College te Oosterhout en begon hij aan het Hoger Laboratorium Onderwijs (Biotechnologie) in Etten-Leur. In 1996 voltooide hij deze opleiding en begon vervolgens aan de studie Biologie in Leiden. De doctoraalfase, in de richting Moleculaire Biologie, werd in 1998 afgerond. Tijdens de studie in Leiden deed hij onderzoek aan een gist 14-3-3 eiwit en zocht naar interactie partners van dit eiwit met behulp van een gist twee-hybriden systeem in de groep van Dr.ir. Yde Steensma (Institute of Molecular Plant Sciences, Sectie Gist Genetica, Rijksuniversiteit Leiden). Verder heeft hij onderzoek gedaan aan een eiwit van het kippen anemie virus genaamd apoptin onder leiding van Dr. Matieu Noteborn en Dr. Astrid Danen-van Oorschot (Leadd B.V., Leiden). Door middel van green fluorescent protein (GFP) fusies van mutanten van het apoptin eiwit werd er gezocht naar functionele domeinen verantwoordelijk voor de apoptosis inducerende activiteit en specificiteit van dit eiwit. In oktober 1998 begon hij aan het in dit proefschrift beschreven onderzoek op het Instituut Hematologie binnen het Erasmus Medisch Centrum te Rotterdam, onder leiding van Prof.dr. Pieter Sonneveld en Dr. Erik Wiemer. Sinds juni 2003 is hij werkzaam bij de afdeling Celbiologie en Genetica van het Erasmus Medisch Centrum te Rotterdam waar hij werkt aan de rol van de transcriptie factor Oct-6 in Schwann cel differentiatie in de groep van Dr. Dies Meijer.

The author of this thesis was born on January 14, 1975 in Gouda, The Netherlands. In 1993 he finished high school (HAVO, Monseigneur Frencken College in Oosterhout) and started his training as a technician in biotechnology (Hoger Laboratorium Onderwijs, Etten-Leur). In 1996 he graduated and went on to Leiden University to study Biology where he obtained his Masters degree in biology (Molecular Biology) in 1998. During his study he performed research on a yeast 14-3-3 protein and searched for interaction partners by means of a yeast two-hybrid system in the group of Dr.ir. Yde Steensma (Institute of Molecular Plant Sciences, Section Yeast Genetics, Leiden Universiteit). Furthermore, he studied the chicken anemia virus protein apoptin, supervised by Dr. Matieu Noteborn en Dr. Astrid Danen-van Oorschot (Leadd B.V., Leiden). By labeling apoptin mutants with a green fluorescent protein he searched for the functional domains responsible for apoptosis induction and the specificity of the protein. In October 1998 he started the reseach described in this thesis at the department of Hematology of the Erasmus Medical Center in Rotterdam, supervised by Prof.dr. Pieter Sonneveld en Dr. Erik Wiemer. Since June 2003 he works at the department Cell Biology and Genetics of the Erasmus Medical Center in Rotterdam, studying the role of the transcription factor Oct-6 in Schwann cell differentiation in the group of Dr. Dies Meijer.

**List of publications**

1. Van Zon, A., Mossink, M. H., Schoester, M., Scheffer, G. L., Scheper, R. J., Sonneveld, P., and Wiemer, E. A. C. Multiple human vault RNAs. Expression and association with the vault complex. J Biol Chem, 276: 37715-37721, 2001.

2. Van Zon A, Mossink M. H., Schoester M., Scheffer G. L., Scheper R. J., Sonneveld P., Wiemer E. A. C. Structural domains of vault proteins: a role for the coiled coil domain in vault assembly. Biochem Biophys Res Commun, 291(3): 535-541, 2002.

3. Mossink M., Van Zon A., Fränzel-Luiten E., Schoester M., Scheffer G. L., Scheper R. J., Sonneveld P., Wiemer E. A. C. The genomic sequence of the murine major vault protein and its promoter. Gene, 294(1-2): 225-232, 2002.

4. Mossink M. H., Van Zon A., Fränzel-Luiten E., Schoester M., Kickhoefer V. A., Scheffer G. L., Scheper R. J., Sonneveld P., Wiemer E. A. C. Disruption of the murine major vault protein (MVP/LRP) gene does not induce hypersensitivity to cytostatics. Cancer Res, 62(24): 7298-7304, 2002.

5. Danen-Van Oorschot A. A., Zhang Y. H., Leliveld S. R., Rohn J. L., Seelen M. C., Bolk M. W., Van Zon A., Erkeland S. J., Abrahams J. P., Mumberg D., Noteborn M.H. Importance of nuclear localization of apoptin for tumor-specific induction of apoptosis. J Biol Chem, 278(30): 27729-27736, 2003.

6. Mossink M. H., de Groot J., Van Zon A., Fränzel-Luiten E., Schoester M., Scheffer G. L., Sonneveld P., Scheper R. J., Wiemer E. A. C. Unimpaired dendritic cell functions in MVP/LRP knockout mice. Immunology,110(1): 58-65, 2003.

7. Van Zon A., Mossink M. H., Scheper R. J., Sonneveld P., Wiemer E. A. C. The vault complex. Cell Mol Life Sci, 60(9): 1828-1837, 2003.

8. Van Zon A., Mossink M. H., Schoester M., Houtsmuller A. B., Scheffer G. L., Scheper R. J., Sonneveld P., Wiemer E. A. C. The formation of vault-tubes: a dynamic interaction between vaults and vault PARP. J Cell Sci, 16: 4391-4400, 2003.

9. Mossink M.H., Van Zon A., Scheper R. J., Sonneveld P., Wiemer E. A. C. Vaults: a ribonucleoprotein particle involveld in drug resistance? Oncogene, 22: 7458-7467, 2003

**Dankwoord**

Begin er maar eens aan…

Je zou denken dat deze zin slaat op het beginnen aan een promotie onderzoek, maar ik heb het over het schrijven van dit dankwoord. Dit komt vooral omdat ik de ruim vier jaar dat ik op de afdeling hematologie heb gelopen als erg gezellig en leerzaam heb ervaren. Daaraan hebben meer mensen bijgedragen dan ik kan noemen in dit korte stukje. Daarom wil ik aan het begin van dit dankwoord iedereen die op de een of andere manier heeft bijgedragen bij het tot stand komen van dit proefschrift hartelijk bedanken. Toch zal ik, zoals dat hoort in een goed dankwoord, een aantal mensen specifiek noemen.

Allereerst wil ik mijn promotor Pieter Sonneveld bedanken. Pieter, je interesse in het fundamentele onderzoek is in de jaren gegroeid maar je hart ligt bij het klinische onderzoek. Daarvan hebben we geprofiteerd tijdens het schrijven van het daunorubicine hoofdstuk en bij de drugresistentie proeven die gedaan zijn met de knockout muizen. Verder wil ik mijn copromotor Erik Wiemer hartelijk bedanken. Ik heb het zeer gewaardeerd dat je altijd tijd voor mij wist vrij te maken. Onze (soms verhitte) discussies hebben uiteindelijk geleid tot een aantal mooie resultaten.

De overige leden van de kleine commissie, Prof.dr. Ivo Touw, Prof.dr. Roland Kanaar en Prof.dr. Rik Scheper wil ik hartelijk bedanken voor hun kritische commentaar op dit proefschrift.

In de tijd dat ik in de MDR groep zat, zijn er nogal wat mensen gekomen en gegaan. Paula, Tineke, Yvonne, Christine, Marry, Peter, Arie, Marianne en Mandy, bedankt voor alle gezelligheid en hulp de afgelopen jaren. Martijn, jij stond altijd klaar met een paar extra handen op de momenten dat het nodig was, bedankt. Erna, bedankt voor de goede impuls die je gegeven hebt aan het vault onderzoek. Heel veel plezier met jullie kleine Nikos. Dan waren er nog twee stagiaires: Sjoerd en Pascal. Bedankt voor jullie bijdrage aan verschillende onderdelen van mijn proefschrift en succes met jullie toekomst.

De FRAP experimenten heb ik gedaan in samenwerking met Adriaan Houtsmuller en Alex Nigg. Adriaan, jouw ervaring met bleaching experimenten en je enthousiasme hebben het vault onderzoek veel goed gedaan. Bedankt.

De werkbesprekingen met de collega's uit Amsterdam waren altijd erg nuttig en stimulerend. Rik, George, Anouk en Anneke bedankt voor de samenwerking en vele nuttige tips.

Karola, jij bent een groot deel van mijn hematologie tijd mijn buurvrouw met een luisterend oor geweest. Bedankt voor de mooie plaatjes die je voor me gemaakt hebt. Ik ben erg blij dat je als paranimf ook mijn buurvrouw tijdens mijn promotie wilt zijn. En dan natuurlijk Marieke. Marieke, ik moet jou voor ontzettend veel dingen bedanken, maar ik ga ze niet allemaal opnoemen. Ook ik vond San Francisco erg gaaf, maar ook de vault-meeting in Amsterdam was erg geslaagd! ('Quick, quick it will only hold for a minute') Jouw steun als paranimf zal ik nodig hebben tijdens mijn verdediging. Bedankt voor alles!

En dan tot slot: Pa en ma, Ramses en Jan-Joost hartelijk dank voor alle steun en begrip door de jaren heen. Ook wil ik bij deze mijn schoonfamilie bedanken. En natuurlijk Wilfred, zonder jouw interesse, steun en geduld had ik het nooit gered.